Plant production of Gonococcal peptide vaccine, candidate peptide display with HPVs

Sarah Lindsay

Thesis presented for the degree of Master of Science

Department of Molecular and Cell Biology

Faculty of Science

University of Cape Town

December 2023

Supervisor: Associate Professor Inga Hitzeroth

Co-supervisors : Dr Alta van Zyl and Dr Georgia Schafer

Plagiarism declaration

I, Sarah Lindsay, declare that this thesis / dissertation, submitted for the degree of Master of Science at the University of Cape Town, under the co-supervision of Dr Inga Hitzeroth and Dr Alta van Zyl, is my own work. Each contribution to, and quotation in, this Dissertation from the work(s) of other people have been attributed and has been cited and referenced. I further confirm that where required, permission was obtained for all images and figures used in this Dissertation and is stated as such, and where permission was not required, the original author was cited.

Signature: Signed by candidate

Date: 10/01/2024

Acknowledgements

To my academic supervisors Associate Professor Inga Hitzeroth and Dr Alta van Zyl for unwavering support they have given me. Thank you for providing me with everything I needed to complete this project and for your patience and guidance whenever I have needed it.

Professor Sanjay Ram from the University of Massachusetts for your endless support and encouragement. Thank you for the incredible opportunity to visit your lab, it is an experience I will keep with me forever.

Dr Georgia Schafer my co-supervisor at the ICGEB for all the help and time. Thank you for all the help with the mammalian cell culture and PsV work as well as the use of her group's facilities for the immunogenicity studies. Thank you to Sinead Carse for all your help with the animal studies, as well as Dr Claire Butters and Dr Alisha Chetty for your help with the mouse work and the IVIS® machine.

The members of the Biopharming Research Unit past and present: particularly Dr Aleyo Chabeda, Kirti Daya, Jenna Bloemetje, for input in my project and the support. As well as all the coffee breaks shared together. I appreciate the time you took to teach me and the friendship that I gained.

Rodney Lucas at the Research Animal Facility, Faculty of Health Sciences, University of Cape Town, for performing the animal experiments.

Mohammed Jaffer for assistance with transmission electron microscopy.

National Institute of Health (NIH) for funding the project, as well as for financial support.

Finally – to my wonderful family in particular my parents, and my special friends. For your love and support every step of the way and until the very end.

Abbreviations

mAb(s)	Monoclonal antibodies
nAb(s)	Neutralizing antibodies
Amp	Ampere
BCIP	5-bromo-4-chloro-3-indolyl-phosphate
bp	Base pairs
BM	Basement membrane
BSA	Bovine serum albumin
CP	Capsid/coat protein
CsCl	Cesium chloride
(k)Da	(kilo) Dalton
dpi	Days post infiltration
DNA	Deoxyribonucleic acid
ELISA	Enzyme-linked immunosorbent assay
EDTA	Ethylenediaminetetraacetic acid
EMC	Extracellular matrix
EtBr	Ethidium bromide
FLuc	Firefly Luciferase
GLuc	Gaussia Luciferase
g	Grams
g	Gravitational force
h	Hour/s
HPV(s)	Human papillomavirus(es)
HS	High salt

IM	Intra muscular
L	Liter/s
LB	Luria broth
m	Meter
M	Molar
min	Minute/s
O/N	Overnight
OD	Optical density
ORF	Open reading frame
PBS	Phosphate-buffered saline
qPCR	Quantitative Polymerase Chain Reaction
PsV(s)	Pseudovirion(s)
mPsV(s)	Mammalian-produced pseudovirion(s)
pPsV(s)	Plant-produced pseudovirion(s)
rpm	Revolutions per minute
RuBisCO	Ribulose-1,5-bisphosphate carboxylase/oxygenase
s	Second/s
SDS	Sodium dodecyl sulphate
NaOAc	Sodium acetate
TEM	Transmission Electron Microscopy
VLP(s)	Virus-like particle(s)
V	Volts
v/v	Volume per volume
w/v	Weight per volume

Symbols

α	Alpha
β	Beta
m	Milli-
μ	Micro-
n	Nano-
γ	Gamma
%	Percentage
°C	Degrees Celsius

Abstract

Human Papillomavirus (HPV) and *Neisseria gonorrhoeae* (*Ng*) are prominent pathogens responsible for a significant proportion of the global burden attributed to sexually transmitted infections. While vaccines targeting HPV have seen success, an effective vaccine against gonorrhea remains elusive, as antimicrobial resistance continues to be a growing threat. This study explores the innovative approach of plant-based production for a dual vaccine against HPV16 and gonorrhea, utilizing *Nicotiana benthamiana* as the expression host.

The vaccine design involves the incorporation of a gonorrhea peptide, mimicking the 2C7 epitope of the surface molecule LOS on gonorrhea, into the surface DE loop of HPV16 virus-like particles (VLPs). These chimeric VLPs as well as HPV16 VLPs were expressed and successfully purified from plants and demonstrated self-assembly into VLPs. The choice of *N. benthamiana* as the expression system is informed by its suitability for efficient and cost-effective recombinant protein production.

Immunological evaluations were conducted in mice to assess the immune response elicited by the dual vaccine. The mice displayed robust antibody responses against both HPV and gonorrhea, indicating the insertion of the peptide does not disrupt the binding of antibodies to HPV16 and highlights the potential of the vaccine candidate to induce a dual protective immunity.

To assess the protective efficacy of the vaccine candidate, a challenge model was developed and optimized, involving the use of HPV16 PsVs containing luciferase (FLuc). The challenge model was refined through a comparison of secreted and non-secreted reporter proteins, followed by comparison of plant and mammalian expression systems. This showed thatHPV16 PsVs containing non-secreted FLuc produced in mammalian cell culture were optimal for the challenge. Mice vaccinated with the plant-produced dual vaccine demonstrated protection against HPV infection upon challenge.

In summary the chimeric and HPV16 VLP vaccine candidates were expressed in an *Agrobacterium*-mediated transient system in plants. The immunogenicity of the vaccine candidates was accessed in a mouse model and a further challenge model. The results demonstrated the potential of using VLPs in the display of foreign epitopes in the fight against gonorrhea and HPV. The findings contribute valuable insights into the development of vaccines against sexually transmitted infections, paving the way for innovative strategies in the field of VLP display molecules and plant molecular pharming.

Chapter 1: Literature review

1.1 Introduction

Neisseria gonorrhoeae (*Ng*) is a coccus shaped bacteria which infects exclusively humans, causing the sexually transmitted disease (STD) gonorrhoea (Liu et al., 2017). Gonorrhoea is the second most common sexually transmitted bacterial infection globally. The World Health Organisation (WHO) recorded ~82 million cases of gonorrhoea in 2020 with the African region accounting for ~ 21.8 million of these cases (Unemo et al., 2021b). Sub-Saharan Africa displays the highest yearly incidence of STDs including gonorrhea (WHO, 2014, Kirkcaldy et al., 2019). The number of sexually transmitted infections (STIs) of gonorrhoea increased 63% between 2014 and 2018 and continues to be a global health issue (Sancta, 2020). Lower income areas tend to have relatively lower numbers of reported cases due to lack of accessibility to appropriate testing, incomplete testing and case reporting as well as lack of sexual health education (Qulu et al., 2023). Therefore, the incidence of gonorrhoea infections is likely to be underreported. This can result in ineffective treatment and increased morbidity which creates further healthcare costs and complications.

Transmission of gonococcal infection usually occurs through sexual activity by direct contact of the mucosal membranes of the urogenital tract, anal canal, oropharynx, or occasionally eye (conjunctivitis), of an infected person with an uninfected person (Rice et al., 2017). Directionality greatly impacts on transmission of *Ng*, as it has been shown that there is 83% transmission from men to women (Su et al., 2022), whereas transmission from women to men is ~20% (Hooper et al., 1978, Holmes et al., 1970) However, infection rates are higher in women and >50% of cases are asymptomatic, resulting in continued spread of infection (Tsevat et al., 2017, Alirol et al., 2017). Thus, there is a desperate need for an effective vaccine, particularly in developing and underdeveloped countries, to prevent the spread of *Ng* infection.

1.1.1 Disease symptoms and severity

Common clinical manifestations of prolonged *Ng* infection include cervicitis, urethritis, and proctitis. The asymptomatic nature of *Ng* infection in women leads to delayed treatment, often resulting in pelvic inflammatory disease (PID). The progression of gonococcal infection can cause permanent scarring of the fallopian tube, causing subsequent infertility and ectopic pregnancies (Kirkcaldy et al., 2019, Haese and 2021). Infected women can also transmit

gonorrhoea infections to infants during child-birth causing ophthalmia neonatorum (Unemo et al., 2019b).

Without treatment gonorrhoea infection can enter the bloodstream and spread to other parts of the body such as the joints, heart and brain. This results in disseminated gonococcal infection (DGI) which can cause further complications such as arthritis, endocarditis, and meningitis (Neto et al., 2021, Dal Conte et al., 2008, Ross, 1996, Vidaurrazaga and Perlman, 2020).

1.1.2 Antimicrobial resistance

Ng has utilised its enhanced ability of horizontal gene transfer to evolve mechanisms of antimicrobial resistance (AMR) to almost all antibiotics and is considered to be multi drug resistant (Figure 1.1) (St Cyr, 2020, Unemo, 2014). *Ng* was deemed a “superbug” by the Centre for Disease Control (CDC) in 2012 (Kirkcaldy et al., 2013, Suay-García and Pérez-Gracia, 2018). Previously-used antimicrobials such as penicillins, macrolides, tetracyclines, fluoroquinolones, and early-generation cephalosporins, as well as sulfonamides are no longer sufficient for treatment (Alirol et al., 2017). There is only one type of drug left that can be used as a monotherapy: extended-spectrum cephalosporins (ESCs) such as cefixime and ceftriaxone. Of particular concern is that it has been observed that there is decreasing susceptibility of gonococcal strains to ESCs globally (Unemo and Nicholas, 2012, Osaka et al., 2008), meaning that gonorrhoea infection may become untreatable. Therefore, the current recommended treatment of gonococcal infection by the CDC involves the use of 2 antimicrobials (azithromycin and ceftriaxone). However, the use of a dual treatment plan can be expensive for lower income regions such as in sub-Saharan Africa (Berndtson, 2020).

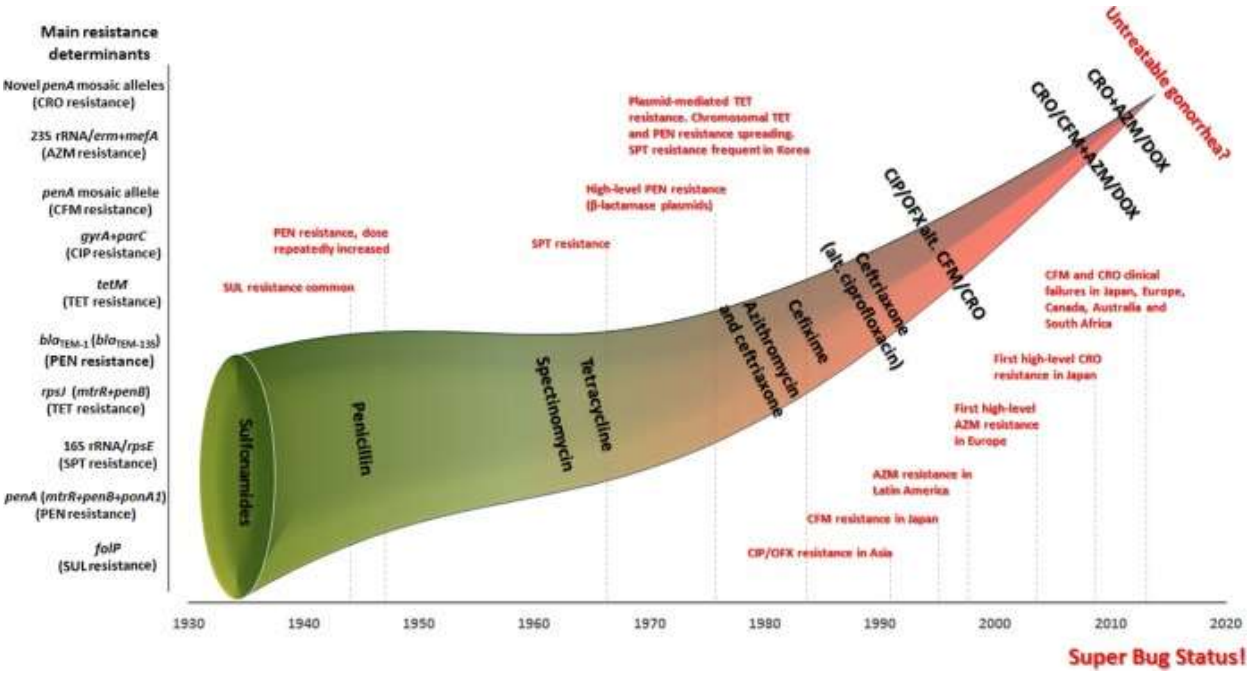

Figure 1.1: Emergence of antimicrobial resistance in *Ng*. Timeline denoting the discovery and recommendation of antimicrobials and subsequent evolution of drug resistance in *Ng*. SUL, sulfonamides; PEN, penicillin; SPT, spectinomycin; TET, tetracycline; CIP, ciprofloxacin; OFX, ofloxacin; CFM, cefixime; CRO, ceftriaxone; AZM, azithromycin; DOX, doxycycline. Figure used with permission from (Unemo, 2014).

Due to unavailability of diagnostic tests, many countries implement symptomatic treatment of *Ng*, and although they have a high incidence there is limited surveillance of AMR strains (Wi et al., 2017). Awareness of gonococcal AMR among policy-makers, clinicians, laboratory professionals, and patients is insufficient in many cases (World Health Organization, 2015, Wi et al., 2017) . Suboptimal testing accompanied with over-the-counter access to antimicrobials and limited access to the most effective antimicrobials give rise the perfect environment for expedited emergence and spread of AMR *Ng* (Unemo et al., 2021a, Unemo et al., 2019a). The WHO implemented the Gonococcal Antimicrobial Surveillance Program (GASP) in 1990 (Wi et al., 2017), however, after 30 years there are only 5 African nations that contribute to the program (Unemo et al., 2019a) (WHO, 2018). Globalization and increased travel has exacerbated the problem of antimicrobial resistance (Berndtson, 2020). This spread of disease across the world makes tracing of resistant strains evermore challenging.

1.2 Pathogenicity of Neisseria gonorrhoeae

Ng is a Gram-negative bacterium which colonises mucus membranes by adhering to epithelial cells (Quillin and Seifert, 2018). Post-infection responses are primarily against lipo-oligosaccharide (LOS), opacity-associated (opa) protein, pili, and porin determinants (Figure 1.2a) (Ngampasutadol et al., 2006, Hook et al., 1984, Lammel et al., 1985). These structures play various roles in the pathogenicity of *Ng*. The opa proteins are integral outer membrane proteins and act primarily as adhesins binding to human epithelial cells. This attachment facilitates the formation of microcolonies which in turn allows for the formation of biofilms (Sadarangani et al., 2011). Type IV pilus facilitate the movement of the bacteria up the genital tract and play important roles in both cell adhesion and genetic exchanges of the bacterium. They are required for effective mucosal membrane colonization (Higashi et al., 2007). Porins are highly abundant channels on outer membrane of *Ng* which are essential for the acquisition of nutrients (Figure 1.2b) (Wetzler et al., 1992, Unemo et al., 2019b).

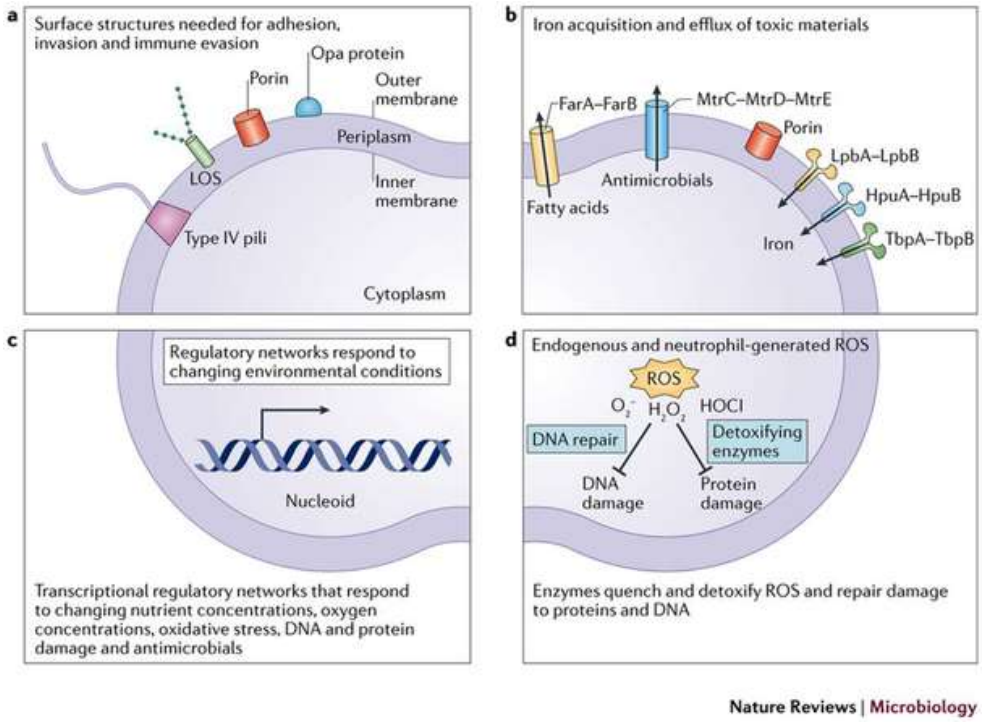

Figure 1.2: Overview of *N. gonorrhoeae* pathogenesis factors. *Ng* encodes a highly effective repertoire of pathogenesis and colonization factors. a) Array of surface structures which responsible for adherence to the surface of host cells, invasion host cells, and evasion of the hosts immune system. These surface structures include Type IV pili, LOS, porin, and Opa proteins. b) Efflux pumps protect *Ng* from antimicrobial peptides and fatty acid stress, and membrane transporters allow *Ng* to co-opt nutrients such as iron, and fatty acids from the surrounding environment. c) *Ng* transcriptional regulators which induce transcriptional pathways to respond and adapt to changing environmental conditions during infection. d) Protective enzymes (e.g. catalyse) neutralize reactive oxygen species (ROS), that are

produced both endogenously and by neutrophils. Figure used with permission from (Quillin and Seifert, 2018).

1.2.1 Strategies of immune evasion

The *Ng* bacteria has developed highly effective mechanisms to evade the host immune system. The ability for *Neisseria* to exchange genetic material allows for rapid adaptation (Quillin and Seifert, 2018). Various transcription factors also play critical roles in responding to environmental changes (Figure 1.2c). All previously mentioned surface proteins present vast antigenic variation due to factors such as phase-variable expression, variation of alleles, and expression of recombined genes (Liu et al., 2017). Recombination of genetic material results in changes to phenotype and therefore evasion of antibody detection.

The first line of protection is the outer membrane that has protective features that are toxic to host cells, namely, LOS, peptidoglycan, and outer-membrane vesicles are released from the surface of the bacteria (Figure 1.2). LOS is sialyated at various sites through the addition of sialic acid which can mimic the sialyation patterns of the host and therefore evade the complement system (Figure 1.3). Sialylation of the α chain of LOS enhances factor H deposition on porin, therefore increasing resistance of sialylated *Ng* to phagocytosis (Shaughnessy et al., 2016). Another mechanism by which *Ng* overcomes complement binding involves reduction modifiable protein M (RmpM), which has been found to bind to peptidoglycan and cover the surface of *Ng* and in doing so does not allow for recognition of surface membrane antigens by the immune system (Jones et al., 2022) .

LOS triggers the innate immune system causing a pro-inflammatory response defined by the release of various cytokines (such as IL-6, IL-8, IL-1β, IL-17, and IFN-γ) resulting in the recruitment of neutrophils to the infected area (Ngampasutadol et al., 2006). Gonococci are able to survive phagocytosis as they possess efflux pumps (Figure 1.2 and 1.3) that will export any antimicrobial molecules. The bacteria also produce enzymes that enable them to avoid killing by reactive oxygen species (ROS) which are released by the neutrophils (Figure 1.2d), enabling them not only to reside but replicate within neutrophils (Smirnov et al., 2023). Because of this, there is a reduced presentation of *Ng* antigens to the CD4 T cells. *In vitro* testing has shown that *Ng* supresses both the CD4 T cell response as well as B cell antibody responses (Zhu and 2011, Liu et al., 2014, Sadarangani et al., 2011).

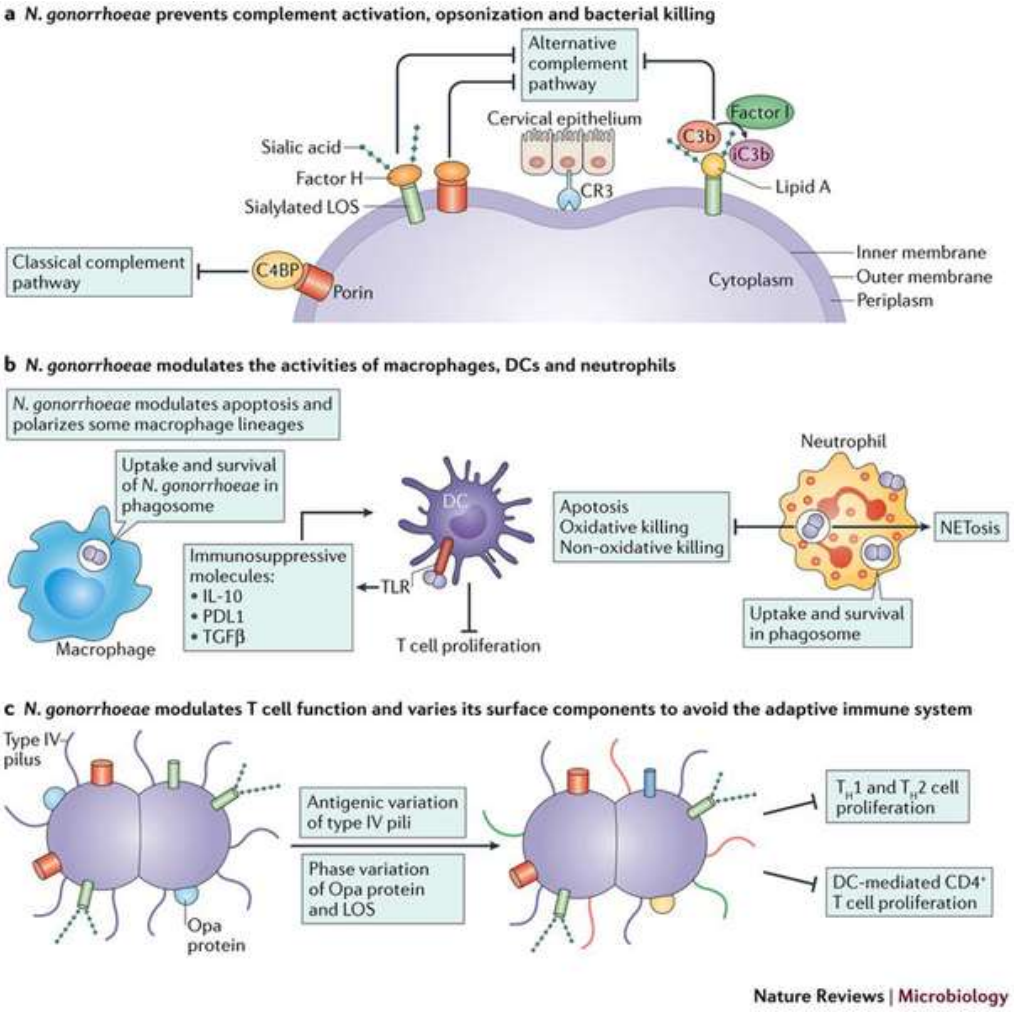

Figure 1.3: *Ng* evades and modulates both innate and adaptive immune system responses. a) *Ng* binds host Factor H and C4bp, becoming serum resistant as well as sialylates its LOS to present as 'self' and hiding itself from complement recognition. *Ng* also binds to the alternative complement pathway as it binds C3b through Lipid A on LOS, factor I rapidly converts C3b to the inactive iC3b. b) *Ng* can survive inside the phagosome of macrophages where it can regulate cell apoptosis and production of cytokines. Dendritic cells exposed to *Ng* are less capable of stimulating T cell proliferation. The interactions of *Ng* and neutrophils is complex whereby *Ng* can escape the phagosome and proliferate with in the neutrophils. c) Due to the ability of *Ng* to undergo frequent antigenic and phase variation of its surface structures including Type IV pili, Opa proteins, and LOS, *Ng* infection does not result in immunological memory. In addition, *Ng* is able to modulate the adaptive immune response by influencing cytokine production which leads to the suppression of T helper cell proliferation. Figure used with permission from (Quillin and Seifert, 2018).

1.2.2 Typical immune response

Infection with *Ng* elicits a strong inflammatory innate immune response. However, this immune response does not result in protective immunity (Liu et al., 2014, Fowler et al., 2010). Therefore,

reinfection with *Ng* is common (Fowler et al., 2010). *Ng* is well equipped to evade the immune system in part due to its resistance to bacteriolytic and opsonophagocytic responses. *Ng* is able to inhibit compliment pathways as well as the activation of Th1 and Th2 cells. It stimulates the activation of the Th17 which results in recruitment of neutrophils to the area (Fox et al., 1999, Schmidt et al., 2001, Ross et al., 1995). It has been found that RmpM antibodies are not bactericidal and that these antibodies block the binding of other surface antigen specific antibodies. These responses result in the lack of *Ng* to elicit a protective immune response. However, this does not mean that protection could not be achieved through vaccination (Zhu and 2011). The development of vaccines will need to focus on generation of Th1 or Th2 responses rather than the natural host response with focus specifically on conserved antigenic sites that provide broad protection and are not subject to phase variation (Edwards and 2004, Liu and Russell, 2011).

1.3 Vaccine research

Vaccination remains the most successful, rapid, and cost-effective method for controlling the spread and preventing infectious diseases (Mohsen et al., 2017, Kushnir et al., 2012). Due to the current AMR emergence, there has never been a greater need for development of a *Ng* vaccine. Recombinant expression of proteins is now a fine-tuned process for the production of many kinds of proteins. Determination of specific antigenic proteins that elicit protective immune responses is the first step in the development of a vaccine (Syomin and Ilyin, 2019).

Previously only 2 *Ng* vaccines have undergone human trials. The first was a killed whole cell vaccine developed by Greenberg et al. The vaccine was able to elicit an antibody immune response in >90% of vaccine recipients. Although the vaccine was composed of whole cells and therefore contained the LOS, it was well tolerated. Despite this the vaccine showed no evidence of protection against *Ng* and no further investigation was done (Greenberg, 1975, Greenberg et al., 1974). The second vaccine was developed based on previous work done on the *Neisseria meningitidis* (*Nm*) vaccine which involved the Pilus. The isolated and purified *Ng* Pili were used in parenteral immunization of recipients. The vaccine evoked a broad antibody response that was detectable in both the serum and the genital secretions and the vaccine showed protection against challenge by urethral infection (Brinton et al., 1982). However, in a proof of principle large-scale trial the vaccine was delivered intradermally, and this resulted in no protection

against *Ng*. The reason may be due to antigenic variation of strains that are present in a natural infection as well as the method of administration. (Boslego et al., 1991).

A retrospective epidemiological study showed that vaccination with MeNZB, a *Nm* outer membrane vesicle (OMV) vaccine designed to protect against sero-group B *Nm* disease, showed 31% effectiveness in reducing *Ng* infection in groups subsequently infected with *Ng* (Semchenko et al., 2019). *Nm* and *Ng* share several similarities and *Nm* protein antigens have shown to elicit antibodies that cross-react with *Ng*. The antibodies elicited by immunizing mice with Bexsero (*Nm* vaccine) or MeNZB were reported to support bactericidal activity against *Ng* (Giuliani et al., 2018). An OMV vaccine approach was also being investigated as a possible vaccine against *Ng* (Matthias et al., 2021, Semchenko and Seib, 2022) .

Substantial progress has been made into research of vaccine development. As previously mentioned, surface antigens have been identified as essential for survival and pathogenicity of *Ng* and therefore can be investigated as vaccine candidates (Jerse and Deal, 2013, Edwards et al., 2016).

Furthermore, mathematical modelling suggests that a vaccine that has only 30% efficacy could decrease gonorrhoea prevalence by >30% within 15 years, if population coverage is sufficiently high and immunity is maintained (Unemo and Sikora, 2017)

1.3.1 LOS as a vaccine target

1.3.1.1 Structure of LOS

LOS is the most abundant outer membrane molecule and is ubiquitously expressed. LOS is made up of a lipid backbone and three oligosaccharide tails which are linked by Heptose sugars Hep I and Hep II with Hep I attached to chain 1 and Hep II attached to chains 2 and 3 (Gulati, 2019). The lengths and branching of each of the chains can vary. These regions have the potential for sialyation which reduces opsonic killing of *Ng* (Kim et al., 1992, Rest and Frangipane, 1992, Gill et al., 1996). These modifications can allow the bacteria to adapt to display sialylation patterns producing up to six different antigenic structures at a time but also that resemble the host cells (Scurtu et al., 2022), and therefore evade antibody detection (Figure 1.4).

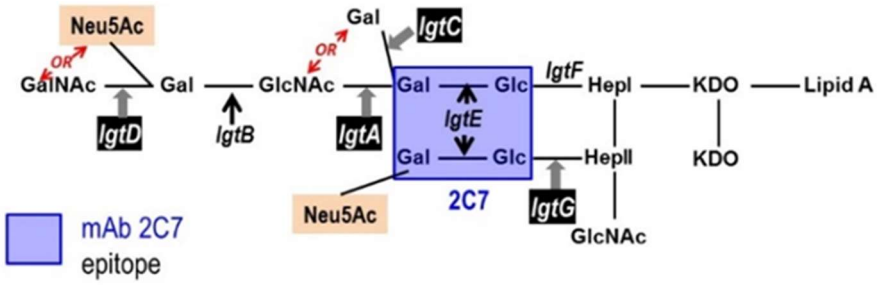

Figure 1.4: Schematic diagram of LOS present on the surface of N. gonorrhea. The black boxes indicate the phase variable genes (lgtA, C, Dand G) that are involved in LOS glycan extensions. The blue box indicates the epitope to which mAb 2C7 binds. Addition of Neu5Ac only occurs in the presence of exogenous CMP-Neu5Ac. KDO, keto-deoxyoctulosonic acid; Hep, heptose; Glc, glucose; Gal; galactose; GlcNAc, N-acetylglucosamine; GalNAc, N-acetylgalactosamine; Neu5Ac, N-acetneuraminic acid.

It has been identified that the lack of the lactose region of oligo chain 2 results in reduced efficacy of the *Ng*. Therefore, it is believed that this region contributes to the virulence of *Ng* and for this reason seems to be conserved and found in almost all *Ng* infections. This specific region is expressed from the IgtE gene and is called the 2C7 epitope as indicated by the blue box in Figure 1.4. The 2C7 epitope consists of 2 Galactose b1-4 Glucose each of which are b-linked to Hep I and Hep II (blue shaded box Figure 1.4) and represents the minimal structure N-linked fatty acids in lipid A which are required for maximal expression of the epitope recognized by mAb 2C7 ((Yamasaki et al., 1999) (Mühlecker et al., 1999)).

1.3.1.2 2C7 epitope

The 2C7 epitope is widely conserved amongst gonococcal strains. The oligosaccharide does not elicit a strong adaptive immune response (i.e. memory cells). It results in production of primarily low affinity IgM antibodies and there is no affinity maturation. Peptide mimics resembling the 2C7 epitope were discovered via screening of a peptide display library, then chosen based on their immunogenicity through immunochemical selection. Ngampasutadol et al successfully identified this mimitope in 2006 which was selected by a monoclonal antibody (Ab) that confers both bactericidal and opsonophagocytic abilities. The mAb 2C7 antibody is complement-dependent (Gulati et al., 1996b, Ngampasutadol et al., 2006, Gulati, 2019). Therefore, using the peptide mimic allows for initiation of a protective immune response and there has been a significant amount of work done using this peptide mimic.

Previously, Ram *et al.* synthesized the 2C7 peptide which was configured into a multiantigen peptide in the form of a tetramer (TMCP2) (Ngampasutadol et al., 2006) and an octamer (Octa-

MAP) (Gulati et al., 2019b) to increase the immunogenicity of the peptide. These vaccine candidates have been tested in mice and show the elicitation of neutralizing antibodies (nAb) which accelerated the clearance of *Ng* infection (Gulati et al., 2019b, Gulati et al., 2013b). Work done using the mimitope showed the elicitation of a Th1 immune response. Notably, use of the 2C7 peptide vaccine outperforms Bexsero when compared in a mouse model (Petousis-Harris et al., 2017). For these reasons the 2C7 vaccine meets the "triple threat" criteria: broad representation, serves as a virulence determinant and plays a critical role in the survival of the organism (Gulati, 2019).

1.3.2 VLPs as display molecules

Virus like particles (VLPs) are self-assembling multimeric nanoparticles that are made up of one or more viral structural proteins that do not contain genetic material (Qian et al., 2020). In particular, these VLPs range in size from 22 nm to 200 nm which is in the optimal range for cellular uptake (40 nm). Larger particles tend to have improved interaction with antigen presenting cells (APCs). Examples include virosomes, particulate adjuvants (microparticles or liposomes), whole cells vaccines, and VLPs (Kovacsovics-Bankowski et al., 1993). The surface structure of VLPs tends to be highly repetitive which therefore allows for increased antibody binding (Bachmann and Jennings, 2010). Due to the targeting of dendritic cells (DCs), VLPs elicit a strong immune response which includes both innate and humoral responses (Kushnir et al., 2012). Because of this there is predominantly no need for the addition of an adjuvant in VLP vaccines as they are self-adjuvating in nature (Grgacic and Anderson, 2006).

For these reasons both VLPs and viral replicon particles (VRPs) show promise as antigen delivery systems (Zhu and 2011). VLPs can be engineered into chimeric particles which display antigens originating from foreign pathogens (Grgacic and Anderson, 2006). Vast research has been done into immunoprophylaxis using VLPs. There are many examples of VLPs used as display particles to combat infectious disease including current efforts to produce a malaria vaccine (Chichester et al., 2018), Influenza vaccine (Chung et al., 2015, Valero-Pacheco et al., 2016), HIV vaccine (Peters et al., 1997) as well as many others (Zhang et al., 2023, Mohsen et al., 2017). The 2C7 mimitope is a small peptide which is not ideal in size or confirmation for eliciting an optimal immune response. It could however be displayed on a VLP thereby enhancing its immunogenicity.

1.4 HPV

Human papillomavirus (HPV) is the causative agent in the development of 99% of cervical cancer cases. Cervical cancer is the 4th most common cancer among women globally with ~600 000 cases reported in 2020 (Singh et al., 2023). The geographic regions primarily effected by higher HPV rates overlap largely with the counties effected by *Ng* infections. This makes a dual vaccine which is affordable for developing regions an extremely useful tool in the fight against the spread of both diseases and would help to reduce the economic burden of both diseases.

1.4.1 HPV VLPs structure

HPVs consist of an 8kb double stranded DNA genome which is encapsidated in L1 (major) and L2 (minor) capsid proteins (de Villiers et al., 2004) and they are nonenveloped viruses. The structure and assembly of HPVs has been well studied and characterised (Chen et al., 2000). The L1 proteins combine to form 72 pentamers which assemble into a T = 7 icosahedral formation with one L2 protein integrating into each of the pentamers (Conway and Meyers, 2009, Naud et al., 2014). The size of the particles varies from 50 - 60 nm. The L1 capsid proteins can self-assemble into stable VLPs even in the absence of L2 proteins. The C-terminal chains of L1 proteins interact hydrophobically to assemble and form capsomeres, which can then further assemble into the full particle structures. The structure of L1 protein forms several loops (BC, DE, EF, FG and HI) which are on the surface of the particle and therefore play a crucial role in production of nAbs (Chen et al., 2000). Therefore, these loops show promise as regions for display of exogenous peptides which can be used for elicitation of an immune response.

1.4.2 Current HPV vaccines

There are 6 HPV vaccines currently licensed: 3 bivalent(Cervarix™, Walrinvax, Cecolin, HPV 16/18 VLP); 2 quadrivalent vaccines (Gardasil®, Cervavax, HPV-6/11/ 16/18 VLP vaccine; and most recently the nonavalent (Gardasil®9 HPV-6/11/16/18/31/33/45/52/58 VLP) vaccine. All of these vaccines make use of L1 as it elicits the immunological response equivalent to that of the native HPV. Vaccination results in production of nAb which prevent infection by any subsequent exposure to the virus. These current vaccines have shown to be highly efficacious and confer protection against HPV infection (Naud et al., 2014, Huh et al., 2017, Chatterjee, 2014). Due to the research and development done to produce these vaccines, it is an attractive option to use

HPV VLPs as display particles. Previous work done using chimeric HPV particles includes the development of an HIV/HPV chimeric vaccine (Dale et al., 2002, Di Bonito et al., 2009, Peng et al., 1998), as well as HPV L1/L2 chimeras (Chabeda et al., 2019) to confer broad protection.

The current HPV vaccines are still expensive in low-income countries costing between US$140 and US$580 per dose (Wang et al., 2023). This leads to further economic burden due to high cancer rates caused by HPV and therefore there is a need to produce a cheaper HPV vaccine.

1.4.3 Concept of a dual vaccine

Another consideration in the development of a dual HPV / *Ng* vaccine is the demographic that would primarily be targeted. People between the ages of 15 and 29 are most at risk for contracting gonorrhea which is similar to the recommended age (11) of vaccination for HPV vaccine (CDC., 2019). However, sex workers and men who have sex with men are also at significant risk for contraction of *Ng,* which may be complicated by social stigma (Unemo and Nicholas, 2012). There is general consensus that a *Ng* vaccine may not provide long term protection but may require regular boosters and therefore it is important that the vaccine is affordable for use in low income regions (Zhu and 2011). Co-transmission of STIs is high and leads to increased risk of HIV infection (CDC., 2019). Considering the protection acquired from the HPV vaccine and the acceptance of this vaccine, coupling this with protection against *Ng* could prove to be effective in increasing vaccine uptake of an *Ng* vaccine and reducing the spread.

1.5 Study Objectives

This study aimed to utilize HPV16 Virus-Like Particles (VLPs) as a structural foundation for presenting the 2C7 peptide mimic, serving as a potential dual vaccine targeting HPV and *Ng*. The initial objective encompassed the recombinant production of chimeric VLPs and HPV16 L1 through Agrobacterium-mediated transient expression in *Nicotiana benthamiana*. Previous successful expressions of HPV16 VLPs in plant systems have been documented (Maclean et al., 2007, Lamprecht et al., 2016) Once successful expression of the VLPs was achieved, the subsequent objective was to purify these particles, intending to employ them as a promising candidate vaccine.

In order to complete a challenge experiment, the second objective was to produce HPV16 PsVs containing a luciferase reporter gene in both plant and mammalian expression systems. This allowed for a head-to-head comparison of the HPV16 PsVs produced in plants and mammalian systems. To effectively conduct the challenge experiment, the third objective entailed the production of HPV16 Pseudo-Virions (PsVs) containing a luciferase reporter gene in both plant and mammalian expression systems. This approach facilitated a direct comparison between the HPV16 PsVs produced in plant and mammalian systems, providing a comprehensive analysis of their efficiency of infection and further use in a challenge experiment.

The fourth objective involved evaluating the immunogenicity of the prophylactic chimeric candidate vaccine in mice. This assessment included antibody detection alongside an HPV challenge experiment to ascertain the immune response generated.

Chapter 2: Transient plant expression of HPV16 L1 chimeras

2.1 Introduction

Neisseria gonorrhoeae, is the etiological agent responsible for gonorrhea, which is an STI causing global concern (Alirol et al., 2017). Despite the availability of antimicrobial treatment, antimicrobial resistance is increasing globally. Prophylaxis has become a primary goal in the fight against gonorrhea as there are currently no vaccines available for protection against gonorrhea infection (Rice et al., 2017). *Ng* is highly skilled at evasion of the immune system which makes vaccine development ever more challenging. The *Ng* 2C7 peptide alone is not highly immunogenic due to its size. As the conformation of the peptide is important for binding, therefore use of HPV as display molecules may elicit a strong immune response. The VLP provides not only a highly repetitive display, but also a structure which keeps the peptide conformation (Chabeda et al., 2019).

Currently there are 3 commercially available HPV vaccines and they have been proven to be effective in the prevention of HPV infections (Naud et al., 2014, Huh et al., 2017). However, completion of the recommended three doses is particularly challenging in low-income countries as HPV vaccines are expensive and less accessible. Therefore, development of a more affordable vaccine would be hugely beneficial for the regions most impacted by HPV (Singh et al., 2023). As with HPV, *Ng* is also highly prevalent in low-income countries. Both diseases affect similar social groups with more severe symptoms affecting women (Unemo et al., 2019b).

2.1.1 Plant production systems

Production of vaccines using eukaryotic expression systems is unaffordable for developing countries. In 2020 a new HPV16/18 vaccine consisting of HPV VLPs was approved for use in China which is expressed in an *Escherichia coli* (*E. coli*) expression system resulting in a cheaper vaccine (Chu et al., 2023). Following this success, a nine valent vaccine produced in *E.coli* is currently under development for increased protection against other high-risk strains of HPV.

While eukaryotic production of recombinant proteins can be expensive, plant-based production systems provide a cost-effective alternative. These production systems have been investigated for expression of various different vaccine candidates including Hepatitis B and C, corona virus and Zika virus as well as many more (Dobrica et al., 2017, Rosales-Mendoza, 2020,

Mohammadzadeh et al., 2016, Diamos et al., 2020, Su et al., 2023). Making use of plants as the expression system has several advantages. Firstly, it should be more affordable, the risk of any contamination with human or animal pathogens is greatly reduced and the waste generated by this production system is more easily contained. Particularly, transient expression in *N. benthamiana* through *Agrobacterium*-mediated infiltration of plants allows for expression of trans genes that will not be incorporated into the plant genome (Lamprecht et al., 2016).

Recombinant transient expression of HPV has shown to be successful in plants, and vaccination of animals with these VLPs induced protective humoral immune responses (Pineo and 2013, Varsani et al., 2003, Maclean et al., 2007, Kohl et al., 2006). It has been shown that localization of HPV expression to different cell compartments influences the accumulation of the protein. Maclean et al showed that using a chloroplast-targeting constructs resulted in highest L1 accumulation (Maclean et al., 2007). Therefore, this study will make use of previously described methods in order to produce chimeric HPV VLPs displaying the *Ng* peptide in *N. benthamiana.*

2.1.2 HPV VLP structure

The structure of L1 is well described (Figure 2.1) and extensive work has been conducted on the function of different regions (Xu et al., 2006), specifically the importance of specific regions in the folding and assembly of the particles. It has been shown that Asp202, Cys175, and Cys428 are essential in the formation of HPV16 L1 VLPs. The EF and CD loop are essential for the formation of larger structures, deletion of these results in formation of capsomeres (Varsani et al., 2003). This is an important consideration when trying to produce chimeric VLPs.

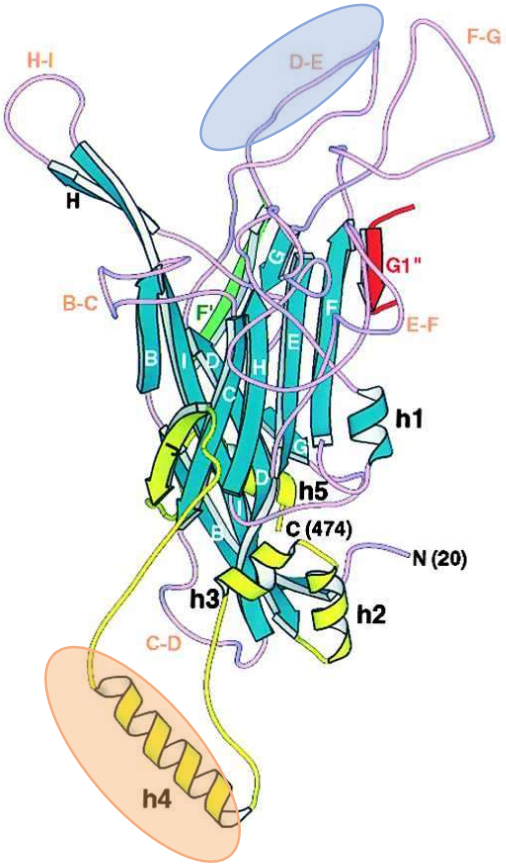

Figure 2.1. Structure of HPV 16 L1 monomer. The amino acid sequence starts at N terminus N(20) and ends at the C terminus C(474). Connecting loops are pink; strands are labelled with capital orange lettering (BC, CD, DE, EF, FG and HI); helices labelled (h1-h5). Adapted from (Chen et al., 2000).

2.1.3 Targeting of LOS using 2C7

The 2C7 epitope is a short peptide, 18 amino acids in length, which mimics the region of the *Ng* surface molecule, LOS that is bound by the 2C7 antibody (mimitope) (Ngampasutadol et al., 2006).

The 2C7 epitope is regulated by a phase variable gene and therefore may not always be present on the surface of the bacteria. However, deletion of this gene resulted in reduced fitness in the infection of *Ng* using a mouse model (Gulati et al., 2013a, Ram et al., 2018). The epitope has also shown to be important for the inhibition of complement binding and inhibition of inflammatory responses (Ram et al., 2018). Epidemiological studies in Boston, USA (early 90s) (Gulati et al., 1996a) and Nanjing, China (2009-2013) (Ram et al., 2018) showed that the epitope was present in 94% and 95% of clinical isolates respectively. All clinical isolates expressing this epitope are killed by the mAb 2C7 in serum bactericidal assay (SBA).

In this chapter we generate various HPV L1/*Ng* chimaeras by inserting the 2C7 peptide into the h4 helix and DE loop. Thereafter, we investigate expression of these chimeras in plants and further purification of the VLPs.

2.2 Materials and methods

2.2.1 Expression plasmid constructs

Previous research carried out in the Biopharming Research Unit (Dr Aleyo Chabeda, unpublished) investigated the effect of VLP formation when the *Ng* 2C7 mimitope was either substituted or inserted into different regions of L1. The following peptide sequence (Cys-Gly-Pro-Ile-Pro-Val-Leu-Asp-Glu-Asn-Gly-Leu-Phe-Ala-Pro-Gly-Pro-Cys) was added specifically to the DE loop indicated by the blue circle in Figure 2.1 and the h4 helix indicated by the orange circle in Figure 2.1. These regions were selected based on previous work done involving the addition of L2 epitopes to the surface of L1 (Chabeda et al., 2019). The expression and the particle assembly as well as binding of the 2C7 mAb was tested to determine the best chimeric particles. As conformation of the 2C7 mimitope is essential for antibody binding, cysteines were added to each end of the peptide chain in order to form a Cys-Cys clamp to display the peptide as a loop (Figure 2.2). This clamp was then removed in the generation II particles to assess whether this may be hindering particle formation. Preliminary testing of various chimeric particles was done to determine the best conformation. After much investigation it was established that the generation I chimeras with the gene inserted into the DE loop (DE i) showed the best expression and the most well-formed particles when compared with the h4 helix (Varsani et al., 2003, Pineo and 2013). Therefore all future experiments were conducted using generation I DE_i. Time trials were conducted as well as infiltration with *Agrobacterium* at various OD_{600} values for optimization of expression.

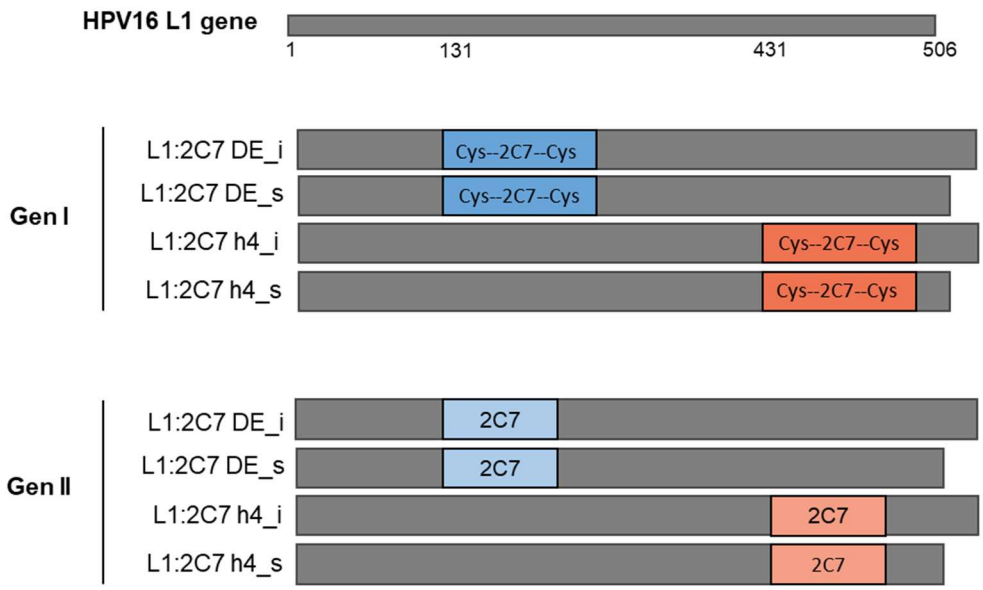

Figure 2.2. Schematic of chimeric constructs. Insertion (_i) or substitution (_s) of 2C7 into HPV-16 L1 at positions within the DE loop or the h4 helix (Figure 2.1) to create generation I and generation II constructs. Not drawn to scale.

2.2.2 *Agrobacterium*-mediated transient expression of HPV L1 and L1-*Ng* VLPs

The expression of HPV chimera (DE_i) and the HPV16 L1 proteins in *N. benthamiana* was previously optimized in the BRU lab by Dr Aleyo Chabeda. The gene sequences were cloned into the pTRAc-rbcs1-CTP vector which is targeted to the chloroplasts (Maclean et al., 2007). Glycerol stocks of the *Agrobacterium* (2mL) were used to inoculate 50 mL of Luria Bertani media (LB; 1% sodium chloride [NaCl], 0.5% yeast extract and 1% tryptone 10mM 2-morpholinoethanesulforic acid (+[MES]) supplemented with relevant antibiotics (30 µg/ml kanamycin, 50 µg/ml carbenicillin and 50 µg/ml rifampicin) and incubated at 27°C for 16 hours with agitation (220rpm). The cultures were subsequently used to inoculate 500 mL of LB media and grown for a further 18 hours. Cultures were diluted in infiltration buffer (10 mM MgCl2, 10 mM MES, and 150 µM acetosyringone in water, pH 5.6) to the required ODs for infiltration (Table 2.1). The strains were incubated at 22°C for 2 hrs to allow for expression of the vir genes prior to infiltration. The chimera was co-infiltrated with *Agrobacterium* harbouring the pBIN-NSs silencing suppressor plasmid found in the tomato spotted wilt virus (TSWV) (Takeda et al., 2002). Approximately 100 6-week-old *N. benthamiana* plants were infiltrated per construct. The plants were submerged in the diluted *Agrobacterium* suspension and subjected to a vacuum of -100 kPa, after which the vacuum was released. Infiltrated and non-infiltrated

plants were grown at 22°C in 8 hours dark, and 16 hours of light cycling. All leaves were harvested at 5 days post infiltration (dpi) and stored at -80°C until use (Maclean et al., 2007).

Table 2.1. Recombinant *Agrobacterium* cell densities (OD_{600}) used for infiltration.

Construct	OD_{600}	Strain of *Agrobacteria*	Vector
Chimera + NSs	0.75 + 0.25	GV3101::pMP90RK LBA4404	pTRAkc-rbsc1-cTP
HPV 16 L1	0.5	GV3101::pMP90RK	pTRAkc-rbsc1-cTP
Empty vector	0.5	GV3101::pMP90RK	pTRAkc-rbsc1-cTP

2.2.3 Extraction and purification of plant-produced VLPs

One kilogram (kg) of plant biomass was homogenized with T-25 digital Ultra-Turrax® (IKA® Works Inc) in 2X volumes of extraction buffer (0.1 M Tris, 0.5 M NaCl, 4% PVPP, 0.01 M ascorbic acid, 0.05 M PMSF, pH 7.8) and incubated at 4 °C with agitation for 1 hour. The extract was filtered through 4 layers of 22-24 µm pore Miracloth™ (Millipore, Sigma) and centrifuged three times for 15 mins at 15 000 *x g*, 4°C. The supernatant was loaded onto sucrose gradients consisting of 1 mL 50% w/v sucrose beneath 5 mL 30% w/v sucrose (Figure 2.3). Sucrose gradients were prepared in high salt Tris (HSTris) buffer (0.1 M Tris, 0.5 M NaCl, pH 7.8). Gradients were centrifuged at 32000 *x g* for 45 mins at 15°C. The 30% sucrose fractions were collected, pooled and dialysed overnight in HSTris buffer at 4°C. The dialysate was loaded onto iodixanol step gradients consisting of the following steps: 50% (1mL), 39% (2mL), 33% (5mL) and 27% (5mL). Gradients were centrifuged at 32000 *x g* for 3.5 hours at 15°C (Chabeda et al., 2019). Fractions (1.5 mL each) were collected from the bottom of the gradients. Fractions 2 – 8 (39%-33% iodixanol) were pooled and dialysed as described above.

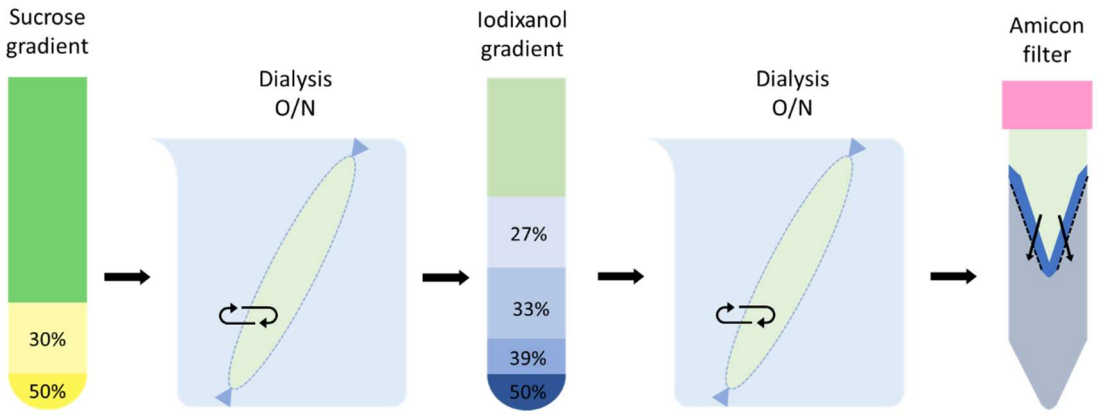

Figure 2.3. Schematic of VLP purification process. Stepwise purification methods

2.2.4 Concentration of purified VLPs

The dialysed samples were loaded onto 5 mL 100K Amicon Millipore filters (Figure 2.3). The samples were centrifuged at 4000 xg at 4°C at 10 min intervals which was repeated until the sample volume was reduced to ~1.5 mL, and subsequently stored at -80°C in siliconized microcentrifuge tubes.

2.2.5 SDS-PAGE of purified VLPs

The protein samples were denatured by heating to 95°C with the addition of 1X sample application buffer (0,001% (w/v) bromothymol blue, 0.5M EDTA, 5% (w/v) SDS, 25% (v/v) glycerol) for 10 minutes (Maniatis et al., 1982, Sambrook et al., 1989). Proteins were resolved on 10% SDS-PAGE gels run at 180 V. The Colour Protein Standard, Broad Range (11-2545 kDa, New England Biolabs) was used as molecular weight marker for all SDS-PAGE gels in this study. Gels were subsequently stained using a silver staining kit (SIGMA) as per the kit's protocol. The gels were fixed in 100 mL fixing solution (50% ethanol, 10% acetic acid) over night to ensure better resolution and lower background.

2.2.6 Western- and dot blot analysis of purified VLPs

SDS-PAGE gels were transferred onto nitrocellulose membranes in transfer buffer (25 mM Tris, 190 mM glycine, 20% methanol, pH ~9.2) at 15 V for 90 mins using a Bio-rad semi-dry transblotter. Non-denatured samples (2 µL) were dotted on the nitrocellulose membrane and allowed to dry. Membranes were blocked in blocking buffer (1x PBS; 5% long life fat-free milk,

1% Tween-20) at room temperature for 30 mins with agitation. To probe for HPV16 L1, CamVir (Abcam, UK) mouse antiserum diluted in blocking buffer (1:5000) was applied to the membranes and incubated at 4 °C overnight with agitation. For detection of RuBisCO, anti-RuBisCO raised in rabbits was used. Anti-2C7 antiserum diluted in blocking buffer (1:500 dilution) was used to probe the dot blots. All blots were washed 4 x 5 minutes in blocking buffer at 37 °C. After washing blots were probed with secondary antibodies goat anti-mouse and goat anti-rabbit IgG alkaline phosphatase-conjugated secondary antibody (Sigma-Aldrich®) diluted in blocking buffer (1:10000) and incubated for 1 hour at 37°C with agitation. Finally, the membranes were washed 4 x 5 minutes with PBST (1x PBS; 1% Tween20) at 37°C with shaking, before proteins were detected by incubating the membranes with 5-bromo-4-chloro-3-indoxyl-phosphate (BCIP) and nitroblue tetrazolium (NBT) phosphatase substrate (BCIP/NBT 1-component) (Whitehead Scientific) for 30 mins.

2.2.7 Structural analysis of VLPs

The VLPs were visualized using transmission electron microscopy (TEM). Aliquots of the purified vaccine antigens were thawed at 4 ºC and resuspended in 1x PBS pH 7.4 at a concentration of 1:50. Copper carbon-coated grids were made hydrophilic, and glow discharged at 25mA for 30 s using a Model 900 SmartSet Cold Stage Controller (Electron Microscopy Sciences). The carbon side of the grids were suspended on a 20 µl drop of sample for 5 mins. The grids were then washed 3x with filter sterilized water. The samples were then negatively stained with 2% w/v uranyl acetate for 1 min and allowed to airdry. The samples were viewed using a FEI Tecnai 20 electron microscope.

2.3 Results

2.3.1 Optimization of expression in plants

Time-trials conducted in previous work done in the BRU showed that best HPV VLPs were obtained 5 days post infiltration. In this study, plants infiltrated with the chimera developed necrotic symptoms by 5 days post infiltration (Figure 2.4A). In contrast plants infiltrated with HPV16 were less necrotic (Figure 2.4B). Negative control plants infiltrated with the empty vector were only mildly necrotic (Figure 2.4C).

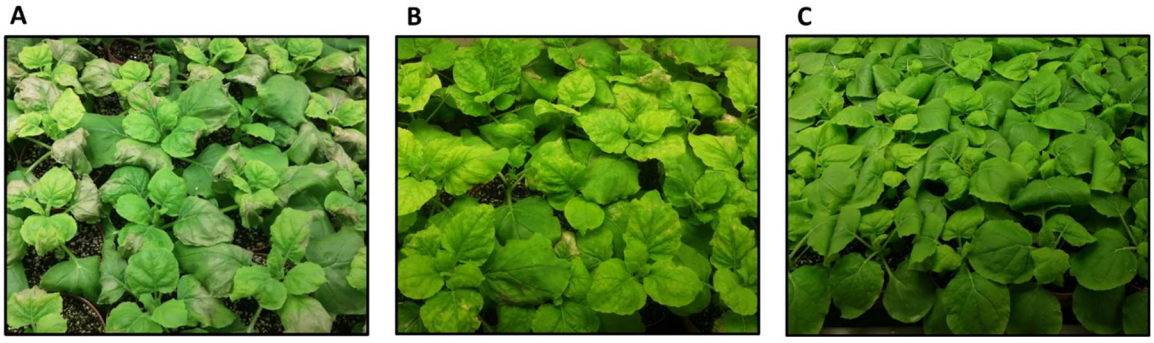

Figure 2.4. Images of Agroinfiltrated *N. benthamiana* 5 days post infiltration. A) *N. benthamiana* agroinfiltrated with pTRAC-CTP-DE_i (chimera) at OD_{600} 0.75 and NSs at OD_{600} 0.25. **B)** *N. benthamiana* agroinfiltrated with pTRAC-ctp-HPV16L1 at OD_{600} 0.5. **C)** *N. benthamiana* agroinfiltrated with pTRAC-CTP at OD_{600} 0.5.

2.3.2 Detection of L1 in protein samples

Western blots were carried out on the purified and concentrated samples to detect L1, using the CamVir antibody (Figure 2.5A). The membranes were also probed with anti- RuBisCO to detect the presence of RuBisCO (Figure 2.5B). Blots probed with CamVir showed distinct bands at the expected sizes of ~58 kDa for the chimera and ~56 kDa in the HPV16 sample. There were very faint bands detected in the lane containing the empty vector negative control which may indicate nonspecific binding of this antibody to various plant proteins. Lanes containing HPV16 L1 and chimera appeared to be smeared which suggests that the protein was not fully denatured, and some may have been trapped in the wells. Blots probed with anti- RuBisCO showed the presence of bands at ~55 kDa in all the samples analyses, indicating the presence of RuBisCO in all purified samples, particularly in the purified empty vector sample. An additional band at ~70 kDa was detected in all samples which may indicate the association of a small RuBisCO subunit (~14 kDa) with the larger subunit (Andersson and Backlund, 2008).

The dot blot of the chimera was clearly stained and resembled the positive controls that were detected using the 2C7 specific antibody shown by Figure 2.5C. This indicated that the 2C7 epitope was present and was being displayed in the correct conformation. These positive controls, octameric 2C7 peptide as well as LOS were also detected by the 2C7 antibody. There was no detection of the 2C7 epitope in the samples containing HPV16 L1 protein and the empty vector as these represented the negative controls.

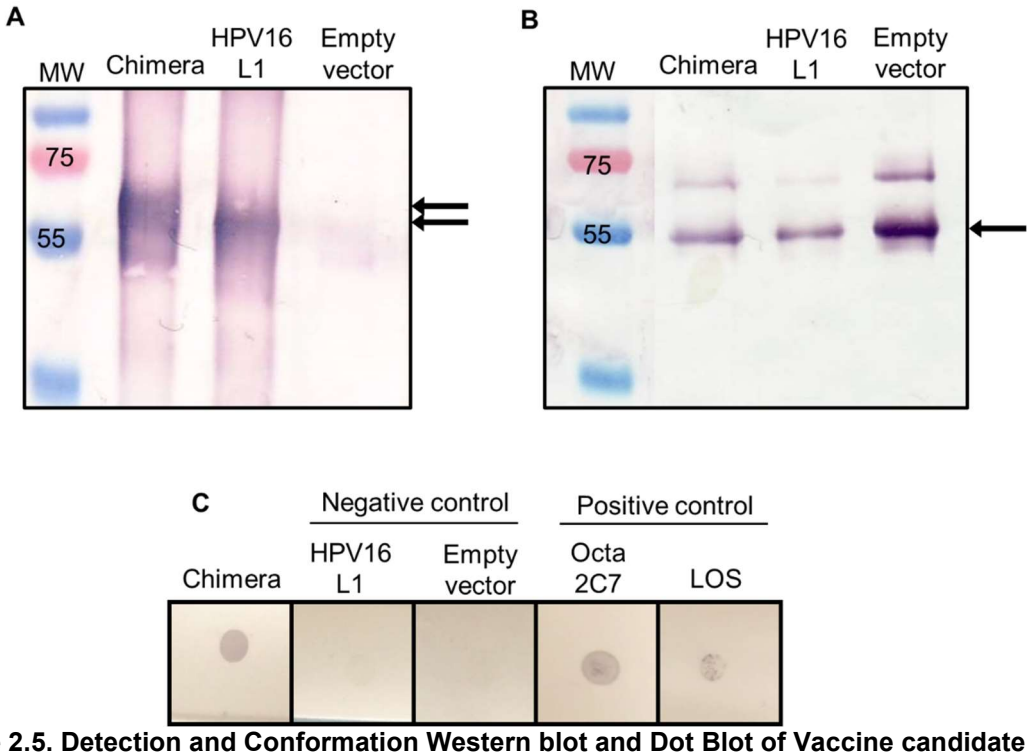

Figure 2.5. Detection and Conformation Western blot and Dot Blot of Vaccine candidate (DE_i). Equal volumes of sample were loaded in each lane. HPV16 L1 was used as a positive control. The empty vector was used as a negative control. **A)** The western blot probed with MAbs CamVir1 (1:5000). Bands representing the chimera and the HPV 16 are indicated by the black arrows. **B)** The western blot probed with anti- RuBisCO (1:1000). The bands representing RuBisCO are indicated by the black arrow. MW is protein marker with the size of the protein in kDa on the relevant bands. Each lane is labelled with the sample. **C)** Non-denatured samples were probed with anti 2C7 antibody (1:500) followed by detection with goat anti-mouse (1:10000). Each sample is labelled. Negative controls: HPV16 L1 and empty vector. Positive controls: Octa 2C7 peptide and LOS.

2.3.3 Silver stain analysis of purified vaccine candidates

Purified samples were analyzed on silver stained SDS-PAGE gels. Figure 2.6 showed four distinct band sizes. The lane containing the chimera sample showed 2 distinct bands, the first is at ~58 kDa which represents the chimera protein. The second band is ~54 kDa which represents RuBisCO. This RuBisCO band was observed in all the samples and is a comparative

thickness to the protein of interest. The HPV16 L1 sample shows a band ~56 kDa which corresponds to the expected size for HPV16 L1. The negative control also shows a band slightly higher than the band in the chimera sample at ~70 kDa which may indicate a nonspecific plant protein. Approximately half of the protein contained in the samples is the protein of interest (Figure 2.5). Quantification of the samples was done using gel densitometry using SYNGENE to determine the protein concentration of the specific proteins compared to a BSA standard curve. The yield of expression of HPV16 L1 was 400 µg/kg of biomass and of the chimera was 480 µg/kg of biomass.

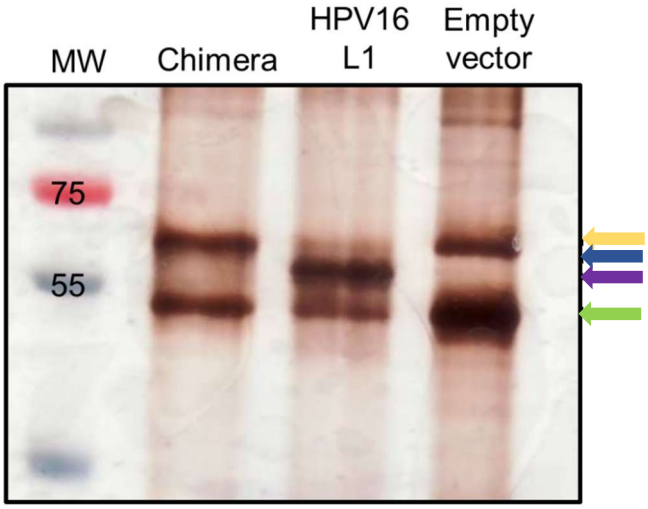

Figure 2.6. Analysis of purity of vaccine candidates using silver stained SDS-PAGE gels. The bands indicated by the arrows are Labels: Blue arrow: Chimeric L1 (~58 kDa) Purple arrow: HPV L1 (~56 kDa), yellow arrow: Host cell protein (~7 0 kDa), and green arrow: RuBisCo (~54 kDa) MW – Molecular weight marker (kDa), Chimera – Chimeric VLPs, HPV16 L1 – HPV16 L1 VLPs, Empty vector – pTRACTP plasmid vector.

2.3.4 Structural analysis of purified vaccine antigens

The concentrated purified VLPs were negatively stained and visualised using TEM. These results show the formation of VLPs in both the chimeric and the HPV16 L1 samples. The chimeric VLPs are indicated by blue arrows in Figure 2.7A. These particles were of the appropriate size (~55 nm). The HPV16 L1 particles shown in Figure 2.7B were of the correct size (~55 nm) and are indicated by the orange arrows. There are also various aggregates and mishaped particles (red arrows Figure 2.7), and capsomeres present in both of these samples. There were no particles visible in the sample purified from plants infiltrated with the empty

expression vector (Figure 2.7C). However, there was significant background, this could be various plant proteins present in all the samples that indicated impurities in the sample.

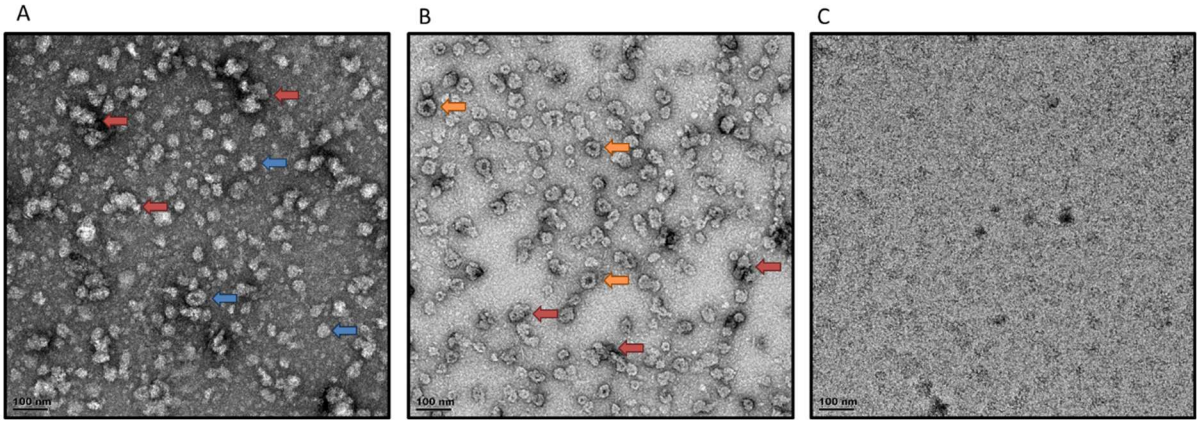

Figure 2.7. TEM for structural analysis of purified and concentrated samples. The samples were negatively stained using uranyl acetate and the particles visualised under TEM. The red arrows indicate examples of misshaped or aggregated particles A) Chimeric VLP sample. Blue arrows indicate examples of Chimeric VLPs (~55 nm); B) HPV 16 L1 VLPs. Orange arrows indicate examples of HPV16 L1 VLPs of the appropriate size (~55 nm); C) Empty vector sample.

2.4 Discussion

The aim of this section was to express and purify chimeric HPV VLPs which could be used as a vaccine candidate as well as HPV16 L1 VLPs to be used as a positive control. The viral proteins were successfully expressed in *N. benthamiana.* The insertion of the 2C7 epitope into the surface loop of HPV16 did not seem to significantly affect the overall expression or the formation of particles.

The commercially available vaccines make use of yeast and insect production systems, respectively. However, these systems have reassembly steps that occur post purification and are very costly. Overall, the yields achieved for both the chimera and for HPV16 L1 are very low compared to yields achieved by other expression and purification systems (Fischer et al., 2004, Chatterjee, 2014). While plant production systems provide all the post translational eukaryotic mechanisms, they can result in low protein yields which may be due to low expression or to instability of the recombinant protein (Fischer et al., 2004, Obembe et al., 2011). The initial expression of the proteins was low, and further losses were incurred in each purification step. Further optimization is required of the plant production system to increase the yields.

Production of particles in the chloroplasts means that they are heavily exposed to RuBisCO throughout translation. Due to the pI values of HPV16 (~7.95) and RuBisCO (~4.4) at neutral pH, they carry opposite charges of positive and negative respectively, causing these proteins to bind electrostatically (Udenigwe et al., 2017, Mistry et al., 2008). The association of these proteins makes them difficult to separate. The samples were analysed in the form of western blots, silver stained SDS-PAGE gels and dot blots in order to determine purity. These results showed that RuBisCO was present in all the samples as there were clear and definite RuBisCO bands that were of similar intensity in both the chimera as well as HPV16 samples. The purity of the vaccine candidates was ~50% and this level of purity does not compare to that of commercially produced HPV vaccines (Harden and Munger, 2017).

Attempts were made to increase the purity of vaccine candidates. Extraction buffers with a wide range of pH values were trialed to disrupt charged-based interaction between the two proteins. The pH of the extraction buffer was lowered to the pI value of RuBisCO (pI of 4.4 – 4.7) to disrupt the electrostatic charges (Udenigwe et al., 2017). While the purity of the sample did slightly improve, there were great losses of the chimera using these extraction buffers. Another purification strategy that was considered was ammonium sulfate precipitation (Zahin et al., 2016). The precipitation concentration of ammonium sulfate for the chimera and for RuBisCO are significantly different. However, once the precipitate was redissolved in buffer the particles did not reassemble which is the same result achieved by Zahin et al. RuBisCO is highly abundant, ~25% of the total proteins in a plant are RuBisCO; it is the most abundant protein on earth and therefore it is difficult to remove (Barbeau and Kinsella, 1988, Andersson and Backlund, 2008).

When viewed under TEM it can be seen that there was formation of VLPs of the correct size (Maclean et al., 2007). However, it seems that there are also capsomeres and misshapen nonuniform particles present in samples (Figure 2.7). This may indicate that the samples were not stable or that self-assembly was not totally efficient. The samples undergo several centrifugal purification steps with the final step involving the Amicon filters. These methods expose the particles to a great amount of force which may be disruptive to the particles, causing them to break apart and refold in a misshapen manner.

The current purification method (density gradients) is not scalable for industrial production of these proteins (Zahin et al., 2016) and this method is also unable to fully purify the proteins (Figure 2.6). Therefore, further work should be done to explore different purification methods to not only improve the yield but to ensure that the results are scalable. This would preserve the

particles and increase yields obtained by the plant production system. A yield of 1% of total soluble protein (TSP) is considered to be the threshold for commercial production (Fischer et al., 2004).

In future, it may be worth exploring the production of these chimeric VLPs in other systems that could result in not only higher yields but also in more uniform assembly of the particles such as callus or another kind of production system i.e. yeast or insect cell culture (Harden and Munger, 2017).

In conclusion, chimeric HPV VLPs were successfully expressed and purified from *N. benthamiana.* These particles displayed the *Ng* 2C7 mimitope in the correct conformation that can be detected by the mAb 2C7. When viewed under TEM it was evident that VLPs have self-assembled into particles of the correct size. For this reason, the chimeric and HPV16 VLPs were used for further immunological studies in an animal model described in Chapter 4.

Chapter 3: Comparison of reporter genes and expression systems in the production of HPV16 L1/L2 PsVs.

3.1 Introduction

3.1.1 Infection mechanism of HPV

Infection of host keratinocytes by HPV is initiated by contact and attachment of the virus to the basement membrane after micro trauma. L1 facilitates attachment of the virions to heparan sulphate proteoglycans (HSPGs) in the extracellular membrane on the cell surface. (Horvath et al., 2010). Conformational changes in the virion that result from intricate interactions which occur between the virus and the basement membrane are essential for viral infection (Kines et al., 2009). These conformational changes result in exposure of L2 epitopes for cleavage by both furin and proprotein convertase (PC) 5/6 which enables binding of the virion to receptors on the basal epithelial cells (Kines et al., 2009). HPV internalization involves intricate interactions between the virus and host cell receptors which is mediated by L1 and L2 (Raff et al., 2013). While cell surface interactions are predominantly mediated by L1, it has been suggested that L2 may interact with specific cell surface receptors to facilitate endocytosis of the virus (Horvath et al., 2010, Roden et al., 2001, Kawana et al., 2001). Upon viral entry into host epithelial cells, an episome surrounds the HPV genome and elicits the host cell machinery for the synthesis of viral DNA (Moody and Laimins, 2010).

3.1.2 PsV assembly and encapsidation

While the presence of L2 is not required for the formation of PsVs intracellularly, it does enhance encapsidation of the plasmid DNA within the particle (Zhao et al., 1998, Roden et al., 2001). L2 has various functions that make it essential for the production of effective HPV PsVs (Sapp and Bienkowska-Haba, 2009). These functions include the role of endosome escape (Richards et al., 2006), and delivery of DNA to the nucleus of the host cells (Florin et al., 2006, Kondo et al., 2009). Thus, L2 is required for efficient self-assembly of functional PsVs.(Buck et al., 2008).

PsVs have been used not only to investigate the papillomavirus life cycle and mechanism of viral internalization pathways (Conway and Meyers, 2009, Ma et al., 2011, Carse et al., 2021), but as a tool for HPV screening by analysing reactivity of human sera (Xu et al., 2006). In addition, HPV PsVs are extremely useful in the development of prophylactic vaccines in

determining neutralizing antibody titre levels (Pastrana et al., 2004, Buck et al., 2005) and have been developed as an *in vivo* challenge model in vaccination studies.

3.1.3 Reporter genes

In the past, radioactive assays were predominately used as reporters of gene expression (Broniarczyk et al., 2019). However, fluorescent and luminescent reporter genes offer a less time-consuming option that do not require the use of radio chemicals and are now widely used. There are several considerations when deciding on luminescent or fluorescent reporter genes, these include: stability of reporter gene, co-factor availability, wavelength, intensity of signal, and whether the signal is secreted or not. All of these factors should be taken into account when selecting a reporter gene for a specific application (Neefjes et al., 2021).

3.1.4 Fluorescent reporter gene assays

Protein products of fluorescent reporter genes produce a bright visible light, and can be visualised using fluorescent microscopy. Advantages of employing fluorescent proteins is the lack of substrates or reagents required (Hakkila et al., 2002) as well as the ability to detect the signal in un-lysed cells (Billinton and Knight, 2001). Common applications of fluorescent reporter genes include, visual imaging, spatio-temporal imaging and *in vivo* experimentation (Bianchi et al., 2015).

3.1.5 Luciferase reporter genes assays

Luciferases are enzymes that bind to luciferin substrates and oxidise them resulting in the release of photons of light (Greer and Szalay, 2002, Gates and DeLuca, 1975). Due to the nature of the reaction, co-factors such as ATP and metal ions are required in the facilitation of the reaction (Neefjes et al., 2021). Luciferases are expressed intracellularly and can be measured in cell lysates or *in vivo,* and some are also secreted from the cells.

Firefly luciferase (FLuc) is the most commonly used luciferase which makes use of D-luciferin as a substrate and requires ATP, Mg^{2+} and O_2 as cofactors of the reaction (Gould and Subramani, 1988). The specific cofactors required for the reaction are derived from metabolic pathways of the cell and therefore the signal produced is dependent on the metabolic state of the cell and availability of energy (Hakkila et al., 2002). To overcome this energy dependency, ATP-independent luciferases can be used including Gaussia luciferase (GLuc) and Nano

luciferase (NLuc) (England et al., 2016). FLuc is retained within the cells and is therefore very useful for locational imaging.

Once expressed within cells, GLuc is secreted enabling the use of media culture for analysis. Secretion of the reporter is particularly useful for real-time monitoring, and high throughput experimentation (Hiramatsu et al., 2005). However, composition of complex bodily fluids may have an effect on the effectivity of the luciferase assay.

3.1.6 Expression systems for the production of HPV PsVs

Production of PsVs in mammalian cell culture is widely used and is currently considered the gold standard (Buck et al., 2005, Adams et al., 2023). When compared to the previously used Semliki Forest virus-derived vector method, particle production efficiency was increased 10 million-fold (Buck et al., 2005). While this method produces excellent quality particles, it can be expensive due to the high cost of reagents and cell culture. Production of recombinant proteins in plants (*N. benthamiana)* provides a cheaper more scalable alternative with a lower risk of contamination with mammalian pathogens and endotoxins (Rybicki, 2010, Faye et al., 2005). Plants also carry the ability to perform post-translational modifications that are similar to humans, and important for the infectivity of HPV16 (Margolin et al., 2018, Broniarczyk et al., 2019).

Production of functional HPV16 PsVs in *N. benthamiana* using *Agrobacterium*-mediated expression has been reported (Lamprecht et al., 2016, Adams et al., 2023). These PsVs functioned similarly to the HEK293TT produced HPV PsVs however they were not tested in an animal model. Following similar strategies to the ones laid out by Lamprecht and co-workers, this study aimed to not only produce PsVs containing the luciferase gene but to directly compare the plant produced PsVs to the mammalian derived PsVs, and to further test the infectivity of plant produced HPV PsVs. At the same time FLuc was compared to a secreted Gluc luciferase to determine which luciferase provided the highest and most reliable readings for the HPV16 challenge model.

3.2 Methods

3.2.1 Mammalian cell production of HPV PsVs (mPsVs)

3.2.2 Cell maintenance

All cell lines were grown and maintained at 37°C in a 5% CO_2 humidified air incubation. Both HEK-293TT transfection cell line and HeLa cell line were grown and maintained in Dulbecco modified Eagle medium (DMEM, Life Technologies) supplemented with 10% heat-inactivated foetal calf serum (FCS) (Gibco), 100 U/mL penicillin (Pen) and 100 µg/mL streptomycin (Strep).

3.2.3 Transfection of HEK293TT cells for production of mPsVs

HEK293TT cells were plated out in DMEM (+10% FCS and Pen/Strep) and grown on a 10 X T175 flasks to 70% confluency. The expression vectors used were: pXULL containing the L1/L2 and reporter gene expression plasmids pGL3 containing FLuc gene (Promega) and pCMV vector containing the GLuc gene (New England Biolabs, Ipswich, MA, USA). The cells were transfected using the calcium phosphate method (Jordan et al., 1998). The reaction mixture (5 µg pXULL plasmid DNA, 12 µg reporter plasmid DNA in TE buffer and 25 µL $CaCl_2$ (2.5 M)) was added to HBS (isotonic saline buffered with HEPES) to a final volume of 200µl in an Eppendorf tube and incubated for 30 mins at room temperature before addition to the cells.

After 48 h the supernatants containing floating cells were collected. The cells were pelleted by centrifuging at 3000 xg for 5 mins. Adherent cells were lifted by trypsinization, then pelleted by centrifugation as above and washed in 5 mL PBS. The cells were centrifuged again, and the pellet resuspended in 1 mL PBS (pH 7.4). The cell suspension was transferred to a round-bottom siliconized tube. The cells were pelleted by centrifuging at 3000 xg for 3 mins and the supernatant was removed. The pellet was resuspended in an equal amount of cell lysis buffer (1x PBS, 9.5mM $MgCl_2$; 0.35% Brij 2 µl Benzonase and 2 µl Exonuclease V, pH 7.4).

3.2.4 Maturation of PsVs

Maturation of putative PsVs results in more uniform and stable particles. The lysed cell suspension was incubated at 37°C with gentle shaking for 24 h. The lysate was chilled on ice for 5 mins followed by the addition 0.17 volumes of PBS containing 5 M NaCl. The high salt concentration aids in stabilization of the PsVs (Buck et al., 2005). The suspensions were

incubated on ice for 10 mins and then freeze/thawed at -80°C to RT (Room Temperature) three times. Matured lysates containing PsVs were stored at -80°C until purification.

3.2.5 Purification and concentration of PsVs

Cell debris was removed from the lysates by centrifuging at 8000 xg for 10 mins at 4°C after which the supernatants were collected. PsVs were purified using ultracentrifugation on 2-step discontinuous CsCl gradients consisting of: 4 mL light CsCl (0.27 g/mL) underlayed with 4 mL of heavy CsCl (0.39 g/mL) dissolved in HSB. The gradients were centrifuged for 16 h at 20 000 xg at 4ºC. The opaque band containing PsVs at the heavy/light interface was collected by insertion of a needle into the tube. The bottom section of the tube was also collected by insertion of a needle and collection of ~500 µL.

To facilitate removal of CsCl and to concentrate the PsVs. samples were loaded onto Amicon Ultra-4 filter devices (100 kDa MWCO) and centrifuged at 3000 xg for 10 mins. HBS (2 mL) was added to the filter devices and the samples centrifuged again to enable complete removal of CsCl. The samples were concentrated to a final volume ~100 µL. Concentrated PsVs were stored in low-binding siliconised tubes at -80ºC. PsV concentration was determined relative to a BSA standard curve using a Bradford assay as per Chapter 2.2.3 according to the manufacturer's instructions.

3.2.6 Plant-based production of HPV PsVs (pPsVs)

3.2.7 Infiltration and Expression of PsVs

Plants were co-infiltrated with the construct listed in Table 3.1 as described in Chapter 2.2.2. The cell densities (OD_{600}) used for each construct are shown in Table 3.1. Infiltrated plants were harvested at 4 dpi.

Table 3.1: The various plasmid constructs and the ODs at which they were infiltrated.

Construct	**Plasmid vector**	**OD_{600}**
HPV16 L1	pTRAkc-rbsc1-cTP	0.25
HPV16 L2	pTRAkc-rbsc1-cTP	0.05
FLuc	pRIC3	0.5

3.2.8 Purification

After harvesting the leaves purification of the pPsVs was carried out in the same manner as the method described in Chapter 2.2.3 and 2.2.4. Pooled iodixanol fractions containing PsVs were loaded onto Amicon Ultra-4 filter devices (100 kDa MWCO) to facilitate removal of iodixanol and to concentrate the PsVs. The samples were centrifuged at 3000 xg for 10 mins. HBS (2 mL) was added to the filter devices and the samples centrifuged again to enable complete removal of iodixanol. The samples were concentrated to a final volume of ~ 2 mL.

3.2.9 Western blotting and silver staining

In order to ensure the presence of L1 and L2 protein in the purified mPsVs and pPsVs samples, they were prepared and analysed on western blots and silver stained SDS-PAGE as described in Chapter 2.2.6.

3.2.10 TEM visualisation of PsVs

In order to confirm the formation of whole PsVs, the purified mPsV and pPsV samples were diluted 1:20 with HSB, and were negatively stained with 2% uranyl acetate and subsequently viewed as described in Chapter 2.2.7.

3.2.11 Rolling circle amplification of encapsidated DNA

Rolling circle amplification (RCA) of purified PsVs was performed as per the illustra™ Templiphi 100 Amplification Kit (GE Healthcare) instructions. PsVs were initially digested using 1 µl of proteinase K for 3 h at 55°C. The proteinase K was subsequently inactivated by heating samples to 95°C for 10 mins. One µL of sample was added to 5 µL of sample buffer. The samples were again denatured for 3 mins at 95°C and cooled to 4°C. A master mix was prepared containing 5 µL reaction buffer and 0.2 µL enzyme mix per reaction and 5 µL of the master mix was added to each sample. Amplification was carried out for 18 h at 30°C, after which the samples were heated to 65°C for 10 mins to stop the reaction. RCA reactions were subsequently linearised with *Hind*III restriction enzyme for 1 h at 37°C. The digested samples were analysed on 1% agarose gels stained with ethidium bromide.

3.2.12 Quantification of encapsidated DNA by qPCR.

3.2.12.1 Sample preparation

Two different sample preparation methods were used in order to determine the amount of total DNA that has been encapsidated. Both methods use the same amount of L1 protein (20 µL). The first method simply involves the samples being heated to 95°C for 10 mins in order to denature the particles. The second method involves the use of the QIAamp® Viral RNA/DNA extraction kit (Qiagen). The DNA was extracted as per kit instructions and the DNA was stored at -20°C before it was sent for qPCR by Inqaba Biotech (South Africa).

3.2.12.2 Quantification of plasmid DNA by qPCR

Primers were designed to amplify the FLuc reporter gene in the pGL3 control vector and are shown in Table 3.2.

Table 3.2: Forward and reverse primers for amplification of the FLuc reporter gene in qPCR.

Direction	Sequence
Forward	ACCAGGGATTTCAGTCGATGTAC
Reverse	TGCAATTGTCTTGTCCCTATCGA

A standard curve ranging from 1 ng to 1 fg of the pGL3 control plasmid was generated. qPCR was carried out in 96 well plates with Luna Universal qPCR Master Mix (New England Biolabs, Ipswich, MA, USA) using a dye-based qPCR assay. Each reaction contained 1 µl of DNA template, 0.25 µm forward and reverse primers and 1X Luna Universal qPCR Master mix. The reactions were carried out in a CFX96 Real-Time PCR System (Bio-Rad) following a standard two-step PCR program as suggested by the Luna Universal qPCR Master Mix manual. Three technical replicates were run for each DNA sample. Amplification of different input templates were evaluated based on quantification cycle (Cq) value.

3.2.13 *In vitro* infectivity testing of particles

The infectivity of the particles was tested *in vitro*. HeLa cells were seeded in a 48 well plate at a density of 1×10^5 cells per well and grown overnight. In order to neutralise the PsVs, they were

incubated in the presence of Gardasil antibody for 30 mins at room temperature. HPV16 PsVs neutralised or not were added to the cells at a final viral density of approximately 0.5 µg/cell for 48 h at 37°C. Media was collected or aspirated from the cells, after which they were lysed with cell lysis buffer and mechanically broken up by scraping of the cells. Thirty microliters of the media or lysates were transferred to a 96 well plate and the luciferase activity was measured using the Gaussia Luciferase Assay Kit (Sigma-Alrich) or Pierce™ Firefly Luciferase Glow Assay Kit (Thermo Fisher Scientific) respectively according to the manufacturer's instructions. Plates were read with the GloMax® Microplate Reader (Promega) at 470 nm. Raw luciferase data were normalised against the uninfected cells-only wells. The experiments were performed in triplicate.

3.2.14 Animal Experiments

Approval for this study was obtained from the Animal Research Ethics Committee at the Faculty of Health Sciences at the University of Cape Town (UCT, AEC 021-023). Female BALB/c mice were bred at the UCT Animal Research Unit. The animals were housed and cared for in the Biosafety Level II (BSL-2) Animal Research Unit. The experiments conducted using the *In Vivo* Imaging System (IVIS®) machine (PerkinElmer) were carried out by Alisha Chetty and Claire Butters.

Six-week-old mice were randomly divided into 3 groups consisting of two experimental groups with 5 mice each and a control group with 3 mice. Mice were acclimatized for 1 week prior to initiation of the experiments. Four days prior to HPV PsV infection, mice were treated with 2 mg/20 g Depo-Provera (Pfizer) suspended in 200 µL PBS by sub-cutaneous injection to ensure equilibration of hormonal levels and to prolong dioestrus which facilitates infection of sexually transmitted diseases. Genital epithelial cells were chemically disrupted 6 h prior to HPV PsV infection, for this procedure mice were lightly anaesthetized via intra-peritoneal injection of 125 µL ketamine (1.5 mg/20 g) and xylazine (0.2 mg/20 g) and intravaginally received 25 µL of 4% Nonoxynol-9 (N-9) (abcam) in a formulation of 3% carboxymethylcellulose (CMC) (Roberts et al., 2007). For infection with HPV PsV, mice were lightly anaesthetized as described above and intravaginally inoculated with 5 µg of mammalian-produced HPV16 PsVs encapsidating either FLuc or GLuc reporter genes or 5 µg of plant produced PsVs (containing the FLuc reporter gene) in a total volume of 20 µL in the presence of 3% CMC.

Vaginal lavages were performed at 24 h, 48 h, and 72 h post infection with the Gluc-expressing virions by rinsing the genital tract with 2×50 µL sterile PBS. Cells and debris were removed by centrifugation at 3000 xg for 5 mins and the remaining supernatants were analysed for secreted Gaussia luciferase expression as a measure for infection using the Gaussia Luciferase Assay Kit (Sigma-Alrich) and the Glomax® microplate reader. Mice infected with PsVs encapsidating firefly luciferase (both mammalian and plant produced) were injected intravaginally with 50 µL firefly luciferase reagent and then immediately imaged using the IVIS® machine. The mice were euthanised 72 h post infection using halothane inhalation.

3.3 Results: Comparison of FLuc and GLuc reporter genes expression

The comparison of the different luciferase reporter genes was carried out to evaluate which reporter gene provides the highest and most reliable luciferase readings for the HPV16 challenge model.

3.3.1 Confirmation of HPV L1 and L2 protein expression

After purification and concentration of the mPsVs containing either the FLuc or GLuc reporter genes, the samples were analysed using silver stained SDS-PAGE gels. Expression of L1 was confirmed by the presence of bands of ~56 kDa and expression of L2 was confirmed by the presence of bands of ~84 kDa in both the GLuc and FLuc samples (Figure 3.1). The bands representing L2 were less intense when compared to the bands representing L1 which is to be expected as one L2 is incorporated with five L1 proteins and therefore is at a lower concentration in the samples. The sample containing the GLuc reporter gene appears to be more concentrated than the sample containing the FLuc reporter gene as these bands are more intense.

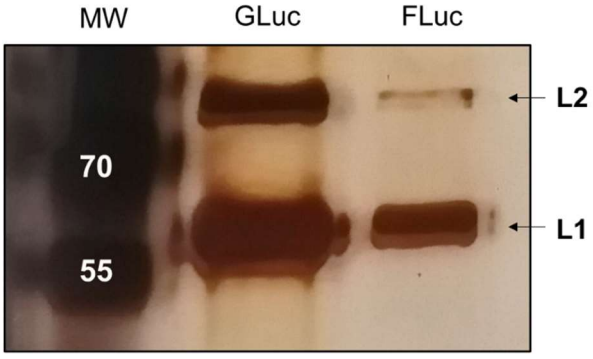

Figure 3.1: **Detection of L1 and L2 in purified PsVs on silver stained SDS-PAGE gels.** SDS-PAGE of the purified and concentrated PsV samples. The bands indicated by the arrows are HPV L1 (bottom) and HPV L2 (top) Labels: MW – Molecular weight marker (kDa), GLuc – Mammalian expressed HPV16 PsVs containing GLuc reporter gene, FLuc – Mammalian expressed HPV16 PsVs containing FLuc reporter gene.

3.3.2 *In vitro* infectivity of PsVs

After confirming the presence of L1 and L2 in the purified PsVs, their infectivity was tested *in vitro* using HeLa cells. All the PsVs tested successfully infected HeLa cells as evidenced by expression and detection of the reporter genes (Figure 3.2, orange bar). The cell lysates of samples cells infected with PsVs encapsidating FLuc showing a higher level of infectivity when compared to the cell supernatants from cells infected with PsVs encapsidating GLuc reporter gene (Figure 3.2) when compared to blank samples. PsVs encapsidating GLuc or FLuc were successfully neutralised in the presence of a Gardasil HPV 16 monoclonal antibody, as shown by the reduction of reporter gene expression in Figure 3.2 (grey bars). The infectivity of the FLuc particles and the GLuc particles was reduced ~13.1 fold and 2.3 fold respectively. These results indicate that neutralising epitopes were properly displayed on the surface of the PsVs.

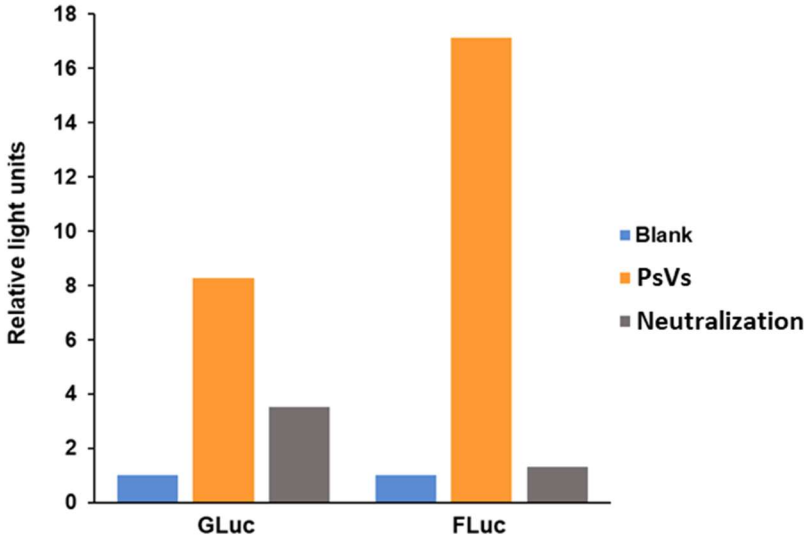

Figure 3.2: ***In vitro* infectivity and neutralization assay of mammalian-produced PsVs encapsidating GLuc or FLuc reporter plasmids.** The luciferase readings were taken from the cell supernatants from the GLuc reporter gene infected cells. The luciferase readings were measured from the cell lysates infected with the FLuc reported genes. The relative light units were measured after 48h post infection on the y-axis taken from the GloMax® Microplate Reader. The luciferase readings have been normalised to the blank.

3.3.3 *In vivo* infectivity of PsVs

Female BALB/c mice were infected with particles containing the 2 different luciferase reporter genes. These mice were randomly assigned to the groups. Each experimental group contained 5 mice and the control group contained 3 mice.

3.3.4 Infectivity of GLuc PsVs in a mouse model

To investigate infectivity of PsVs encapsidating GLuc, mice were infected with mPsVs containing this gene. One group of 5 mice was infected with PsVs containing the GLuc reporter gene. As GLuc is a secreted reporter protein, mice were vaginally lavaged every 24 h for 3 days to ensure that readings were taken at the time of most optimal expression. Figure 3.3 shows that 24 h post-infection no GLuc expression had occurred as the GLuc showed no difference between uninfected control mice and PsV- infected mice. Forty-eight hours post-infection, 4 of the 5 mice in the experimental group showed infection, with large variance between the readings. The most uniform infection was measured 72 h after infection, where 4 out of 5 mice showed successful luciferase expression. Luciferase expression readings were significantly higher in the PsV-infected mice compared to the control group. Across all 3 days none of the mice from the control group showed any infection and therefore no variation was noted in the fluorescent readings.

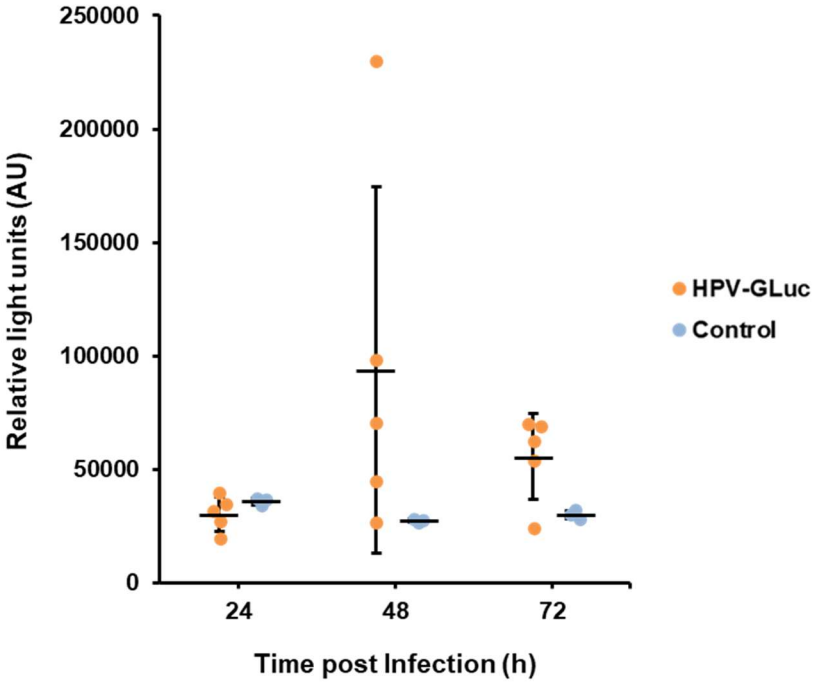

Figure 3.3: GLuc readings 24 h, 48 h and 72 h post infection. Dot plot of the individual mice plotted for each time point the readings given are in relative light units recorded by the IVIS. The experimental group (GLuc) is represented by the orange points and the control group is represented by the blue points. The black bar represents the average for each group. The error bars indicate the standard deviation for the group.

3.3.5 Infectivity of FLuc PsVs in a mouse model

To assess the infectivity of the PsVs encapsidating FLuc, mice were infected with the mPsVs encapsidating this gene. Due to the FLuc being retained within the cells of the vaginal canal the infection levels were determined by imaging the mice with the IVIS® machine. The mice were imaged every 24 h for 3 days to monitor the mice for optimal infection. The readings taken from the IVIS® machine are reported as average radiance (p/sec/cm^2/sr) which normalises for the area over which the fluorescent is measured. The initial readings taken after 24 h showed a signal in only one mouse Figure3.4(A). Forty-eight hours after infection it was observed that 3 out of 5 mice displayed expression of luciferase shown by the signal in Figure 3.4(B). The most uniform infection was measured after 72 h, where all 5 of the mice were infected, which is evident from the image in Figure 3.4(B). There was the least amount of variation between the mice after 72 h (Figure 3.4 (A)). Luciferase expression readings were significantly higher in the PsV-infected mice compared to the control group. Throughout the duration of the experiment none of the mice from the control group showed any infection.

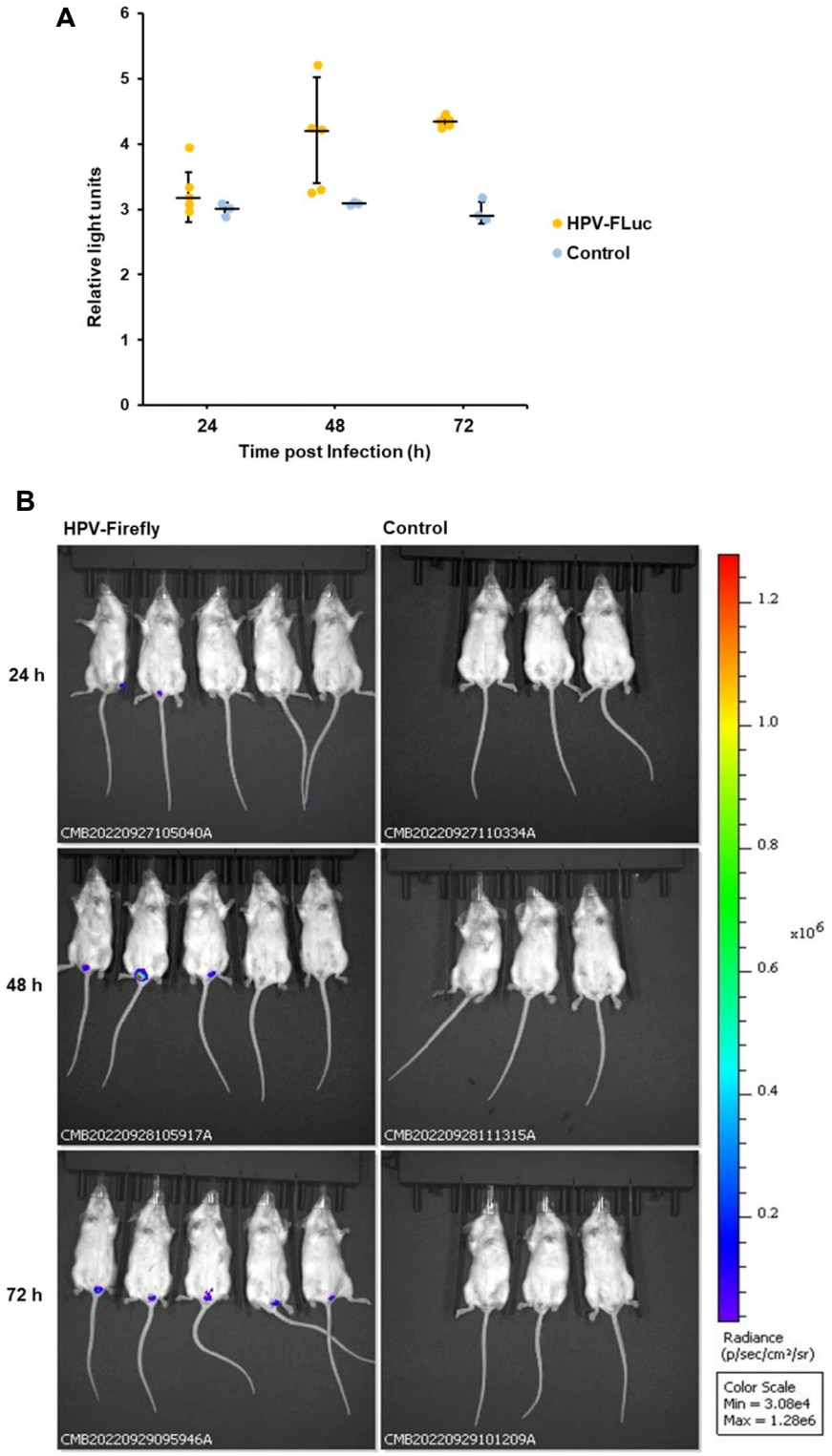

Figure 3.4: HPV16 PsVs encapsidating firefly luciferase reporter gene show infectivity. A) Dot plot of the average radiance recorded as relative light units of the individual mice plotted for each time point that readings were taken. **B)** Images of mice while in the IVIS® machine. The mice were placed in the same position for every reading.

The infectivity of the PsVs containing the FLuc gene was more uniform. All the mice showed gene expression at 96 h. The GLuc expression showed more variation in the signals.

3.4 Plant-produced PsVs vs Mammalian-produced PsVs

3.4.1 Expression of pPsV coat proteins

In order to detect whether L1 and L2 were present in the purified pPsVs samples, they were analysed on western blots by probing with anti-L1 or anti-L2 antibodies. Both the L1 and the L2 proteins were expressed and detected in the purified samples, indicated by bands at sizes ~56 kDa (purple arrow) and ~84 kDa (yellow arrow) respectively (Figure 3.5). The lane probed with L2 showed bands of different sizes which might be present due to non-specific binding of this antibody. The sample showed presence of RuBisCO which indicates that the sample was not pure (green arrow). Production of the pPsVs also resulted in co-purification of host cell proteins which produces higher background. This indicated that this sample was of lower purity when compared with the mPsVs.

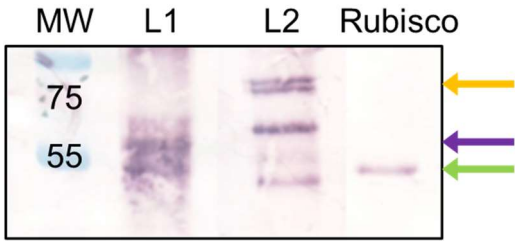

Figure 3.5: **Detection of pPsV coat proteins L1 and L2 by western Blot.** All lanes contain pPsV sample. Purple arrow: HPV L1 (~56 kDa), yellow arrow: HPV L2 (~84 kDa), and green arrow: RuBisCo (~54 kDa) Labels: MW – Molecular weight marker (kDa), L1 – probed with MAbs CamVir1 (1:5000), L2 – Probed with anti-L2 (1:2000) (from the lab ask inga), RuBisCO - probed with anti- RuBisCO (1:1000).

To determine if the expressed proteins self-assembled into particles, samples were analysed with TEM (Figure 3.6). Both the mPsV and pPsV samples appeared to contain secondary HPV structures, such as capsomere aggregates, small VLPs (~25 - 40 nm) or full-sized PsVs (~55 - 60 nm). TEM analysis showed that mammalian expressed HPV16 L1 and L2 assembled into uniform mPsVs that were approximately ~55 nm in diameter. In comparison, the plant expressed HPV16 L1 and L2 did not produce a homogenous pPsVs sample. The sample was a mixed heterogenous population of amorphous particles and protein aggregates.

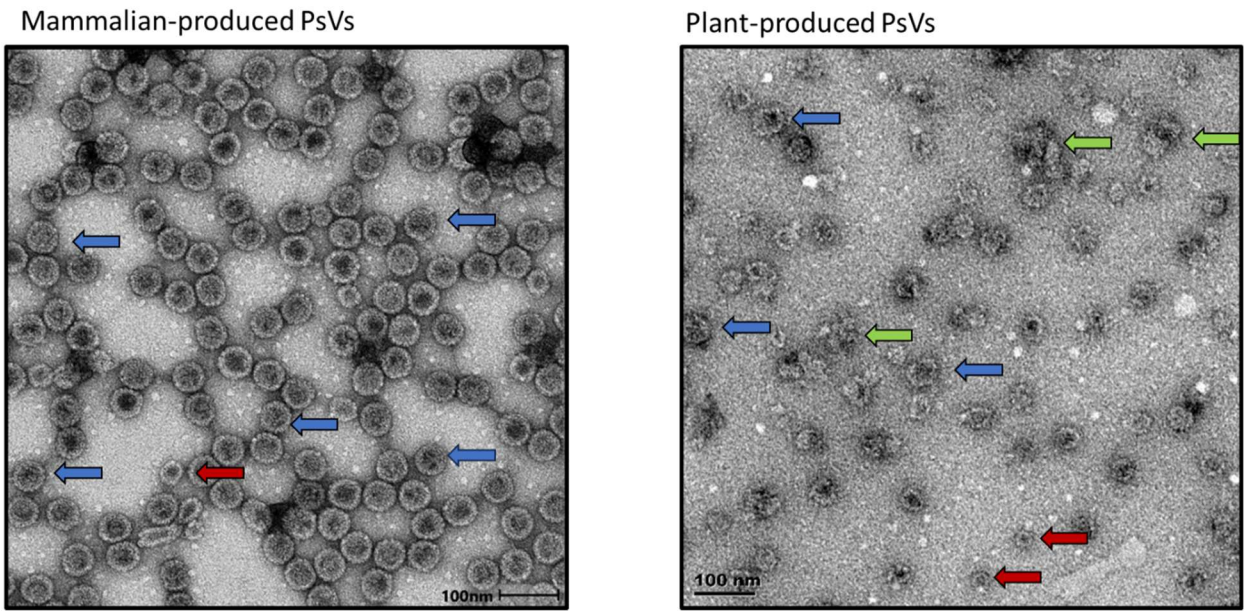

Figure 3.6: TEM analysis of purified and concentrated PsVs. The samples were negatively stained using uranyl acetate. A) Mammalian expressed mPsVs. B) Plant produced pPsVs. The blue arrows indicate full PsVs (~55 - 60 nm); red arrows indicate smaller VLPs (~20 - 40 nm); green arrows indicate capsomere aggregates or misshapen particles. Scale bar = 100nm. The VLPs were viewed using Zeiss 912 Omega Cryo EFTEM.

3.4.2 Quantification of reporter gene encapsidation

To determine whether the reporter gene plasmid was successfully encapsidated, PsVs were disassembled by digestion and boiling and subjected to RCA. After RCA and plasmid linearization with RE, encapsidation was confirmed by the presence of ~5100 bp amplified fragments observed in the lanes containing both pPsVs and mPsVs (Figure 3.7 (A)). The band observed after RCA of the mammalian-produced PsVs was more intense than the bands observed for the plant-produced PsVs, potentially indicating a higher concentration of DNA present in the mammalian-produced PsVs sample. A band of the expected size (2686 bp) was observed for the positive control, with no bands detected in the negative control lane.

After the presence of the reporter plasmids within the purified PsVs was confirmed, the amount of FLuc reporter gene present in each of the samples was assessed by qPCR. To standardise analysis of PsVs in qPCR assays, equal amounts of L1 protein was processed which enabled comparison of the amount of DNA associated with the PsVs between the mammalian- and plant-produced PsVs. The qPCR assays were carried out on DNA extracted from the particles, as well as DNA from heat denatured particles. When comparing the DNA that was extracted

from the particles with the unextracted DNA there was a significant difference for the mPsVs. The plant produced PsVs showed a 3.7-fold increase in the absolute copies found in the unextracted sample. Comparison of the extracted samples showed that the amount of plasmid in the mammalian sample was not significantly different from that of the plant. However, comparison of the unextracted samples shows that there was a significantly higher plasmid copy number for the plant sample.

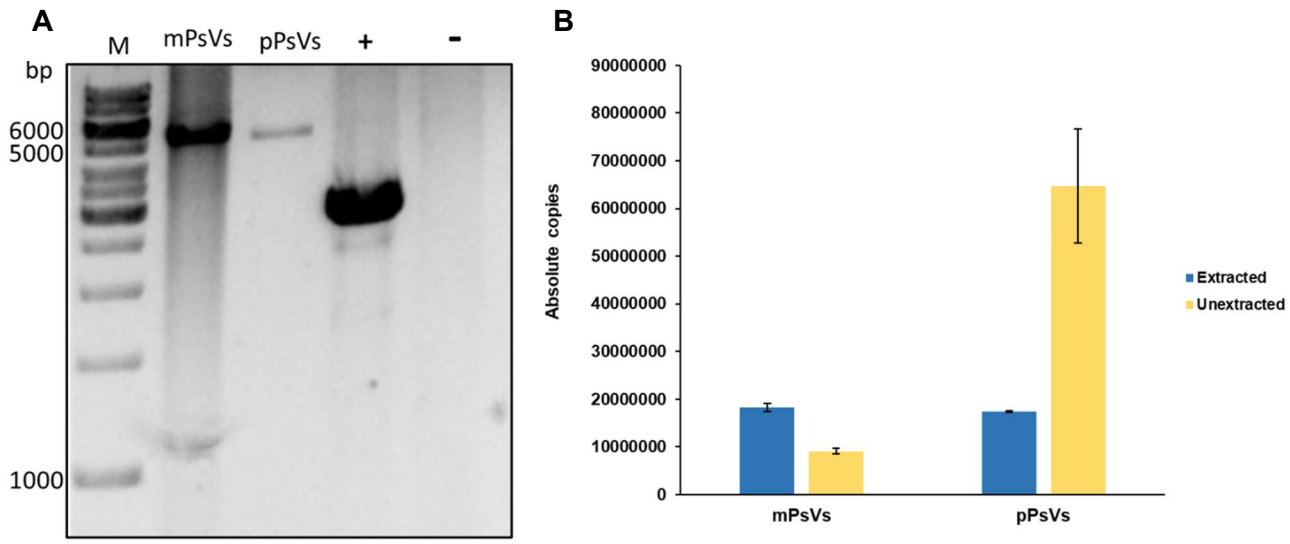

Figure 3.7: **Detection and quatification of plasmids with RCA and qPCR. (A)** Lanes M - DNA marker with size in kb indicated on the left, mPsVs - sample with mPsVs containing GLuc reporter gene, pPsVs - sample with pPsVs containing GLuc reporter gene (+) – positive control pUC 19 vector, (-) – negative control with no DNA added. **(B)** The graph represents the absolute copies of FLuc reporter gene plasmid in samples of equal L1 concentration. The blue bars indicate extracted sample, the yellow bars indicate the unextracted samples. The error bars give the standard deviation. The experiments were done in triplicate.

3.4.3 Infectivity of PsVs *in vitro*

To assess and compare the infectivity of the differently produced PsVs, HeLa cells were infected with both the mPsVs and the pPsVs. The results indicated that there was more effective infectivity of the mPsVs, when compared to the pPsVs (Figure 3.8). While cells were infected with the same amount of L1, the concentration of the pPsVs was lower and therefore, a significantly larger volume of pPsV sample was required to be added. The addition, high volumes of sample appeared to have a negative effect on the cells. In an attempt improve the infectivity, the pPsVs were incubated in the presence of furin, however no change was observed in the infectivity of the particles (data not shown).

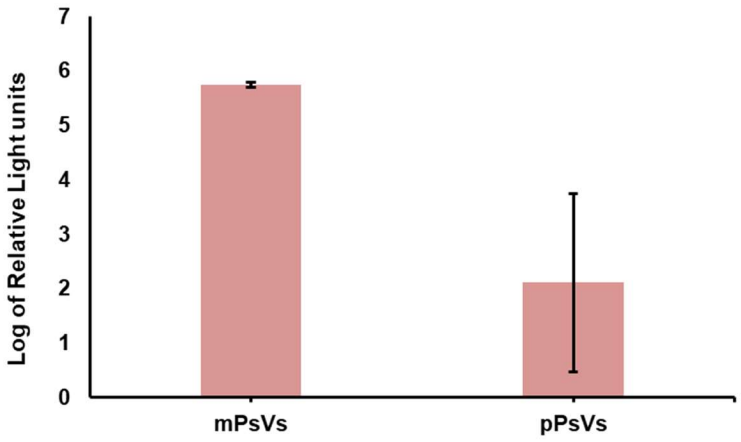

Figure 3.8: Infectivity of the PsVs incubated with HeLa cells after 48 h. FLuc reporter gene activity as a measure for infection was assessed in the HeLa cell lysates 48 h after addition of the virions to the cells. Log of the relative light units is plotted for both the mPsVs and the pPsVs. The error bars indicate the standard deviation.

3.4.4 Infectivity of pPsVs compared to mPsVs *in vivo*

Mammalian and plant-produced PsVs underwent comparative infectivity testing using the *in vivo* mouse model mentioned before. Infection was evaluated by measuring Fluc gene expression, indicative of HPV PsVs infection, through fluorescence readings obtained using the IVIS® system. The readings taken from the IVIS® machine are reported as average radiance (p/sec/cm^2/sr) which normalises for the area over which the fluorescence is measured. The results showed a notably higher infection level in mice exposed to mPsVs compared to pPsVs, evident in the considerably greater fluorescence readings at 48 h and 72 h post-infection in mPsVs-exposed mice when contrasted with the control group. There was little variation within the group infected with mPsVs as all 5 of the mice showed fluorescent signals after 72 h affirming their expression of the reporter gene (Figure 3.9). The pPsVs showed fluorescent signals in 4 out of the 5 mice after 72 h (Figure 3.9 (B)). However, the average of these responses was ~100 fold lower than the average radiance observed by the mPsVs (Figure 3.9 A). The control group exhibited no infection and there was minimal variation in average radiance readings.

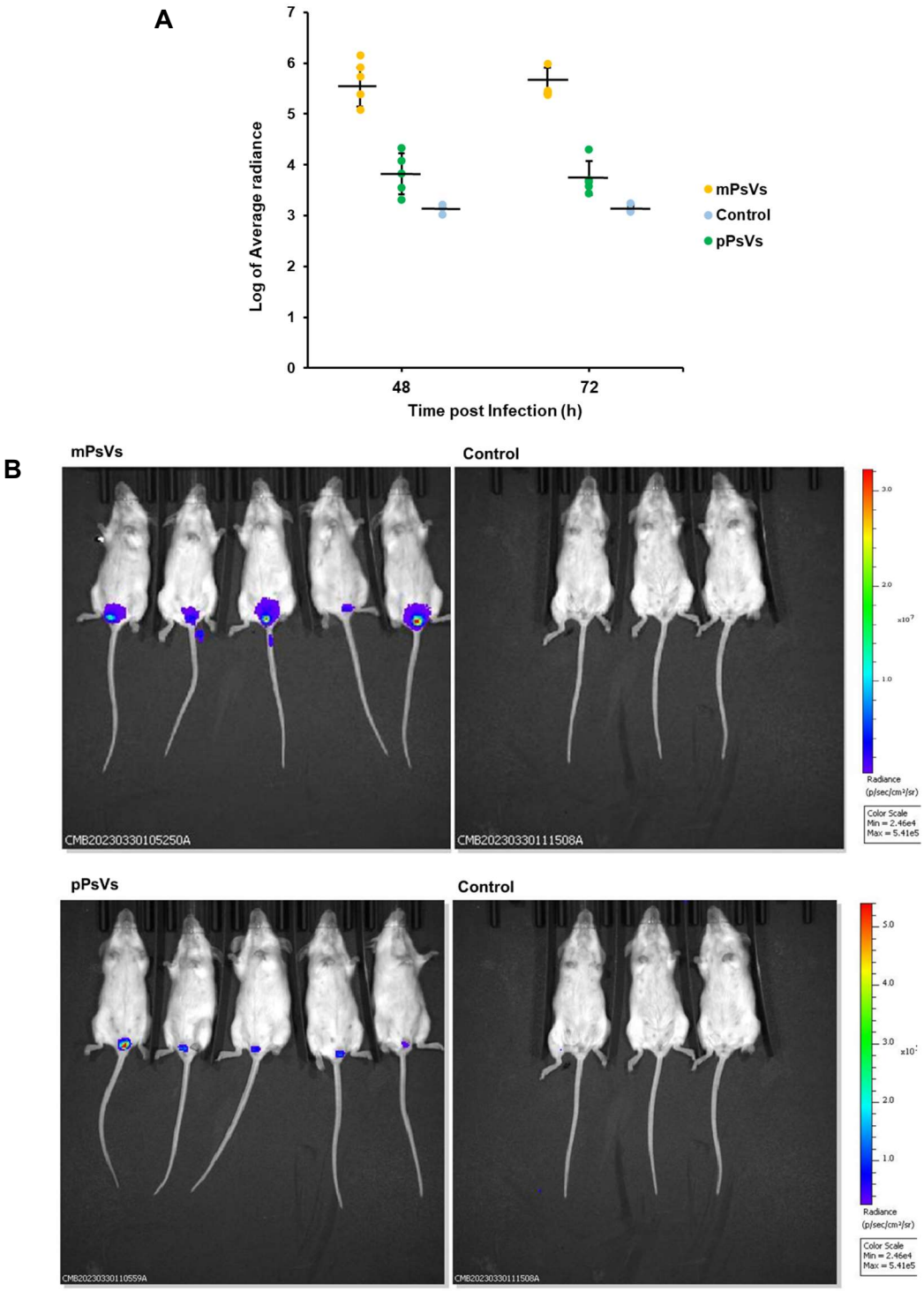

Figure 3.9: **Infectivity of the mPsVs and pPsVs in an animal model. (A)** The graph shows the log of the average radiance (p/sec/cm^2/sr) for each individual mouse for each time point. The yellow points represent the mPsV infected mice; the green points represent the pPsV infected mice and the grey points represent the control mice The average of each group is indicated by the black bar. The error bars indicate the standard deviation. **(B)** IVIS® images of the mice 72 hours after infection with the colour intensity indicated on the scale bar.

3.5 Discussion

HPV PsVs are comprised of capsid proteins L1 and L2 that self-assemble to form a virus-like particle that can encapsidate plasmid DNA containing a reporter gene (Xu et al., 2006). This study compared FLuc and GLuc in a mammalian expression system to determine which luciferase would provide the most reliable challenge results in a mouse model. The optimal luciferase was then used to directly compare expression of HPV16 PsVs in plant and mammalian expression systems.

3.5.1 Comparison of luciferase reporter genes

The comparison of GLuc and FLuc in this *in vivo* study highlighted some key differences and considerations when deciding on reporter genes used for encapsidation. Both PsVs were produced using the same expression vector for the PsV coat proteins and showed good expression. PsVs containing either reporter gene constructs showed successful infection in the *in vitro* assay as well as in the *in vivo* mouse model. Encapsidation of plasmids in HPV PsVs is not dependent on the DNA sequence encoded, but rather on the genomic size (Roden et al., 1996). Thus, it is expected that although the reporter genes are contained within different plasmids, it should not affect their encapsidiation within PsVs (Xu et al., 2006).

The *in vitro* infection of HeLa cells showed that the PsVs encapsidating FLuc produced a higher signal relative to the blank when compared to the GLuc PsVs. However, due to the differences in the reagents, enzymes and samples use these results cannot be directly compared. Neutralization assays were carried out to determine if these PsVs would be able to be neutralized by antibodies. Results from these assays showed that both FLuc and GLuc PsVs were successfully neutralised in the presence of HPV16 neutralising antibodies (Nab) and therefore could be used as infection challenge post vaccination. The PsVs encapsidating the FLuc reporter showed a greater reduction in the signal when incubated with Nab indicating that these were more effectively neutralised by the HPV16 Nab (Figure 3.2).

While the FLuc and GLuc cannot be directly compared due to the fluorescent readings being recorded with different units from the *in vivo* experiment, the results show that there was less variation in the group infected with the PsVs containing the FLuc gene (Figure 3.3 and 3.4). A consideration of the GLuc reporter is that expression and secretion of the protein occurs continually (Hiramatsu et al., 2005), while readings are only taken every 24 h. Vaginal lavages carried out to collect secreted luciferase introduce another variation factor due to the viscosity of

the vaginal fluid and difficulties in ensuring uniformity in the samples collected. In contrast, mice expressing the FLuc reporter gene retain the luciferase within the cells and can be imaged using IVIS® at any time point without the need for collecting vaginal washes (Gould and Subramani, 1988), and allows for visualization of the infected areas (Figure 3.3). Mice infected with either kind of PsVs showed that 4 out of the 5 mice were infected, which shows the natural variably of *in vivo* animal studies. Upon analysis of these results, it was evident that FLuc showed less variation and a more intense fluorescent signal therefore it was decided that FLuc would be the most optimal reporter gene to use in challenge experiments in the present study.

3.5.2 Comparison of expression systems

This chapter directly compared the formation, encapsidation and infectivity of pPsVs with the gold standard mPsVs using the same reporter gene. PsVs encapsidating the FLuc reporter gene were successfully expressed in *N. benthamiana* (Adams et al., 2023). In recent years, plant-based expression systems have become an area of great interest for recombinant protein production, the advantages of using plant production systems include the low production costs, the lower risk of contamination with mammalian pathogens, and capability of post translational modifications (Rybicki, 2010).

Similar difficulties with yield and purity were experienced with the production of the HPV VLPs in Chapter 2, as with production of HPV16 VLPs, when producing the HPV16 PsVs in plants (Adams et al., 2023). While HPV16 PsVs were successfully produced in plants, the yield and the purity of the particles obtained with this production system are not feasible for large scale production. The purity of the pPsVs sample was not as high as the mPsVs and there were significant amounts of host cell proteins post purification, as observed by TEM analysis (Figure 3.6). One of the main challenges was removal of the abundantly present photosynthetic enzyme RuBisCO (Figure 3.5) which is co-purified along with the HPV16 PsVs due to the electrostatic forces that exist between them (Andersson and Backlund, 2008, Chen et al., 2000) making the purification and the removal of this protein exceedingly difficult without lowering the yield of the PsVs.

The infiltration OD_{600} values for L1:L2 is at 5:1 which was based on structure of HPV16 which has one L2 for every L1 pentamer (Conway and Meyers, 2009, Varsani et al., 2003). However, the mammalian expression system has the L1 and L2 genes on the same expression vector and therefore these are present at a ratio of 1:1 in each cell to ensure co-expression. An expression

vector such as pEAQexpress may be a consideration for the plant expression system, where L1 and L2 are able to be expressed on the same T-DNA, as it ensures that both L1 and L2 will be expressed within the same cell (Sainsbury et al., 2009). To account for the different amounts of L1 and L2 required for VLP assembly, promotors of differing strength can be used for expression of each gene to ensure that L1 is expressed at a higher level than L2.

3.5.3 Particle assembly

When assessing the formation of PsVs under TEM, it was evident that the mPsVs were more uniform in shape and size, and appeared to be of higher quality particles which more closely resembling the native virions (Buck et al., 2005), when compared to the pPsVs. The pPsVs particles appeared to be of a much larger range of sizes (20 nm - 60 nm) and shapes, with more aggregates present and less fully formed intact particles when compared with the mPsVs. These results are consistent with that of other plant-derived VLPs. (Adams et al., 2023). These non-uniform particles indicated suboptimal particle assembly and a lower encapsidation efficiency of the reporter plasmid DNA in the pPsVs. Moreover, the mPsVs appeared to be more stable than the pPsVs due to the more uniformly formed particles and the increased thermal stability (Figure 3.6 and 3.7) (Zhao et al., 2012, Kim et al., 2016). This is supported by the higher amount of FLuc plasmid amplified from the extracted mPsVs sample (Figure 3.7(B)) when compared to the unextracted samples. These results indicated that the PsVs were highly stable, as heating of the particles to 95°C was not effective in denaturing the particles, or the particles may have partially reformed on cooling and therefore not all the DNA was available for amplification (Zhao et al., 2012). Extraction of the DNA from the pPsVs resulted in a 3.7 fold increase in absolute copy number, which may indicate that DNA was associated with L1 and L2 rather than being encapsidated within the PsVs.

3.5.4 Infectivity of the particles *in vitro*

The infectivity of PsVs made in plants and mammalian cells was compared by infection of HeLa cells in an *in vitro* system. The *in vitro* infection investigation of the PsVs showed that the pPsVs were not able to infect these cells as no signal was detected with the luciferase assay (Figure 3.9). The initial step of infection in cultured cells is binding to the extra cellular matrix (ECM) however, this is not equivalent to binding to the basement membrane *in vivo*. Binding of PsVs of the ECM does not result in interaction with HSPG and therefore there is less efficient cleavage

of L2 (Culp et al., 2006). This means that there will be a lower infection rate of cultured cells as this model relies on interactions at the cell surface (Day et al., 2010). Another critical consideration is the differences in protein concentration of the pPsVs and the mPsVs. Due to the co-purification of host cell proteins the pPsVs could not be effectively concentrated to a low enough volume using the Amicon filters that would result in a similar concentration to the mPsVs and therefore, significantly higher volumes were added to the cells in order to add the same amount of protein as the mPsVs. This large volume of sample therefore diluted the growth media of the cells and created suboptimal growing conditions for the cells which may have affected expression levels of the reporter gene. It has also been shown by other groups that particle heterogeneity resulted in variability of infectivity assays (Horvath et al., 2010). Further testing should be done on the particles to assess for any surface changes or structural differences within the cells that may be inhibiting the particles from infecting in the *in vitro* cultured cell assays.

3.5.5 Infectivity of PsVs *in vivo*

The PsVs made in plants and mammalian cells was assessed for their infectivity in an *in vivo* mouse model. mPsVs showed infectivity in the mouse model that was ~100 fold higher than that of the pPsVs (Figure 3.16 (A)). Variation between mice of all the groups tested was lowest 72 h after infection which corresponded to the results obtained when mice were infected with PsVs encapsidating FLuc or GLuc (Figure 3.10 and 3.11). This challenge study showed successful infection of all experimental mice with both the mPsV group as well as the pPsV group. While the infectivity of the pPsVs was low when compared to the mPsVs, it was evident from the IVIS® images in Figure 3.10 (B) that infection of these mice was successful when compared with the negative control groups. Due to the lower concentration of the pPsVs used to infect the mice, a lower ratio of the sample to CMC was used for infection, this may have resulted in reduced viscosity of the mixture and might have allowed for the infection medium containing PsVs to leak out (Roberts et al., 2007). This reduces the amount of time the PsVs are in contact with the vaginal canal and therefore lowers the chance of the PsVs binding to the BM, leading to lower infectivity (Ma et al., 2011). Improvements to the purity and concentration of the samples could have resulted in higher infection levels of the pPsVs.

In summary, both the mPsVs and pPsVs were successfully produced and tested both *in vitro* and in an *in vivo* mouse model. The PsVs produced from the two different expression systems were compared and it was determined that production in the mammalian system was more

effective as higher yields and purity were obtained when using this system. The purified mPsVs were more uniform in shape, and displayed more effective DNA encapsidation, which resulted in the mPsVs showing greater infectivity in the mouse model and *in vitro*.To the best of our knowledge, this is the first study that shows that plant produced HPV PsVs are infective *in vivo*.

Chapter 4: Immunogenicity of plant-produced vaccine candidates

4.1 Introduction

The burden of STIs poses a significant challenge to public health particularly in low to middle income countries. Africa, in particular, grapples with this burden, exacerbated by socio-economic challenges such as insufficient education, pervasive social stigma, and limited resources, which include the high costs associated with testing and treatments. (Badawi et al., 2019, Gerbase and Mertens, 1998). Among the most prevalent STIs globally are HPV and gonorrhea (CDC., 2019). While the current HPV vaccine has demonstrated remarkable efficacy in preventing infection and cervical cancer, its adoption in the African context remains hindered by financial constraints and limited accessibility (Kutz et al., 2023). *Ng* has been declared as a superbug and is rapidly gaining resistance to all antimicrobial treatments heightening the urgency for the development of a vaccine against *Ng* (Fifer et al., 2016, Wi et al., 2017). The proposition of a dual vaccine capable of conferring protection against both HPV and gonorrhea holds immense promise, not only for disease reduction but also from a pragmatic standpoint, streamlining vaccinations and targeting similar age groups and social demographics.

4.1.2 *In vivo* mouse model

The use of animal models is well established to investigate the immunogenicity of vaccine candidates (Day et al., 2010, Raterman and Jerse, 2019). This technique is widely used in assessment of prophylactic vaccines (Doorbar, 2016). The mouse model is frequently used to assess the ability of antibodies elicited by vaccines to block HPV infection. However, *Ng* is species specific and therefore a challenge with *Ng* is not possible in the standard mouse model (Ngampasutadol et al., 2008). Animal models can be used for detection of antibody responses which can confer protection against infection (Gulati et al., 2019a), specifically, the elicitation of IgG antibodies. IgA antibodies predominate at the mucosal lining of the GI (gastrointestinal) tract, while IgG occurs at higher levels in the female genital tract (Johansson and Lycke, 2003). IgG is transferred bidirectionally across epithelial cells by the Fc receptor which is expressed in epithelial cells of both the human and mouse. More recently, protocols have been developed to humanize mice by supplementing them with human factors or transgenically altering the mice to be able to better understand infection and immune protective mechanisms (Raterman and Jerse, 2019).

4.1.3 LOS as a vaccine target

Lipooligosaccharide (LOS) is the most abundant molecule on the surface of *Ng* and is responsible for virulence factors exhibited by the pathogen. It has been well studied and identified as a promising vaccine target (Gulati et al., 2019a, Haese and 2021). LOS can undergo sialyation and there are various different sites at which this can occur which gives rise to different epitopes that maybe all be present at different times (Ram, 2018). The gene responsible for the formation of the 2C7 epitope is phase variable and therefore is not constitutively expressed; however, it is still widely expressed among clinical isotopes (Gulati et al., 1996b, Gulati, 2019). Due to LOS being membrane bound, free LOS displays a flexibility and instability in its structure that is not optimal for antibody binding. Therefore, the use of a peptide mimic can overcome this and provide a stable conformation allowing for the elicitation of a more effective immune response (Gulati, 2019).

4.1.4 Vaccine adjuvants

Adjuvants exert their influence by modulating and enhancing both the innate and adaptive arms of the immune system. There are various vaccine adjuvants that can elicit specific immune responses depending on the desired protective immunity against a particular pathogen (Firdaus et al., 2022). The successful combination of antigens and adjuvants is crucial in formulating effective vaccines.

Aluminium-based (Alum) adjuvants primarily form a depot at the injection site, allowing for the slow release of antigens prolonging the antigen exposure, thereby enhancing antigen uptake by antigen-presenting cells (APCs). Alum adjuvants act to enhance the production of both IgG1 and IgE antibodies through the promotion Th2 cell responses (Zhao et al., 2023). Alum adjuvants are known to be safe, reliable, and inexpensive. For these reasons they are widely used for the prevention and treatment of various diseases including HPV (Shi et al., 2019). The current HPV vaccines make use of an aluminium-based adjuvant which is combined with a TLR4 agonist ASO_4, amplifying antigen presentation and immune cell activation (Firdaus et al., 2022).

Previous immunogenicity experiments carried out with the 2C7 peptide utilised Glucopyranosyl Lipid Adjuvant in a Stable Emulsion (GLA-SE) as an adjuvant. GLA-SE is a Th1-biased TLR4 agonist, which has been shown to boost the effectiveness of vaccines targeting LOS (Gulati et al., 2019b, Coler et al., 2010).

4.1.5 Immune interactions

The goal of vaccine design is to elicit multifaceted immune reactions, comprising both humoral and T-cell responses, in order to confer effective and durable protection against pathogenic invaders (Pulendran and Ahmed, 2011). A humoral response is mainly characterized by the activation of B cells, culminating in the production of antigen-specific antibodies, typically of the IgG isotype (Plotkin, 2010). These antibodies are characterized by high affinity for specific antigens and longevity, thus constituting a primary immune defence mechanism (Pulendran and Ahmed, 2011). Th1 and Th2 responses have been shown to be important for conferring protection against *Ng*. Th1 are proinflammatory responses which a play a role in amplifying the cellular arm of immunity, and aid in activation of B cells and signal downstream responses which result in enhanced pathogen clearance (Swain et al., 2012). In contrast, Th2 responses, contribute to antibody class-switching, resulting in the production of diverse antibody isotypes (Mosmann and Coffman, 1989). It is vital to evoke a mixed adaptive immune response to establish enduring immunity against both HPV and *Neisseria gonorrhoeae*.

It has been shown that the HPV vaccine its able to elicit a response that is strong enough to fully protect against infection (Naud et al., 2014, Chatterjee, 2014). The size of the VLPs as well as their repetitive structure are optimal for interaction with APCs (Bachmann and Jennings, 2010). The currently used HPV vaccines have shown good efficacy in the prevention of viral infection and the subsequent onset of cervical cancer.

The candidate vaccine employs the strategy of presenting the 2C7 peptide to the immune system by using the highly immunogenic HPV16 L1 VLPs. The size and the self-assembly of highly repetitive structures of these particles makes them ideal display particles (Day et al., 2010). It is hoped that by exposing the *Ng* peptide to the immune system in the presence of the response elicited by the HPV VLPs will induce a more protective response than that of a native infection.

Thus far this study has described the production of HPV and HPV-*Ng* vaccine candidates as well as the optimization of an HPV challenge model using PsVs. In this chapter, immunogenicity of the plant-produced HPV16 L1 and HPV16-*Ng* chimeric VLPs as a candidate vaccine produced in Chapter 2 was evaluated in a murine model. The immunogenicity of the plant-produced vaccine candidates were analysed with respect to their ability to elicit both anti-L1 and anti-LOS antibodies, as well as their ability to prevent *in vivo* infection with HPV PsVs.

4.2 Materials and Methods

4.2.1 Vaccination of mice

This study was approved by the Animal Research Ethics Committee at the Faculty of Health Sciences at the University of Cape Town (UCT, AEC 021-023). Female BALB/c mice were bred at the UCT Animal Research Unit. The animals were housed and cared for in the Biosafety Level II (BSL-2) Animal Research Unit. The experiments conducted using the IVIS® were carried out by Alisha Chetty and Claire Butters. Welfare monitoring of the animals as well as any procedures was carried out by a registered, experienced animal technologist at the University of Cape Town Animal Research Unit.

Six-week-old female BALB/c mice were used to test the immunogenicity of the plant-produced vaccine candidates. The vaccine doses were produced as described in Chapter 2.2.3 Mice were randomly divided into 4 groups of 5 mice each (Table 4.1) and were acclimatised for one week prior to the start of the experiment.

	µg protein	Alum concentration	Number of doses
Chimera + Alum	5	1:1	1
Chimera	5	-	3
HPV16 L1	5	-	3
Empty Vector (negative control)	5	-	3

Table 4.1: Vaccination groups and dosages

Mice were vaccinated according to the schedule shown in Figure 4.1. Pre-bleeds were taken before administration of the first vaccine doses. Three vaccine doses were administered at intervals of 3 weeks, except for the group receiving adjuvant which only received the primary dose. The vaccine administered with adjuvant was mixed at a 1:1 ratio of Alum (Afrigen) to

sample prior to vaccination. Each dose contained 5 µg of antigen diluted in PBS (endotoxin free pH 7.5) to a total volume of 100 µL which was injected intra-muscularly (IM) 50 µL per hind leg as this was the preferred route of administration, based on optimization experiments that evaluated immunogenicity, bactericidal activity and efficacy in mice (Gulati et al., 2019b). Two weeks after the final vaccination blood was collected from the mice, serum was isolated from the blood and stored at 4°C (short term) or -20°C (long term).

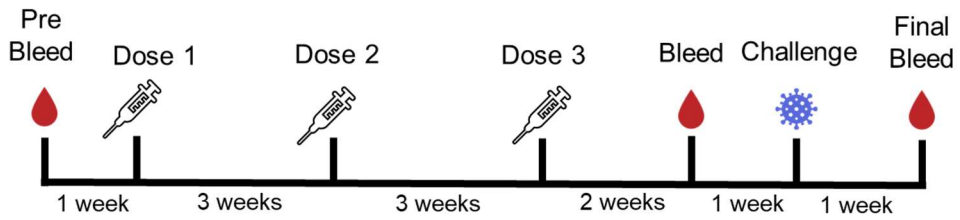

Figure 4.1: Schematic diagram of vaccination timeline. The duration of the experiment is 11 weeks. Red drops indicate mouse bleeds, vaccine doses are indicated by the injections and the challenge with HPV PsVs is indicated by the pathogen.

4.2.2 *In vivo* challenge with HPV PsVs

Mice were challenged with mammalian cell-produced PsVs three weeks after the final vaccine dose (Figure 4.1) to test if the plant-produced vaccine candidates were able to protect mice from HPV infection. The challenge experiment was carried out as described in Chapter 3.2.11 where mice were inoculated intravaginally with 5 µg of mPsVs encapsidating FLuc. Infection of the mice with the PsVs was measured 2-, 3- and 4-days post challenge with the IVIS® imaging system as per manufacturer instructions. Living Image V4.1 (Perkin Elmer) was used to analyse a fixed-sized area of interest, to obtain total flux (photons/seconds).

4.2.3 Evaluation of the humoral immune response elicited by the plant-produced vaccine candidates

4.2.4 Western- and dot blot analysis of mouse sera

In order to detect antibodies present in the mice sera, HPV L1 or LOS was analysed by western blot and dot blot respectively. Western- and dot blots were carried out as described in Chapter 2, Section 2.2.11. Mammalian produced HPV16 L1 was loaded onto the western blot and LOS

was used for dot blot analysis. Pooled mice sera for each group was used as the primary antibody at a dilution of 1:200 alkaline phosphatase-conjugated anti-mouse IgG antibody (Sigma-Aldrich®) diluted at 1:5000 was used as a secondary antibody. The positive controls used were probed with CamVir (Abcam UK) (1:5000) (for HPV16) and Anti-2C7 (1:500) (for the LOS) as primary antibodies. All secondary antibodies used were goat anti-mouse (Sigma-Aldrich®). Pre-bleeds were used as negative control serum, with an additional empty vector control for plant-made vaccine candidates.

4.2.5 Pre-absorption of mice sera

For detection of anti-HPV16 L1 antibodies purified plant-produced HPV16 L1 (see Chapter 2) was used as antigen. Prior studies have indicated that cellular proteins from the host (specifically co-purified plant proteins) can induce the production of antibodies against these proteins (Chabeda et al., 2019, Pineo et al., 2013). As discussed in Chapter 2, the vaccine candidates displayed the presence of a significant amount of host cell proteins. Substantiating this, initial ELISAs conducted on test final bleeds for antibodes revealed notable background detection of plant proteins in the serum from the empty vector control. Moreover, the identification of plant-derived L1 in the final bleeds from VLPs produced in plants, as well as the empty vector, led to the identification of intense non-specific bands in western blots.

In order to mitigate the cross-reactivity between the host cell proteins and antibodies present in the sera, the final bleed samples from mice were pre-absorbed employing the "Lunchbox" Immunoabsorbent Technique (Rybicki 1990, 2000: http://www.mcb.uct.ac.za/mcb/resources/molbio_techniques/lunchbox) (Rybicki et al., 1990). This method was utilized to potentially eliminate or reduce the presence of antibodies against plant host cell proteins within the sera of the mice as these antibodies will bind to the plant proteins. Crude plant extract was prepared by homogenising 6g of plant leaves in 2x volumes of HSPBS (pH 7.4) followed by filtration through 4 layers of 22-24µm pore Miracloth™ (Millipore Sigma) to remove plant debris. Nitrocellulose membrane was submerged in the crude plant extract and incubated at 37°C for 1 h with agitation. The membrane was washed 4x with blocking buffer (5% long life fat-free milk, 1x Tris-Cl [pH7.5]) before incubation in 1:200 diluted mice serum overnight at 4°C.

4.2.6 ELISA detection of antibodies in mouse sera

Indirect ELISAs were carried out to assess antibody titres elicited by the plant-produced vaccine candidates, buffer conditions and coating antigens are listed in Table 4.2 below. Ninety-six well plates were coated with the appropriate amount of antigen (Table 4.2) in coating buffer and incubated overnight at 4°C with gentle shaking. The plates were blocked with 300 µL of the appropriate blocking buffer for 2 h with gentle shaking at RTP. Plates were washed four times with 200 µL per well of the appropriate wash buffer and subsequently probed with sera diluted in wash buffer for 1 hour at 37°C. After incubation plates were washed three times with wash buffer and probed with goat anti-mouse alkaline phosphatase conjugated (Sigma-Aldrich®) secondary antibody diluted 1:10000 in wash buffer for 1 h at 37°C with gentle agitation. The plates were washed four times with wash buffer and finally, 200 µL *SIGMAFAST*™ *p*-nitrophenyl phosphatase substrate (Sigma Aldrich) was added to each well and incubated in the dark for times specified in Table 4.2. The absorbance was read at 405 nm using a Bio-Tek Powerwave XS spectrophotometer. All experiments were repeated three times, an average of the three experiments for each vaccine group is reported here.

Table 4.2: ELISA methods for detection of humoral immune response to HPV16 L1, 2C7 peptide and LOS

Antigen	HPV16 L1	Octa 2C7	LOS
Coating antigen amount	100 ng/well	100 ng/well	80 µg/well
ELISA plates (ThermoFisher Scientific)	Nunc Maxisorp	Pierce® Streptavidin High Binding Capacity Coated	Nunc Polysorp
Coating buffer	1x Tris-Cl (TBS), pH 7.5, 5% NFDM	1x PBS pH 7.5 0.1% BSA, 0.05% Tween 20	1x PBS pH 7.5, 0.05% Tween 20
Wash buffer	1x TBS, 0.05% Tween 20 pH 8.5	1x PBS pH 7.5 0.1% BSA, 0.05% Tween 20	1x PBS pH 7.5
Final wash buffer	1x TBS, 0.05% Tween 20 pH 9	1x PBS pH 7.5 0.1% BSA, 0.05% Tween 20	1x PBS pH 7.5
Detection time	30 minutes	20 minutes	25 minutes

4.2.7 Statistical analysis

Statistical significance of quantitative ELISA data and IVIS® readings were evaluated using a two-tailed non-paired t-test to compare the experimental and control groups. The significance threshold (*p* value) was set at a value of 5% (p=0.05).

4.3 Results

4.3.1 Detection of humoral immune responses elicited by the plant-produced vaccine candidates

4.3.1.1 Western- and dot blot detection of HPV16 L1 and LOS:

To determine if an antibody response was elicited against the plant-produced candidate vaccines, the respective antigens were probed with pooled sera collected from vaccinated mice. The sera contained antibodies to both HPV and *Ng* as shown in Figure 4.2. Western blots (Figure 4.2 A) showed presence of anti-L1 antibodies by the detection of bands at ~56 kDa in the groups vaccinated with chimera both in the absence and presence of adjuvant as well as in the group of mice vaccinated with HPV16, which served as the positive control group. The intensity of the bands was comparable between the chimera groups and the positive HPV16 control. Faint bands were detected in the pre-bleeds and negative controls. These bands may potentially constitute host cell proteins, such as RuBisCO that are detected due to cross reactivity of other antibodies present in the mice sera. The chimeric vaccine candidate elicited an antibody response against LOS as shown by detection of LOS on dot blots in Figure 4.2 B. As expected, both the HPV16 and negative control vaccine groups did not show antibody detection for LOS.

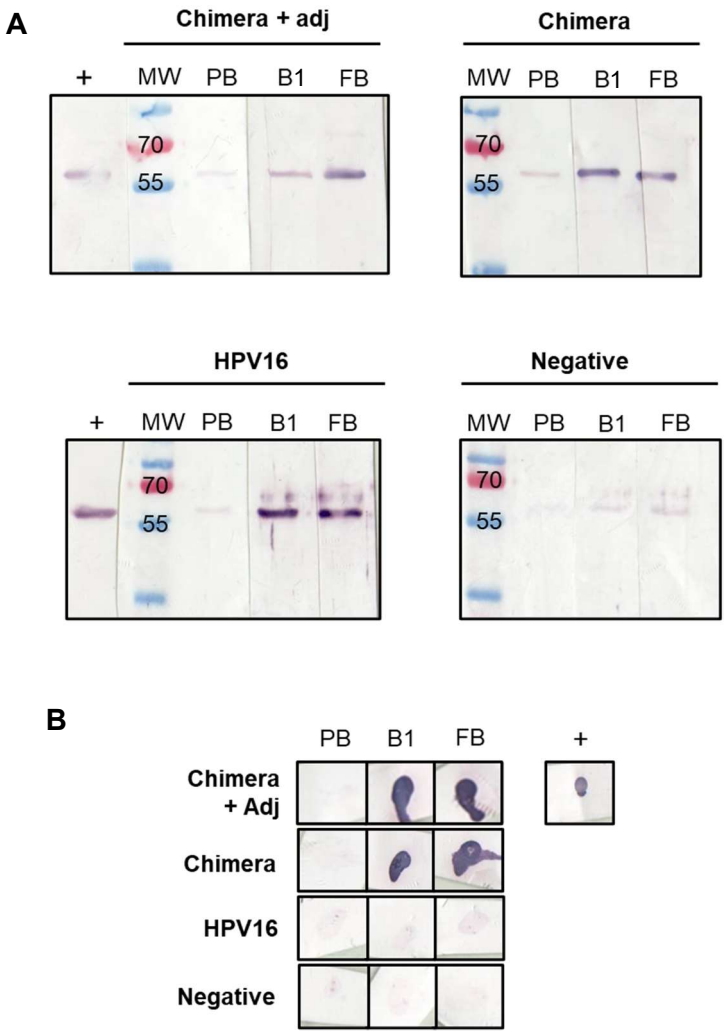

Figure 4.2: Western- and dot blot analysis of sera. (**A**) Each lane contains HPV16 L1, blots were cut into strips each one containing one lane and each strip was probed with pooled mice sera of all bleeds collected from each experimental group. Lanes: + - positive control probed with CamVir (Abcam, UK), MW – Molecular weight marker (kDa), PB – Pre-bleed sera, B1 – the initial bleed before the challenge, FB – Final bleed. (**B**) Dot blot detection of anti-LOS antibodies in mouse sera of vaccinated groups. The positive control was probed with mAb 2C7 diluted 1:500.

4.3.1.2 Quantification of humoral response against candidate vaccine antigens

To determine antibody titres elicited against both HPV and *Ng*, indirect ELISAs were carried out on pooled mice sera using either HPV16 L1, cyclic-2C7 peptide and LOS as coating antigen. These titres represent the maximum dilution factor that results in an absorbance greater than pre-bleed sera. The pre-bleed sera served as a negative control and no antibodies specific for HPV L1, 2C7, or LOS was detected in any of the groups which agrees with the results observed in the western- and bot blots (Figure 4.2).

4.3.2 Detection of Anti-HPV16 L1 antibodies

Indirect ELISAs were carried out to determine antibody titres elicited against HPV16 L1 in the pooled mice sera (Figure 4.3). Sera were titrated using a 4-fold serial dilution ranging from 1:200-1:204800. The anti-HPV16 titres were expressed as the reciprocal of the maximum serum dilution containing higher absorbance readings than that of the corresponding pre-bleed serum at 1:200. Rabbit-raised anti-Gardasil® antibody (1:5000) served as a positive control and was used to validate the experiments.

Sera collected from mice vaccinated with chimeric and HPV16 L1 VLPs displayed antibody levels that were statistically different from the pre-bleed sera ($p < 0.00001$). In addition, the titres achieved for all the VLP-vaccinated groups were statistically significant when compared to the negative control group vaccinated with crude plant extract. The plant-produced HPV16 and chimeric VLPs (with adjuvant) elicited anti-L1 titres of 1:204800, and the chimera without adjuvant elicited anti-L1 titres of 1:51200 (Figure 4.3 B).

The presence of adjuvant increased the antibody titre levels even though these mice only received one vaccine dose, suggesting that the adjuvant increases the immunogenicity of the vaccine candidate. These levels were comparable to the HPV16 L1 vaccinated mice which served as a positive control.

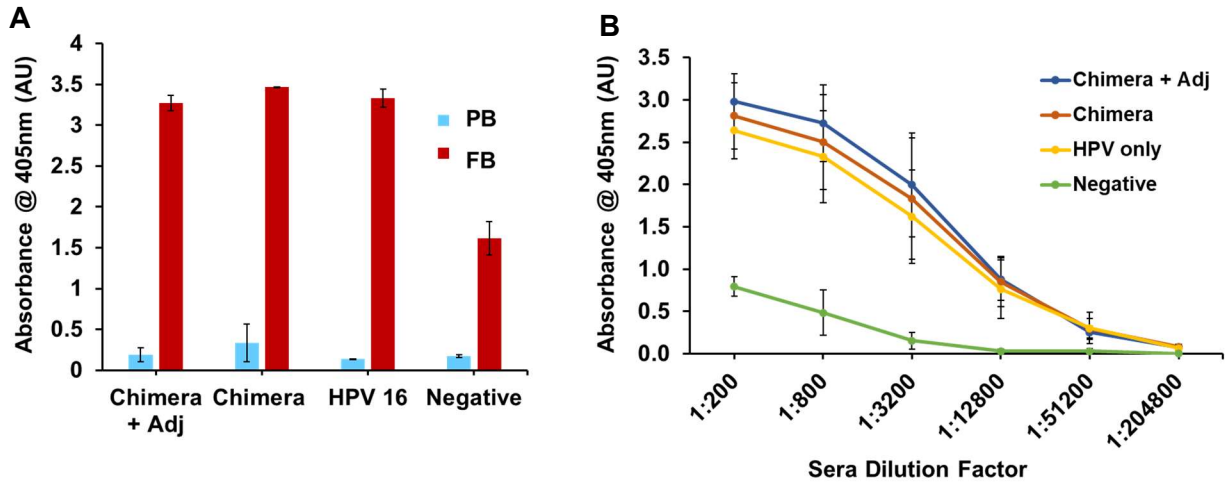

Figure 4.3: Indirect ELISA of pooled mouse sera using plant-produced HPV16 L1 as coating antigen. (A) Vaccine pre-bleeds (PB) sera and final bleeds (FB) sera absorbances at 405 nm at dilutions of 1:200. **(B)** Titration curve of the mouse sera for the vaccine and control groups. The markers represent the average of the 3 repeats. Error bars represent 95% confidence interval.

4.3.3 Anti-2C7 antibodies detected in mouse sera

Detection of antibodies elicited against the 2C7 peptide was carried out using biotinylated peptide coated onto streptavidin plates. Anti-2C7 titres were expressed as the reciprocal of the maximum serum dilution containing higher absorbance readings than that of the corresponding pre-bleed serum at 1:200. Sera were titrated using a 4-fold serial dilution ranging from 1:500-1:128000 (Figure 4.4 B).

There was no response elicited against 2C7 by vaccination with the HPV16 and the plant-only negative controls. The chimeric vaccine candidate elicited antibody titre of 1:32000 both in the presence and absence of Alum (Figure 4.4 B), these titres were significantly different when compared to the negative control group. Vaccination with the chimeric vaccine candidate in the absence of adjuvant resulted in a slightly higher antibody response at 10 weeks, which may be due to the difference in doses received, as the adjuvant group only received one dose of the vaccine compared to the other vaccine groups. Sera collected from mice vaccinated with the chimeric vaccine candidate displayed antibody levels that were statistically different from the pre-bleed sera both in the presence ($p < 0.0004$) and absence ($p < 0.00005$) of adjuvant.

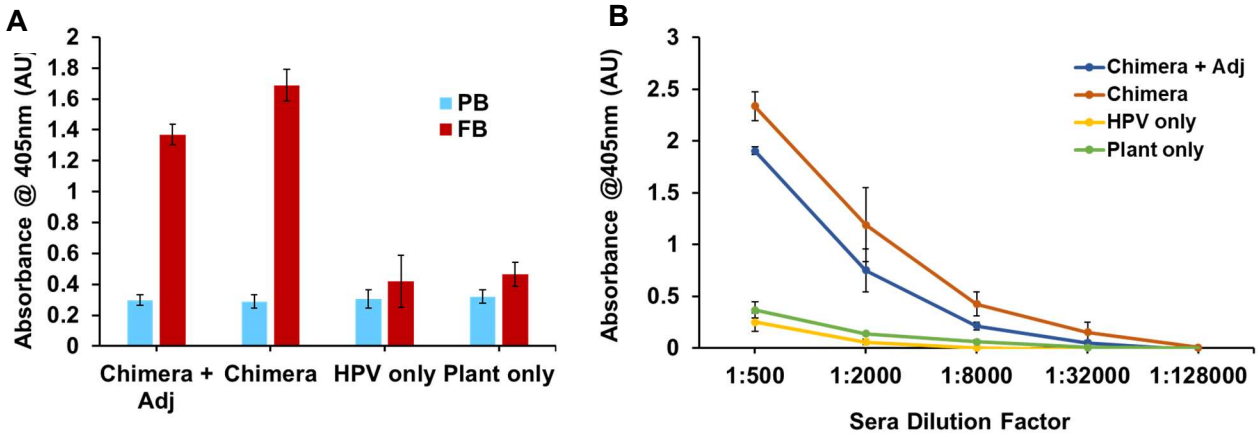

Figure 4.4: Indirect ELISA of pooled mouse sera using biotinylated 2C7 peptide as coating antigen. (A) Vaccine pre-bleed and final bleed absorbances in arbitrary units (AU) at dilutions of 1:1000. **(B)** Titration curve of the mouse sera for the vaccine and control groups. The bars represent the means of the triplicate readings. Error bars represent the 95% confidence interval.

4.3.4 Detection of Anti-LOS antibodies in mouse sera

Indirect ELISAs where plates were coated with LOS extracted from *Ng* were carried out to ensure that the 2C7 antibodies detected are specific and will bind to LOS. The anti-LOS titres were expressed as the reciprocal of the maximum serum dilution containing higher absorbance readings than that of the corresponding pre-bleed serum at 1:500. The initial readings were taken at sera diluted to 1:100 and then titrated using a 2-fold serial dilution ranging from 1:500-1:8000.

The negative controls, HPV16 and the empty vector control showed no response against LOS (Figure 4.5 A). The chimera elicited antibody titres of 1:8000 both in the presence and absence of adjuvant (Figure 4.5 B). As with the anti-2C7 titre levels vaccination without Alum elicited a slightly higher response, potentially the result of the discrepancy in the number of doses as group vaccinated with the chimera and adjuvant only received a single dose. The sera collected from the mice vaccinated with the chimera displayed antibody levels that were statistically different from the pre-bleed sera both in the presence ($p = 0.0024$) and absence ($p = 0.000084$) of adjuvant.

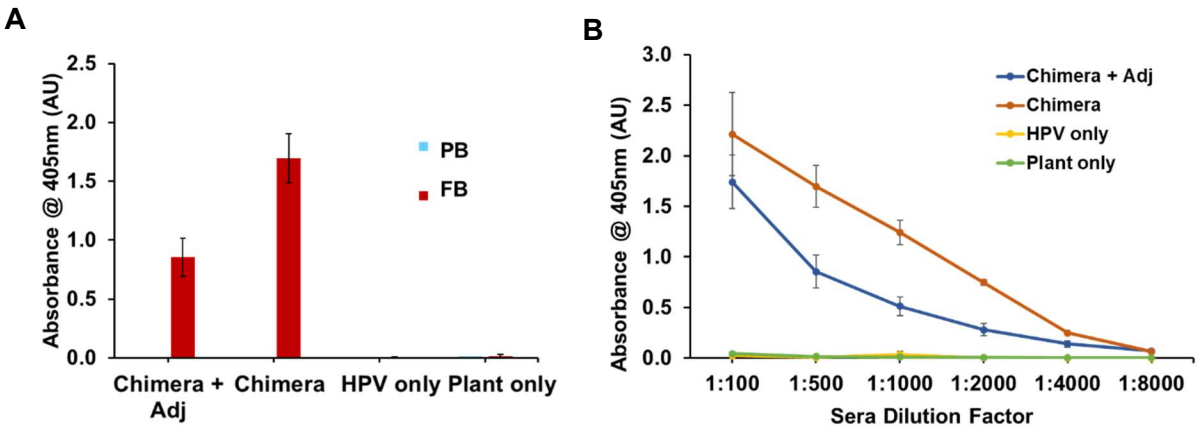

Figure 4.5: Indirect ELISA of pooled mouse sera using LOS as coating antigen. (A) Vaccine pre-bleed and final bleed absorbances in arbitrary units (AU) at dilutions of 1:200. **(B)** Titration curve of the mouse sera for the vaccine and control groups. The bars represent the means of the triplicate readings. Error bars represent the 95% confidence interval.

4.3.5 Protection of mice against HPV challenge

To test if the chimeric and HPV16 L1 vaccines were able to provide protection against HPV infection, the vaccinated mice were challenged with mammalian cell-produced HPV16 PsVs

encapsidating FLuc as produced in Chapter 3. Challenge results are represented in Figure 4.6, these results show that all the vaccine candidates were able to provide protection in all of the mice vaccinated with the chimera and adjuvant, and in the group vaccinated with the chimera alone as well as in the group vaccinated with HPV16. The HPV16 group serves as a positive control and showed no infection as indicated by the lack of fluorescence detected. Therefore, the vaccine candidates were able to fully neutralise the HPV PsVs which imitate an infection. The negative control group vaccinated with the plant extract showed infection in 3 out of the 5 mice with the most uniform readings recorded 72 hours after infection as reported in Chapter 3 (Figure 4.6 B). The infection of 3 out of 5 mice may have been due to biological variation. The lack of infection in 2 of the mice results in a lower average reading which produces *p* values which indicate that there is no significance between the experimental groups and the negative control group.

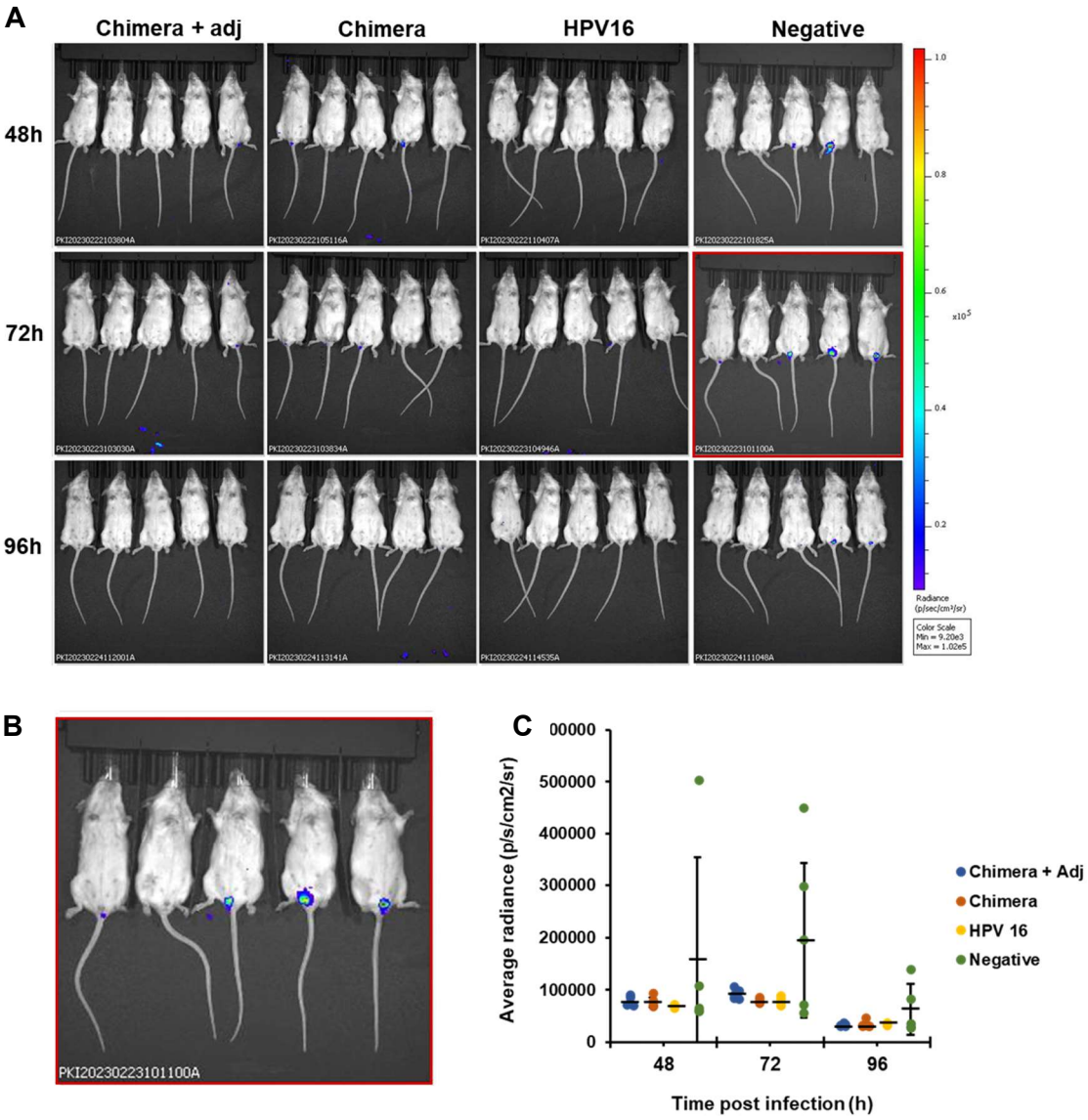

Figure 4.6: Protection of vaccinated mice against HPV challenge. (A) Images taken in the IVIS® machine 2-, 3- and 4-days post infection. The images have been normalised and the scale bar on the right indicates the radiance (p/sec/cm^2/sr). **(B)** Image taken in the IVIS® machine 72 hours post infection of the negative control group **(C)** The average radiance (p/s/cm^2/sr) for each mouse at each time point. The readings were taken 48, 72 and 96 hours post infection. The average for each group is indicated by the black line and the bars represent the standard deviation.

4.4 Discussion

VLPs have demonstrated potent immunogenicity attributed to the repetitive presentation of epitopes on their surfaces, their interaction with APCs and the resulting stimulation of B cells. HPV VLPs, are comprised of 360 copies of L1, and are used as the foundation for current prophylactic vaccines, which result in the production of high-titre nAbs (Zhang et al., 2023, Chen et al., 2000). (Qian et al., 2020)The structure of HPV VLPs can be used to produce chimeric particles which display foreign epitopes. Due to HPV16 being the most common cause of cervical cancer, HPV16 L1 VLPs were used as the backbone to display the Ng 2C7 peptide mimic in the DE loop of L1 to develop a potential dual vaccine candidate. The challenge faced when accessing the dual vaccine candidate in this study is that the immune responses required for protection against viruses (i.e. HPV) and bacteria, specifically *Ng,* are not the same. Protection against HPV infection is dependent on the presence of neutralising antibodies (IgG1 and IgG3 subclasses), while correlates of protection against *Ng* in humans is not fully understood and the mechanisms are undefined (Pasmans et al., 2022). The current mechanisms of interest are the binding of antibodies which will activate complement and lead to bactericidal activity. The binding of complement may also lead to opsonophagocytic killing or recruitment of T helper cells responses (Gulati et al., 2019b, Shaughnessy et al., 2022). Th1 responses have also been suggested to be important for efficacy of *Ng* OMV vaccine designed for intravaginal delivery (Liu et al., 2017).

In this chapter we aimed to assess the immunogenicity of plant produced HPV16 VLPs and HPV/*Ng* chimeric VLPs as vaccine candidates. The antibody responses were compared directly to the responses elicited by HPV16 L1 as a positive control to determine how the insertion of the 2C7 peptide effects the elicitation of anti HPV16 response. The mice were immunised with 5 µg of candidate vaccine in the presence and absence of Alum as an adjuvant. The mice were also vaccinated with purified plant extract to ensure responses observed were specific to the recombinantly expressed proteins. The group receiving the adjuvanted chimeric VLPs received one vaccine dose, while the other groups received 3 does over the span of 6 weeks.

The humoral immune response is characterized by the production of specific antibodies by B cells and plasma cells in response to foreign antigens. These antibodies play a pivotal role in neutralizing pathogens, providing protection against infection, and contributing to immunological memory (Plotkin, 2010, Pulendran and Ahmed, 2011). The humoral immune response for both vaccine candidates were evaluated on immunoblots and indirect ELISAs by detecting HPV16 L1 and *Ng*-specific antibodies in sera collected from mice.

The level of HPV16 L1 antibodies detected was similar between the chimeric VLPs and the positive control with each group exhibiting equivalent titres of 1:204800 (Figure 4.3). The titres achieved are high when compared to the levels achieved by plant-produced HPV L1 in previous studies, which ranged from 12800-40960 (Pineo and 2013, Maclean et al., 2007, Fernández-San Millán et al., 2008). The study by Pineo et al reported lower end point titre levels from mice that were vaccinated with 10 µg per dose and received 4 doses (Pineo and 2013). Considering that mice were vaccinated in this study with 5 µg VLPs per dose and only received 3 doses, the vaccine candidate shows strong immunogenicity. It is clear that the insertion of the peptide into the surface of the VLPs did not reduce immunogenicity of the VLPs with respect to HPV-antibody binding as antibody titres elicited by the chimeric vaccine candidate are comparable to that of the response of HPV16 vaccinated group.

The antibody titre levels achieved by the VLP-based vaccine candidates (both the chimeric VLPs and the HPV16 VLPs) were significantly different from the negative control group. A higher antibody titre indicates a greater concentration of antibodies, which often correlates with a greater immune response. However, there was relatively high background present in the negative control group (Figure 4.3) which indicates the presence of antibodies against plant host proteins that were co-purified with the VLPs. These co-purified proteins when exposed to the immune system will elicit an immune response leading to the generation of antibodies specific for these off-target proteins. When examining the results of Chapter 2 and the purity of the vaccine samples this is not unexpected as can be seen by the silver-stained gels (Figure 2.6), where other proteins could be detected in the vaccine samples. These results are consistent with previous studies that also showed marked co-extraction of plant proteins with HPV VLPs purified from plants (Chabeda et al., 2019).

Adjuvants are added to vaccines to enhance immunogenicity and Alum is an aluminium based adjuvant which is commonly used in commercial vaccines (Shi et al., 2019). While VLPs have shown to be self-adjuvating, Alum is added to the currently-used HPV vaccine and therefore was a suitable adjuvant for this study (Mohsen et al., 2017, WHO, 2022). It is difficult to compare the vaccines in this study in the presence and absence of the adjuvant because of the discrepancy in the number of doses that were given. The addition of the adjuvant to the chimeric vaccine candidate did not seem to drastically increase the level of antibody detected (Figure 4.3). However, the group which received the adjuvant received only one dose still showed a strong immune response 10 weeks later without any booster doses. This vaccine candidate was also able to protect against HPV challenge. These results show that even at one dose only the

vaccine with the adjuvant was able to protect against HPV infection. It would be interesting to compare the same vaccine without the adjuvant at a one dose application to determine if it could also protect against HPV infection.

The primary objective of vaccination lies in its efficacy in preventing infections (Pinto et al., 2018) Notably, the current HPV vaccines have proven efficacious in this regard (Naud et al., 2014, WHO, 2022). The HPV16 L1 and chimeric VLPs demonstrated the capacity to elicit an immunogenic response in mice, conferring immunity against PsV-induced infections in the challenge experiment. The lack of fluorescent readings indicated that the infectious PsVs were fully neutralised by nAbs and therefore there was no infection of the vaccinated mice. The combination of the humoral response and the protection by challenge shows great promise for the vaccine candidate against HPV infection.

When conducting the challenge experiment the mice are imaged in the IVIS® to detect the fluorescence of the luciferase and therefore infection. The lack of signal indicates no infection. One of the challenges faced using this method is that the mouse faeces gives off a fluorescent reading which can be misinterpreted as infection. This was the case in several mice in Figure 4.6 in the chimera groups with and without adjuvant. This was taken into account when selecting the areas which are used for detection of the fluorescence readings (Figure 4.6 A).

Ng exhibits a remarkable capacity to evade host immune responses through a repertoire of sophisticated mechanisms that have been finely honed by evolutionary pressures. These mechanisms enable the bacterium to establish and maintain colonization within various mucosal surfaces, impeding effective immune clearance and contributing to its persistent pathogenicity (Scurtu et al., 2022, Liu and Russell, 2011). *Ng*'s adaptability has also allowed it to become a superbug which is resistant to almost all available antibiotics (Alirol et al., 2017). A natural infection with *Ng* does not elicit an immune response that can provide protection against future infection (Fowler et al., 2010, Liu et al., 2014). Eliciting an immune response that targets the generation of Th1 or Th2 responses will provide greater levels of protection (Liu and Russell, 2011, Edwards et al., 2016).

LOS is the most abundant molecule on the surface of *Ng* (Gulati, 2019) has been chosen as a vaccine target, more specifically the 2C7 epitope of LOS. Previous studies involved the use of an octameric and tetrameric multi-antigenic peptide to display the 2C7 peptide in a linear conformation (Gulati et al., 2019b). Vaccination with the peptide in this conformation resulted in the elicitation of antibodies in the mouse model that were able to bind to LOS and displayed

killing ability against *Ng*. Previously mice vaccinated with the 2C7 peptide resulting in the elicitation of antibodies which were shown to bind to LOS have exhibited bactericidal activity against *Ng* (Gulati et al., 1996, Gulati et al., 2013, Gulati et al., 2019b). The chimeric vaccine candidate tested in this study displayed the peptide on a much larger and more rigid structure. The chimeric VLPs were able to induce a humoral response against the LOS (Figure 4.5) which was further confirmed by the detection of antibodies specific for the 2C7 peptide (Figure 4.4). These antibody levels were significantly different from the pre-bleed sera as well as the negative control groups (HPV16 L1 and plant extract). While the antibody titres against LOS appear to be lower than the titres against the 2C7 peptide, this may be due to differences in sialylation of the LOS which results in the presence of differing structures and binding sites (Gulati, 2019).

As with the HPV response, the effect of the addition of adjuvant to the vaccine candidate is difficult to assess due to the differences in doses received. However, it is noted that the responses seen against LOS *Ng* were also higher in the absence of adjuvant, however this may be due to this group receiving 3 doses and the results of this were not significantly different when accessing the end point titre levels. Overall the levels of antibodies elicited against LOS were comparable to previous experiments and remained so over the duration of the experiment. Considering the importance of antibody binding, the results of the vaccination showed promise in that 2C7 antibodies that were detected are specific to LOS. This study makes use of Alhydrogel® adjuvant 2% (Invitrogen) which is an aluminium hydroxide wet gel suspension. This adjuvant induces an innate immune response through the activation of pattern recognition receptors (PPRs) as well as a Th2 response. Previous studies done with the peptide have made use of GLASE in order to enhance the Th1 response (Gulati et al., 2019b) and may be a consideration in future experiments.

In conclusion the plant-produced chimeric and HPV16 VLPs were able to elicit immunogenic responses in the mice against both LOS and HPV16 L1. The anti 2C7 response showed that the antibodies were able to bind to both the 2C7 peptide as well as LOS. The vaccinated mice were protected against the challenge infection with HPV16 as they did not show any fluorescent luciferase readings and therefore the PsVs were fully neutralised in vivo. Further testing of the mouse sera such as serum bactericidal assays could be used to determine the killing ability of the antibodies detected and then pursue further vaccination experiments and undergo a *Ng* challenge model in the humanised mice (Raterman and Jerse, 2019).

Chapter 5: Final discussion

STDs constitute a global public health challenge, exerting a significant burden on communities worldwide. In the context of Africa, the prevalence of STDs compounds existing health and economic disparities (CDC., 2019). Among the noteworthy STDs is *Ng*, which has been classified as a superbug due to its alarming antibiotic resistance. The bacterium's ability to evolve rapidly and evade immune responses not only complicates treatment but also contributes antibiotic resistance which has resulted in its superbug status (Unemo et al., 2019b). Infections often begin asymptomatically, facilitating silent transmission. If left untreated, *Ng* can progress to symptomatic stages marked by painful urination, genital discharge, and, in women, pelvic inflammatory disease (PID) which can lead to infertility as well as DGI (Su et al., 2022).

Meanwhile, HPV, with a global impact on women's health, is a leading cause of cervical cancer and is of particular concern in sub-Saharan Africa (WHO, 2018, Qulu et al., 2023). The success of the HPV vaccine in preventing cervical cancer highlights the potential of vaccination strategies (Kutz et al., 2023). Demographically, both diseases disproportionately affect marginalized populations. *Ng* prevalence is elevated among young adults, men who have sex with men, and individuals with limited access to healthcare (Unemo et al., 2019b). In the case of HPV, the burden falls disproportionately on women in low-resource settings, where routine screening and vaccination are often challenging to implement. Thus, the imperative for comprehensive interventions is underscored, addressing both the infectious dynamics of *Ng* and the oncogenic potential of persistent HPV infections, especially in vulnerable populations (Singh et al., 2023).

5.1 Production and Purification of VLPs

Plant production systems offer a cost effective alternative method for the recombinant production of proteins (Rosales-Mendoza, 2020). The utilization of plants mitigates the risk of contamination with animal pathogens and the waste generated by this production system is more easily contained. Transient expression in *N. benthamiana* through *Agrobacterium*-mediated infiltration of plants allows for expression of trans genes that will not be incorporated into the plant genome (Lamprecht et al., 2016). These methodologies are currently a focal point of scientific interest and have demonstrated successful application in generating a diverse array of recombinant proteins (Rybicki, 2010, Obembe et al., 2011, Su et al., 2023).

Nevertheless, challenges arise when applying this approach to the production of HPV VLPs resulting in low yields and complexities associated with protein purification (Chabeda et al., 2019, Lamprecht et al., 2016). In previous studies, expression of the protein was targeted to the chloroplasts to improve yield and stability of the particles (Maclean et al., 2007), however the yields achieved by this study were still insufficient to be deemed as industrially scalable (Fischer et al., 2004). In the present study, a notable limitation was observed, which is the co-purification of RuBisCO with L1 VLPs. RuBisCO, possessing an opposite electrostatic charge to HPV, allows for interaction between the molecules, rendering purification challenging with substantial losses in HPV or chimeric VLPs (Udenigwe et al., 2017).

While ammonium sulphate precipitation fails to yield intact particles (Fernández-San Millán et al., 2008), exploring alternative purification methods, such as two-phase separation or ultrafiltration techniques, presents viable avenues for improvement of purity (Fouladvand et al., 2020, Sun et al., 2016). These approaches offer the potential to enhance particle homogeneity and overall yield.

Furthermore, considering a shift to a distinct production system, such as *Escherichia coli (E. coli)* or a yeast expression system which is the current system implemented in Gardasil vaccine production (Pinto et al., 2018). This alternative system not only holds the potential to augment protein yield but also offers the prospect of achieving greater particle homogeneity at a cost-effective scale (Chu et al., 2023). This approach aligns with the ongoing pursuit of optimizing production methods to meet the dual objectives of improved efficiency and cost-effectiveness in virus-like particle synthesis.

5.2 Development of HPV PsV Challenge model

Similar challenges were encountered during the production of HPV16 PsVs in plant systems. There were challenges involving the purity of the samples as well as the yields which was described in Chapter 3. While plant-produced PsVs have previously been produced and examined *in vitro*, (Adams et al., 2023, Módolo et al., 2017) the present study showcases the first *in vivo* challenge experiment, demonstrating infection in a mouse model. However, plant-made PsVs were outperformed by the gold standard mammalian made PsVs which resulted in stronger reporter gene expression and therefore more effective infection in the mouse model (Buck et al., 2005, Módolo et al., 2017).

Further optimization of plant production systems and purification are required. Suggestions include relocation of the L1 and L2 genes onto the same vector to ensure expression of both

proteins within the same cells, utilization of different promotors could allow for differences in expression levels allowing for higher expression levels of L1 (Yeager et al., 2000). As previously mentioned for the plant-produced VLPs, further optimization of the PsVs could also improve encapsidation, uniformity and stability of the PsVs. These aspects of the plant produced PsVs will need to be improved and this would contribute to more effective infection (Adams et al., 2023). The choice of reporter gene used for PsVs is also an important consideration, a comparison of the Gaussia vs Firefly luciferase demonstrated that the FLuc was more effective in infection than the Gaussia in this particular model (Neefjes et al., 2021). However, since the same reagents are not used for detection of each reporter, the *in vitro* infection were normalised to the blank.

5.3 Immunogenicity of Vaccine candidates

Within the domain of vaccinology, the primary aim is to induce a robust adaptive immune response, strategically harnessing both humoral and T-cell responses to engender potent and enduring defence against pathogenic incursions. The humoral response is chiefly characterized by the activation of B cells, culminating in the production of antigen-specific antibodies, typically of the IgG isotype (Pulendran and Ahmed, 2011). These antibodies, characterized by high affinity and longevity, are instrumental in neutralizing extracellular pathogens and their associated toxins, thus constituting a primary defence mechanism. The effective stimulation of the humoral response is a fundamental objective in vaccine design, ensuring the generation of a reservoir of specific antibodies to establish durable immune memory (Plotkin, 2010). The candidate vaccine was able to elicit a humoral immune response in mice against both HPV and *Ng* as evidenced by the detection of antigen specific antibodies. The humoral response against HPV was not only comparable to the HPV16 L1 positive control but was able to provide protection against challenge with HPV PsVs where no infection was observed in the vaccinated mice.

Protective immunity against *Ng* in humans is not fully understood and the mechanisms are undefined. One of the current mechanisms of interest is the binding of antibodies which will activate complement and lead to bactericidal activity. The binding of complement may also lead to opsonophagocytic killing or recruitment of T helper cells responses (Gulati et al., 2019b, Shaughnessy et al., 2022). Considering the importance of antibody binding, the results of the vaccination showed promise in that 2C7 antibodies were detected which are specific to LOS. Previously 2C7 antibodies have shown to have bactericidal activity against *Ng* (Gulati et al., 1996b, Gulati et al., 2013b, Gulati et al., 2019b).

5.4 Conclusions and Future work

Following on from these results, the testing of the vaccines would need to be repeated as there is variation of living systems. Serum bactericidal assays should be carried out in order to determine whether the antibodies elicited against *Ng* will result in killing of the bacteria (Gulati et al., 2019a). This is crucial in determining the effectiveness of the vaccine against *Ng*. A humanised mouse model could be used to determine whether the immune response elicited by the vaccine speeds up disease clearance (Raterman and Jerse, 2019).

HPV has shown to be highly immunogenic and has a large repetitive structure and therefore serves as an ideal display molecule (Pinto et al., 2018). However, producing uniform stable particles involves downstream disassembly and reassembly processes which are expensive. As an alternative the base HPV16 VLPs could be replaced with another type of HPV that forms more uniform particles and is easier to purify such as HPV35 or BPV (Módolo et al., 2017). Another consideration would be to utilize alternative display methods which make use of VLP tagging such as spy-tag spy-catcher technology (Hatlem et al., 2019), streptavidin biotin coupling (Fredsgaard et al., 2021). These enable the use of a myriad of different particles to display the 2C7 peptide enabling the production of a vaccine cocktail (Jerse and Deal, 2013). The display may benefit from a cyclic peptide as the confirmation would be ‘looser’ than insertion into a particle itself. Production of the display particle would be simplified which would lower the cost of production. Loss of dual vaccine activity however could use this method to display several different antigenic peptides more easily on the surface of the VLPs.

In conclusion while there is further optimization of production and purification required, the dual vaccine candidate shows promise in the elicitation of a protective immune response against both target diseases.

Appendix

Appendix

Table 6.1: Amino acid sequences of the generation I constructs of the insertion (_i) or substitution (_s) of 2C7 peptide sequence into HPV-16 L1 at positions within the DE loop indicated by the blue boxes or the h4 helix indicated by the orange boxes.

Generation I constructs
DE_i MSLWLPSEAT VYLPPVPVSK VVSTDEYVAR TNIYYHAGTS RLLAVGHPYF PIKKPNNNKI LVPKVSGLQY RVFRIHLPDP NKFGFPDTSF YNPDTQRLVW ACVGVEVGRG QPLGVGISGH PLLNKLDDTE NCGPIPVLDE NGLFAPGPC ASAYAANAG VDNRECISMD YKQTQLCLIG CKPPIGEHWG KGSPCTNVAV NPGDCPPLEL INTVIQDGDM VDTGFGAMDF TTLQANKSEV PLDICTSICK YPDYIKMVSE PYGDSLFFYL RREQMFVRHL FNRAGAVGEN VPDDLYIKGS GSTANLASSN YFPTPSGSMV TSDAQIFNKP YWLQRAQGHN NGICWGNQLF VTVVDTTRST NMSLCAAIST SETTYKNTNF KEYLRHGEEY DLQFIFQLCK ITLTADVMTY IHSMNSTILE DWNFGLQPPP GGTLEDTYRF VTSQAIACQK HTPPAPKEDP LKKYTFWEVN LKEKFSADLD QFPLGRKFLL QAGLKAKPKF TLGKRKATPT TSSTSTTAKR KKRKL
DE_s MSLWLPSEAT VYLPPVPVSK VVSTDEYVAR TNIYYHAGTS RLLAVGHPYF PIKKPNNNKI LVPKVSGLQY RVFRIHLPDP NKFGFPDTSF YNPDTQRLVW ACVGVEVGRG QPLGVGISGH PLLNKLDDTE NCGPIPVLDEN GLFAPGPCMD YKQTQLCLIG CKPPIGEHWG KGSPCTNVAV NPGDCPPLEL INTVIQDGDM VDTGFGAMDF TTLQANKSEV PLDICTSICK YPDYIKMVSE PYGDSLFFYL RREQMFVRHL FNRAGAVGEN VPDDLYIKGS GSTANLASSN YFPTPSGSMV TSDAQIFNKP YWLQRAQGHN NGICWGNQLF VTVVDTTRST NMSLCAAIST SETTYKNTNF KEYLRHGEEY DLQFIFQLCK ITLTADVMTY IHSMNSTILE DWNFGLQPPP GGTLEDTYRF VTSQAIACQK HTPPAPKEDP LKKYTFWEVN LKEKFSADLD QFPLGRKFLL QAGLKAKPKF TLGKRKATPT TSSTSTTAKR KKRKL
h4_i MSLWLPSEAT VYLPPVPVSK VVSTDEYVAR TNIYYHAGTS RLLAVGHPYF PIKKPNNNKI LVPKVSGLQY RVFRIHLPDP NKFGFPDTSF YNPDTQRLVW ACVGVEVGRG QPLGVGISGH PLLNKLDDTE NASAYAANAG VDNRECISMD YKQTQLCLIG CKPPIGEHWG KGSPCTNVAV NPGDCPPLEL INTVIQDGDM VDTGFGAMDF TTLQANKSEV PLDICTSICK YPDYIKMVSE PYGDSLFFYL RREQMFVRHL FNRAGAVGEN VPDDLYIKGS GSTANLASSN YFPTPSGSMV TSDAQIFNKP YWLQRAQGHN NGICWGNQLF VTVVDTTRST NMSLCAAIST SETTYKNTNF KEYLRHGEEY DLQFIFQLCK ITLTADVMTY IHSMNSTILE DWNFGLQPPP GGTLCGPIPV LDENGLFAPG PCEDTYRFV TSQAIACQK HTPPAPKEDP LKKYTFWEVN LKEKFSADLD QFPLGRKFLL QAGLKAKPKF TLGKRKATPT TSSTSTTAKR KKRKL
h4_s MSLWLPSEAT VYLPPVPVSK VVSTDEYVAR TNIYYHAGTS RLLAVGHPYF PIKKPNNNKI LVPKVSGLQY RVFRIHLPDP NKFGFPDTSF YNPDTQRLVW ACVGVEVGRG QPLGVGISGH PLLNKLDDTE NASAYAANAG VDNRECISMD YKQTQLCLIG CKPPIGEHWG KGSPCTNVAV NPGDCPPLEL INTVIQDGDM VDTGFGAMDF TTLQANKSEV PLDICTSICK YPDYIKMVSE PYGDSLFFYL RREQMFVRHL FNRAGAVGEN VPDDLYIKGS GSTANLASSN YFPTPSGSMV TSDAQIFNKP YWLQRAQGHN NGICWGNQLF VTVVDTTRST NMSLCAAIST SETTYKNTNF KEYLRHGEEY DLQFIFQLCK ITLTADVMTY IHSMNSTILE DWNFGLQPPP GGTLCGPIPV LDENGLFAPG PCTPPAPKEDP LKKYTFWEVN NLKEKFVTSQA IACQKHTPPA PKEDPSADLD QFPLGRKFLL QAGLKAKPKF TLGKRKATPT TSSTSTTAKR KKRKL

Table 6.2: Amino acid sequences of the generation I constructs of the insertion (_i) or substitution (_s) of 2C7 peptide sequence without the Cys clamp into HPV-16 L1 at positions within the DE loop indicated by the blue boxes or the h4 helix indicated by the orange boxes.

Generation II constructs
DE_i MSLWLPSEAT VYLPPVPVSK VVSTDEYVAR TNIYYHAGTS RLLAVGHPYF PIKKPNNNKI LVPKVSGLQY RVFRIHLPDP NKFGFPDTSF YNPDTQRLVW ACVGVEVGRG QPLGVGISGH PLLNKLDDTE NIPVLDENGLF APASAYAANAG VDNRECISMD YKQTQLCLIG CKPPIGEHWG KGSPCTNVAV NPGDCPPLEL INTVIQDGDM VDTGFGAMDF TTLQANKSEV PLDICTSICK YPDYIKMVSE PYGDSLFFYL RREQMFVRHL FNRAGAVGEN VPDDLYIKGS GSTANLASSN YFPTPSGSMV TSDAQIFNKP YWLQRAQGHN NGICWGNQLF VTVVDTTRST NMSLCAAIST SETTYKNTNF KEYLRHGEEY DLQFIFQLCK ITLTADVMTY IHSMNSTILE DWNFGLQPPP GGTLEDTYRF VTSQAIACQK HTPPAPKEDP LKKYTFWEVN LKEKFSADLD QFPLGRKFLL QAGLKAKPKF TLGKRKATPT TSSTSTTAKR KKRKL
DE_s MSLWLPSEAT VYLPPVPVSK VVSTDEYVAR TNIYYHAGTS RLLAVGHPYF PIKKPNNNKI LVPKVSGLQY RVFRIHLPDP NKFGFPDTSF YNPDTQRLVW ACVGVEVGRG QPLGVGISGH PLLNKLDDTE NIPVLDENGL FAPRECISMD YKQTQLCLIG CKPPIGEHWG KGSPCTNVAV NPGDCPPLEL INTVIQDGDM VDTGFGAMDF TTLQANKSEV PLDICTSICK YPDYIKMVSE PYGDSLFFYL RREQMFVRHL FNRAGAVGEN VPDDLYIKGS GSTANLASSN YFPTPSGSMV TSDAQIFNKP YWLQRAQGHN NGICWGNQLF VTVVDTTRST NMSLCAAIST SETTYKNTNF KEYLRHGEEY DLQFIFQLCK ITLTADVMTY IHSMNSTILE DWNFGLQPPP GGTLEDTYRF VTSQAIACQK HTPPAPKEDP LKKYTFWEVN LKEKFSADLD QFPLGRKFLL QAGLKAKPKF TLGKRKATPT TSSTSTTAKR KKRKL
h4_i MSLWLPSEAT VYLPPVPVSK VVSTDEYVAR TNIYYHAGTS RLLAVGHPYF PIKKPNNNKI LVPKVSGLQY RVFRIHLPDP NKFGFPDTSF YNPDTQRLVW ACVGVEVGRG QPLGVGISGH PLLNKLDDTE NASAYAANAG VDNRECISMD YKQTQLCLIG CKPPIGEHWG KGSPCTNVAV NPGDCPPLEL INTVIQDGDM VDTGFGAMDF TTLQANKSEV PLDICTSICK YPDYIKMVSE PYGDSLFFYL RREQMFVRHL FNRAGAVGEN VPDDLYIKGS GSTANLASSN YFPTPSGSMV TSDAQIFNKP YWLQRAQGHN NGICWGNQLF VTVVDTTRST NMSLCAAIST SETTYKNTNF KEYLRHGEEY DLQFIFQLCK ITLTADVMTY IHSMNSTILE DWNFGLQPPP GGTLIPVLDE NGLFAPEDTYRF VTSQAIACQK HTPPAPKEDP LKKYTFWEVN LKEKFSADLD QFPLGRKFLL QAGLKAKPKF TLGKRKATPT TSSTSTTAKR KKRKL
h4_s MSLWLPSEAT VYLPPVPVSK VVSTDEYVAR TNIYYHAGTS RLLAVGHPYF PIKKPNNNKI LVPKVSGLQY RVFRIHLPDP NKFGFPDTSF YNPDTQRLVW ACVGVEVGRG QPLGVGISGH PLLNKLDDTE NASAYAANAG VDNRECISMD YKQTQLCLIG CKPPIGEHWG KGSPCTNVAV NPGDCPPLEL INTVIQDGDM VDTGFGAMDF TTLQANKSEV PLDICTSICK YPDYIKMVSE PYGDSLFFYL RREQMFVRHL FNRAGAVGEN VPDDLYIKGS GSTANLASSN YFPTPSGSMV TSDAQIFNKP YWLQRAQGHN NGICWGNQLF VTVVDTTRST NMSLCAAIST SETTYKNTNF KEYLRHGEEY DLQFIFQLCK ITLTADVMTY IHSMNSTILE DWNFGLQPPP GGTLIPVLDE NGLFAPACQK HTPPAPKEDP LKKYTFWEVN LKEKFSADLD QFPLGRKFLL QAGLKAKPKF TLGKRKATPT TSSTSTTAKR KKRKL

References

ADAMS, A., HENDRIKSE, M., RYBICKI, E. P. & HITZEROTH, II 2023. Optimal size of DNA encapsidated by plant produced human papillomavirus pseudovirions. *Virology,* 580**,** 88-97.

ALIROL, E., WI, T. E., BALA, M., BAZZO, M. L., CHEN, X.-S., DEAL, C., DILLON, J.-A. R., KULARATNE, R., HEIM, J., HOOFT VAN HUIJSDUIJNEN, R., HOOK, E. W., LAHRA, M. M., LEWIS, D. A., NDOWA, F., SHAFER, W. M., TAYLER, L., WORKOWSKI, K., UNEMO, M. & BALASEGARAM, M. 2017. Multidrug-resistant gonorrhea: A research and development roadmap to discover new medicines. *PLOS Medicine,* 14**,** e1002366.

ANDERSSON, I. & BACKLUND, A. 2008. Structure and function of Rubisco. *Plant Physiology and Biochemistry,* 46**,** 275-291.

BACHMANN, M. F. & JENNINGS, G. T. 2010. Vaccine delivery: a matter of size, geometry, kinetics and molecular patterns. *Nature Reviews Immunology,* 10**,** 787-796.

BADAWI, M. M., SALAHELDIN, M. A., IDRIS, A. B., HASABO, E. A., OSMAN, Z. H. & OSMAN, W. M. 2019. Knowledge gaps of STIs in Africa; Systematic review. *PLOS ONE,* 14**,** e0213224.

BARBEAU, W. E. & KINSELLA, J. E. 1988. Ribulose bisphosphate carboxylase/oxygenase (rubisco) from green leaves-potential as a food protein. *Food Reviews International,* 4**,** 93-127.

BERNDTSON, A. E. 2020. Increasing Globalization and the Movement of Antimicrobial Resistance between Countries. *Surgical Infections,* 21**,** 579-585.

BIANCHI, R., TEIJEIRA, A., PROULX, S. T., CHRISTIANSEN, A. J., SEIDEL, C. D., RÜLICKE, T., MÄKINEN, T., HÄGERLING, R., HALIN, C. & DETMAR, M. 2015. A Transgenic Prox1-Cre-tdTomato Reporter Mouse for Lymphatic Vessel Research. *PLOS ONE,* 10**,** e0122976.

BILLINTON, N. & KNIGHT, A. W. 2001. Seeing the wood through the trees: a review of techniques for distinguishing green fluorescent protein from endogenous autofluorescence. *Analytical Biochemisty,* 291**,** 175-97.

BOSLEGO, J. W., TRAMONT, E. C., CHUNG, R. C., MCCHESNEY, D. G., CIAK, J., SADOFF, J. C., PIZIAK, M. V., BROWN, J. D., BRINTON JR, C. C. & WOOD, S. W. 1991. Efficacy trial of a parenteral gonococcal pilus vaccine in men. *Vaccine,* 9**,** 154-162.

BRINTON, C., WOOD, S., BROWN, A., LABIK, A., BRYAN, J., LEE, S., POLEN, S., TRAMONT, E., SADOFF, J. & ZOLLINGER, W. 1982. Seminars in Infectious Diseases. *Bacterial Vaccines,* 4.

BRONIARCZYK, J., MASSIMI, P., PIM, D., BERGANT MARUŠIČ, M., MYERS, M. P., GARCEA, R. L. & BANKS, L. 2019. Phosphorylation of Human Papillomavirus Type 16 L2 Contributes to Efficient Virus Infectious Entry. *Journal of Virology,* 93.

BUCK, C. B., CHENG, N., THOMPSON, C. D., LOWY, D. R., STEVEN, A. C., SCHILLER, J. T. & TRUS, B. L. 2008. Arrangement of L2 within the papillomavirus capsid. *J Virol,* 82**,** 5190-7.

BUCK, C. B., PASTRANA, D. V., LOWY, D. R. & SCHILLER, J. T. 2005. Generation of HPV Pseudovirions Using Transfection and Their Use in Neutralization Assays. Humana Press.

CARSE, S., LANG, D., KATZ, A. A. & SCHÄFER, G. 2021. Exogenous Vimentin Supplementation Transiently Affects Early Steps during HPV16 Pseudovirus Infection. *Viruses,* 13**,** 2471.

CDC., C. F. D. C. A. P. 2019. Sexually transmitted disease surveillance 2018. *Atlanta: U.S. Department of Health and Human Services*.

CHABEDA, A., VAN ZYL, A. R., RYBICKI, E. P. & HITZEROTH, II 2019. Substitution of Human Papillomavirus Type 16 L2 Neutralizing Epitopes Into L1 Surface Loops: The Effect on Virus-Like Particle Assembly and Immunogenicity. *Front Plant Sci,* 10**,** 779.
CHATTERJEE, A. 2014. The next generation of HPV vaccines: nonavalent vaccine V503 on the horizon. *Expert Review of Vaccines,* 13**,** 1279-1290.
CHEN, X. S., GARCEA, R. L., GOLDBERG, I., CASINI, G. & HARRISON, S. C. 2000. Structure of Small Virus-like Particles Assembled from the L1 Protein of Human Papillomavirus 16. *Molecular Cell,* 5**,** 557-567.
CHICHESTER, J. A., GREEN, B. J., JONES, R. M., SHOJI, Y., MIURA, K., LONG, C. A., LEE, C. K., OCKENHOUSE, C. F., MORIN, M. J., STREATFIELD, S. J. & YUSIBOV, V. 2018. Safety and immunogenicity of a plant-produced Pfs25 virus-like particle as a transmission blocking vaccine against malaria: A Phase 1 dose-escalation study in healthy adults. *Vaccine,* 36**,** 5865-5871.
CHU, K., BI, Z.-F., HUANG, W.-J., LI, Y.-F., ZHANG, L., YANG, C.-L., JIANG, H.-M., ZANG, X., CHEN, Q., LIU, D.-L., PAN, H.-X., HUANG, Y., ZHENG, F.-Z., ZHANG, Q.-F., SUN, G., SU, Y.-Y., HUANG, S.-J., PAN, H.-R., WU, T., HU, Y.-M., ZHANG, J., ZHU, F.-C. & XIA, N.-S. 2023. Safety and immunogenicity of an Escherichia coli-produced 9-valent human papillomavirus L1 virus-like particle vaccine (types 6/11/16/18/31/33/45/52/58) in healthy adults: an open-label, dose-escalation phase 1 clinical trial. *The Lancet Regional Health – Western Pacific,* 34.
CHUNG, K. Y., COYLE, E. M., JANI, D., KING, L. R., BHARDWAJ, R., FRIES, L., SMITH, G., GLENN, G., GOLDING, H. & KHURANA, S. 2015. ISCOMATRIX™ adjuvant promotes epitope spreading and antibody affinity maturation of influenza A H7N9 virus like particle vaccine that correlate with virus neutralization in humans. *Vaccine,* 33**,** 3953-3962.
COLER, R. N., BALDWIN, S. L., SHAVERDIAN, N., BERTHOLET, S., REED, S. J., RAMAN, V. S., LU, X., DEVOS, J., HANCOCK, K., KATZ, J. M., VEDVICK, T. S., DUTHIE, M. S., CLEGG, C. H., VAN HOEVEN, N. & REED, S. G. 2010. A synthetic adjuvant to enhance and expand immune responses to influenza vaccines. *PLoS One,* 5**,** e13677.
CONWAY, M. J. & MEYERS, C. 2009. Replication and Assembly of Human Papillomaviruses. *Journal of Dental Research,* 88**,** 307-317.
CULP, T. D., BUDGEON, L. R. & CHRISTENSEN, N. D. 2006. Human papillomaviruses bind a basal extracellular matrix component secreted by keratinocytes which is distinct from a membrane-associated receptor. *Virology,* 347**,** 147-59.
DAL CONTE, I., FIANCHINO, B., DELMONTE, S., ROBBIANO, F., D'ANTUONO, A., MIRONE, E., MATTEELLI, A., DE FRANCESCO, M. A., CUSINI, M., SCIOCCATI, L., DI CARLO, A., PRIGNANO, G., SALFA, M. C., STARNINO, S., SULIGOI, B., REGINE, V., BILEK, N. & STEFANELLI, P. 2008. Phenotypic and genotypic characterization of Neisseria gonorrhoeae in parts of Italy: detection of a multiresistant cluster circulating in a heterosexual network. *Clinical Microbiology and Infection,* 14**,** 949-954.
DALE, C. J., LIU, X. S., DE ROSE, R., PURCELL, D. F., ANDERSON, J., XU, Y., LEGGATT, G. R., FRAZER, I. H. & KENT, S. J. 2002. Chimeric human papilloma virus-simian/human immunodeficiency virus virus-like-particle vaccines: immunogenicity and protective efficacy in macaques. *Virology,* 301**,** 176-87.
DAY, P. M., KINES, R. C., THOMPSON, C. D., JAGU, S., RODEN, R. B., LOWY, D. R. & SCHILLER, J. T. 2010. In Vivo Mechanisms of Vaccine-Induced Protection against HPV Infection. *Cell Host & Microbe,* 8**,** 260-270.
DE VILLIERS, E. M., FAUQUET, C., BROKER, T. R., BERNARD, H. U. & ZUR HAUSEN, H. 2004. Classification of papillomaviruses. *Virology,* 324**,** 17-27.
DI BONITO, P., GRASSO, F., MOCHI, S., PETRONE, L., FANALES-BELASIO, E., MEI, A., CESOLINI, A., LACONI, G., CONRAD, H., BERNHARD, H., DEMBEK, C. J., COSMA, A., SANTINI, S. M., LAPENTA, C., DONATI, S., MURATORI, C., GIORGI, C. &

FEDERICO, M. 2009. Anti-tumor CD8+ T cell immunity elicited by HIV-1-based virus-like particles incorporating HPV-16 E7 protein. *Virology,* 395**,** 45-55.
DIAMOS, A. G., PARDHE, M. D., SUN, H., HUNTER, J. G., MOR, T., MEADOR, L., KILBOURNE, J., CHEN, Q. & MASON, H. S. 2020. Codelivery of improved immune complex and virus-like particle vaccines containing Zika virus envelope domain III synergistically enhances immunogenicity. *Vaccine,* 38**,** 3455-3463.
DOBRICA, M.-O., LAZAR, C., PARUCH, L., SKOMEDAL, H., STEEN, H., HAUGSLIEN, S., TUCUREANU, C., CARAS, I., ONU, A. & CIULEAN, S. 2017. A novel chimeric Hepatitis B virus S/preS1 antigen produced in mammalian and plant cells elicits stronger humoral and cellular immune response than the standard vaccine-constituent, S protein. *Antiviral research,* 144**,** 256-265.
DOORBAR, J. 2016. Model systems of human papillomavirus-associated disease. *The Journal of Pathology,* 238**,** 166-179.
EDWARDS, J. L., JENNINGS, M. P., APICELLA, M. A. & SEIB, K. L. 2016. Is gonococcal disease preventable? The importance of understanding immunity and pathogenesis in vaccine development. *Critical Reviews in Microbiology,* 42**,** 928-941.
EDWARDS, J. L. A., MICHAEL. A. & 2004. The molecular mechanisms used by Neisseria gonorrhoeae to initiate infection differ between men and women. 17**,** 965-981.
ENGLAND, C. G., EHLERDING, E. B. & CAI, W. 2016. NanoLuc: A Small Luciferase Is Brightening Up the Field of Bioluminescence. *Bioconjugate Chemistry,* 27**,** 1175-1187.
FAYE, L., BOULAFLOUS, A., BENCHABANE, M., GOMORD, V. & MICHAUD, D. 2005. Protein modifications in the plant secretory pathway: current status and practical implications in molecular pharming. *Vaccine,* 23**,** 1770-8.
FERNÁNDEZ-SAN MILLÁN, A., ORTIGOSA, S. M., HERVÁS-STUBBS, S., CORRAL-MARTÍNEZ, P., SEGUÍ-SIMARRO, J. M., GAÉTAN, J., COURSAGET, P. & VERAMENDI, J. 2008. Human papillomavirus L1 protein expressed in tobacco chloroplasts self-assembles into virus-like particles that are highly immunogenic. *Plant Biotechnol J,* 6**,** 427-41.
FIFER, H., NATARAJAN, U., JONES, L., ALEXANDER, S., HUGHES, G., GOLPARIAN, D. & UNEMO, M. 2016. Failure of Dual Antimicrobial Therapy in Treatment of Gonorrhea. *New England Journal of Medicine,* 374**,** 2504-2506.
FIRDAUS, F. Z., SKWARCZYNSKI, M. & TOTH, I. 2022. Developments in Vaccine Adjuvants. Springer US.
FISCHER, R., STOGER, E., SCHILLBERG, S., CHRISTOU, P. & TWYMAN, R. M. 2004. Plant-based production of biopharmaceuticals. *Current opinion in plant biology,* 7**,** 152-158.
FLORIN, L., BECKER, K. A., LAMBERT, C., NOWAK, T., SAPP, C., STRAND, D., STREECK, R. E. & SAPP, M. 2006. Identification of a dynein interacting domain in the papillomavirus minor capsid protein l2. *J Virol,* 80**,** 6691-6.
FOULADVAND, F., BEMANI, P., MOHAMMADI, M., AMINI, R. & AZIZI JALILIAN, F. 2020. A Review of the Methods for Concentrating M13 Phage. *Journal of Applied Biotechnology Reports,* 7**,** 7-15.
FOWLER, T., CALEY, M., JOHAL, R., BROWN, R. & ROSS, J. D. C. 2010. Previous history of gonococcal infection as a risk factor in patients presenting with gonorrhoea. *International Journal of STD & AIDS,* 21**,** 277-278.
FOX, K. K., THOMAS, J. C., WEINER, D. H., DAVIS, R. H., SPARLING, P. F. & COHEN, M. S. 1999. Longitudinal Evaluation of Serovar-specific Immunity to Neisseria gonorrhoeae. *American Journal of Epidemiology,* 149**,** 353-358.
FREDSGAARD, L., GOKSØYR, L., THRANE, S., AVES, K. L., THEANDER, T. G. & SANDER, A. F. 2021. Head-to-Head Comparison of Modular Vaccines Developed Using Different Capsid Virus-Like Particle Backbones and Antigen Conjugation Systems. *Vaccines (Basel),* 9.

GATES, B. J. & DELUCA, M. 1975. The production of oxyluciferin during the firefly luciferase light reaction. *Archives of Biochemistry and Biophysics,* 169**,** 616-621.
GERBASE, A. C. & MERTENS, T. E. 1998. Sexually transmitted diseases in Africa: time for action. *Afr Health,* 20**,** 10-2.
GILL, M. J., MCQUILLEN, D. P., VAN PUTTEN, J. P., WETZLER, L. M., BRAMLEY, J., CROOKE, H., PARSONS, N. J., COLE, J. A. & SMITH, H. 1996. Functional characterization of a sialyltransferase-deficient mutant of Neisseria gonorrhoeae. *Infect Immun,* 64**,** 3374-8.
GIULIANI, M., MONACI, E., LEUZZI, R., PEZZICOLI, A., GIANFALDONI, C., FONTANA, L., TAVARINI, S., BONCI, A., NORAIS, N. & MORI, E. Exploiting in vitro and in vivo assays to evaluate the potential ability of 4CMenB to confer protection against Neisseria gonorrhoeae, abstr P139. 21st Int Pathogenic Neisseria Conf. Asilomar, CA, 2018.
GOULD, S. J. & SUBRAMANI, S. 1988. Firefly luciferase as a tool in molecular and cell biology. *Analytical Biochemistry,* 175**,** 5-13.
GREENBERG, L. 1975. Field trials of a gonococcal vaccine. *J Reprod Med,* 14**,** 34-6.
GREENBERG, L., DIENA, B. B., ASHTON, F. A., WALLACE, R., KENNY, C. P., ZNAMIROWSKI, R., FERRARI, H. & ATKINSON, J. 1974. Gonococcal vaccine studies in Inuvik. *Can J Public Health,* 65**,** 29-33.
GREER, L. F. & SZALAY, A. A. 2002. Imaging of light emission from the expression of luciferases in living cells and organisms: a review. *Luminescence,* 17**,** 43-74.
GRGACIC, E. V. & ANDERSON, D. A. 2006. Virus-like particles: passport to immune recognition. *Methods,* 40**,** 60-5.
GULATI, S., BEURSKENS, F. J., DE KREUK, B.-J., ROZA, M., ZHENG, B., DEOLIVEIRA, R. B., SHAUGHNESSY, J., NOWAK, N. A., TAYLOR, R. P., BOTTO, M., HE, X., INGALLS, R. R., WOODRUFF, T. M., SONG, W.-C., SCHUURMAN, J., RICE, P. A. & RAM, S. 2019a. Complement alone drives efficacy of a chimeric antigonococcal monoclonal antibody. *PLOS Biology,* 17**,** e3000323.
GULATI, S., MCQUILLEN, D. P., MANDRELL, R. E., JANI, D. B. & RICE, P. A. 1996a. Immunogenicity of *Neisseria gonorrhoeae* lipooligosaccharide epitope 2C7, widely expressed in vivo with no immunochemical similarity to human glycosphingolipids [published erratum appears in J Infect Dis 1997 Apr;175(4):1027]. *J Infect Dis,* 174**,** 1223-37.
GULATI, S., PENNINGTON MICHAEL, W., CZERWINSKI, A., CARTER, D., ZHENG, B., NOWAK NANCY, A., DEOLIVEIRA ROSANE, B., SHAUGHNESSY, J., REED GEORGE, W., RAM, S. & RICE PETER, A. 2019b. Preclinical Efficacy of a Lipooligosaccharide Peptide Mimic Candidate Gonococcal Vaccine. *mBio,* 10**,** 10.1128/mbio.02552-19.
GULATI, S., ZHENG, B., REED, G. W., SU, X., COX, A. D., ST MICHAEL, F., STUPAK, J., LEWIS, L. A., RAM, S. & RICE, P. A. 2013a. Immunization against a Saccharide Epitope Accelerates Clearance of Experimental Gonococcal Infection. *PLoS Pathog,* 9**,** e1003559.
GULATI, S., ZHENG, B., REED, G. W., SU, X., COX, A. D., ST. MICHAEL, F., STUPAK, J., LEWIS, L. A., RAM, S. & RICE, P. A. 2013b. Immunization against a Saccharide Epitope Accelerates Clearance of Experimental Gonococcal Infection. *PLoS Pathogens,* 9**,** e1003559.
GULATI, S. S., JUTAMAS. RAM, SANJAY. RICE, PETER A., MCQUILLEN, D. P., MANDRELL, R. E., JANI, D. B. & RICE, P. A. 1996b. Immunogenicity of Neisseria gonorrhoeae Lipooligosaccharide Epitope 2C7, Widely Expressed In Vivo with No Immunochemical Similarity to Human Glycosphingolipids. *The Journal of Infectious Diseases,* 174**,** 1223-1237.

GULATI, S. S., JUTAMAS. RAM, SANJAY. RICE, PETER. 2019. Targetting lipooligosaccharide (LOS) for a gonococcal vaccine. *Frontiers in Immunology,* 10.
HAESE, E. C. T., VAN C. KAHLER, CHARLENE M. & 2021. Vaccine candidates for the control and prevention of the sexually transmitted disease gonorrhea. *Vaccines,* 9.
HAKKILA, K., MAKSIMOW, M., KARP, M. & VIRTA, M. 2002. Reporter Genes lucFF, luxCDABE, gfp, and dsred Have Different Characteristics in Whole-Cell Bacterial Sensors. *Analytical Biochemistry,* 301**,** 235-242.
HARDEN, M. E. & MUNGER, K. 2017. Human papillomavirus molecular biology. *Mutat Res Rev Mutat Res,* 772**,** 3-12.
HATLEM, D., TRUNK, T., LINKE, D. & LEO, J. C. 2019. Catching a SPY: Using the SpyCatcher-SpyTag and Related Systems for Labeling and Localizing Bacterial Proteins. *Int J Mol Sci,* 20.
HIGASHI, D. L., LEE, S. W., SNYDER, A., WEYAND, N. J., BAKKE, A. & SO, M. 2007. Dynamics of Neisseria gonorrhoeae attachment: microcolony development, cortical plaque formation, and cytoprotection. *Infect Immun,* 75**,** 4743-53.
HIRAMATSU, N., KASAI, A., MENG, Y., HAYAKAWA, K., YAO, J. & KITAMURA, M. 2005. Alkaline phosphatase vs luciferase as secreted reporter molecules in vivo. *Anal Biochem,* 339**,** 249-56.
HOLMES, K. K., JOHNSON, D. W. & TROSTLE, H. J. 1970. An Estimate of the Risk of Men Acquiring Gonorrhea by Sexual Contact with Infected Females. *American Journal of Epidemiology,* 91**,** 170-174.
HOOK, E. W., OLSEN, D. A. & BUCHANAN, T. M. 1984. Analysis of the antigen specificity of the human serum immunoglobulin G immune response to complicated gonococcal infection. *Infection and Immunity,* 43**,** 706-709.
HOOPER, R. R., REYNOLDS, G. H., JONES, O. G., ZAIDI, A., WIESNER, P. J., LATIMER, K. P., LESTER, A., CAMPBELL, A. F., HARRISON, W. O., KARNEY, W. W. & HOLMES, K. K. 1978. Cohort study of venereal disease. I: the risk of gonorrhea transmission from infected women to men. *Am J Epidemiol,* 108**,** 136-44.
HORVATH, C. A., BOULET, G. A., RENOUX, V. M., DELVENNE, P. O. & BOGERS, J. P. 2010. Mechanisms of cell entry by human papillomaviruses: an overview. *Virol J,* 7**,** 11.
HUH, W. K., JOURA, E. A., GIULIANO, A. R., IVERSEN, O. E., DE ANDRADE, R. P., AULT, K. A., BARTHOLOMEW, D., CESTERO, R. M., FEDRIZZI, E. N., HIRSCHBERG, A. L., MAYRAND, M. H., RUIZ-STERNBERG, A. M., STAPLETON, J. T., WILEY, D. J., FERENCZY, A., KURMAN, R., RONNETT, B. M., STOLER, M. H., CUZICK, J., GARLAND, S. M., KJAER, S. K., BAUTISTA, O. M., HAUPT, R., MOELLER, E., RITTER, M., ROBERTS, C. C., SHIELDS, C. & LUXEMBOURG, A. 2017. Final efficacy, immunogenicity, and safety analyses of a nine-valent human papillomavirus vaccine in women aged 16-26 years: a randomised, double-blind trial. *Lancet,* 390**,** 2143-2159.
JERSE, A. E. & DEAL, C. D. 2013. Vaccine research for gonococcal infections: where are we? *Sexually Transmitted Infections,* 89**,** iv63-iv68.
JOHANSSON, M. & LYCKE, N. Y. 2003. Immunology of the human genital tract. *Curr Opin Infect Dis,* 16**,** 43-9.
JONES, R. A., YEE, W. X., MADER, K., TANG, C. M. & CEHOVIN, A. 2022. Markerless gene editing in Neisseria gonorrhoeae. *Microbiology (Reading),* 168.
JORDAN, M., KÖHNE, C. & WURM, F. M. 1998. Calcium-phosphate mediated DNA transfer into HEK-293 cells in suspension: control of physicochemical parameters allows transfection in stirred media. Transfection and protein expression in mammalian cells. *Cytotechnology,* 26**,** 39-47.
KAWANA, Y., KAWANA, K., YOSHIKAWA, H., TAKETANI, Y., YOSHIIKE, K. & KANDA, T. 2001. Human papillomavirus type 16 minor capsid protein l2 N-terminal region

containing a common neutralization epitope binds to the cell surface and enters the cytoplasm. *J Virol,* 75**,** 2331-6.
KIM, H. J., KWAG, H. L. & KIM, H. J. 2016. Characterization of human papillomavirus type 16 pseudovirus containing histones. *BMC Biotechnol,* 16**,** 63.
KIM, J. J., ZHOU, D., MANDRELL, R. E. & GRIFFISS, J. M. 1992. Effect of exogenous sialylation of the lipooligosaccharide of Neisseria gonorrhoeae on opsonophagocytosis. *Infection and Immunity,* 60**,** 4439-4442.
KINES, R. C., THOMPSON, C. D., LOWY, D. R., SCHILLER, J. T. & DAY, P. M. 2009. The initial steps leading to papillomavirus infection occur on the basement membrane prior to cell surface binding. *Proceedings of the National Academy of Sciences,* 106**,** 20458-20463.
KIRKCALDY, R. D., BOLAN, G. A. & WASSERHEIT, J. N. 2013. Cephalosporin-Resistant Gonorrhea in North America. *JAMA,* 309**,** 185.
KIRKCALDY, R. D., WESTON, E., SEGURADO, A. C. & HUGHES, G. 2019. Epidemiology of gonorrhoea: a global perspective. *Sexual Health,* 16**,** 401.
KOHL, T., HITZEROTH, I., STEWART, D., VARSANI, A., GOVAN, V., CHRISTENSEN, N., WILLIAMSON, A.-L. & RYBICKI, E. 2006. Plant-produced cottontail rabbit papillomavirus L1 protein protects against tumor challenge: a proof-of-concept study. *Clinical and vaccine immunology,* 13**,** 845-853.
KONDO, K., ISHII, Y., MORI, S., SHIMABUKURO, S., YOSHIKAWA, H. & KANDA, T. 2009. Nuclear location of minor capsid protein L2 is required for expression of a reporter plasmid packaged in HPV51 pseudovirions. *Virology,* 394**,** 259-265.
KOVACSOVICS-BANKOWSKI, M., CLARK, K., BENACERRAF, B. & ROCK, K. L. 1993. Efficient major histocompatibility complex class I presentation of exogenous antigen upon phagocytosis by macrophages. *Proceedings of the National Academy of Sciences,* 90**,** 4942-4946.
KUSHNIR, N., STREATFIELD, S. J. & YUSIBOV, V. 2012. Virus-like particles as a highly efficient vaccine platform: diversity of targets and production systems and advances in clinical development. *Vaccine,* 31**,** 58-83.
KUTZ, J. M., RAUSCHE, P., GHEIT, T., PURADIREDJA, D. I. & FUSCO, D. 2023. Barriers and facilitators of HPV vaccination in sub-saharan Africa: a systematic review. *BMC Public Health,* 23**,** 974.
LAMMEL, C. J., SWEET, R. L., RICE, P. A., KNAPP, J. S., SCHOOLNIK, G. K., HEILBRON, D. C. & BROOKS, G. F. 1985. Antibody-Antigen specificity in the immune response to infection with neisseria gonorrhoeae. *Journal of Infectious Diseases,* 152**,** 990-1001.
LAMPRECHT, R. L., KENNEDY, P., HUDDY, S. M., BETHKE, S., HENDRIKSE, M., HITZEROTH, II & RYBICKI, E. P. 2016. Production of Human papillomavirus pseudovirions in plants and their use in pseudovirion-based neutralisation assays in mammalian cells. *Sci Rep,* 6**,** 20431.
LIU, Y., HAMMER, L. A., LIU, W., HOBBS, M. M., ZIELKE, R. A., SIKORA, A. E., JERSE, A. E., EGILMEZ, N. K. & RUSSELL, M. W. 2017. Experimental vaccine induces Th1-driven immune responses and resistance to Neisseria gonorrhoeae infection in a murine model. *Mucosal Immunology,* 10**,** 1594-1608.
LIU, Y., LIU, W. & RUSSELL, M. W. 2014. Suppression of host adaptive immune responses by Neisseria gonorrhoeae: role of interleukin 10 and type 1 regulatory T cells. *Mucosal Immunol,* 7**,** 165-76.
LIU, Y. & RUSSELL, M. W. 2011. Diversion of the immune response to Neisseria gonorrhoeae from Th17 to Th1/Th2 by treatment with anti-transforming growth factor β antibody generates immunological memory and protective immunity. *mBio,* 2**,** e00095-11.
MA, B., RODEN, R. B., HUNG, C. F. & WU, T. C. 2011. HPV pseudovirions as DNA delivery vehicles. *Ther Deliv,* 2**,** 427-30.

MACLEAN, J., KOEKEMOER, M., OLIVIER, A. J., STEWART, D., HITZEROTH, I. I., RADEMACHER, T., FISCHER, R., WILLIAMSON, A. L. & RYBICKI, E. P. 2007. Optimization of human papillomavirus type 16 (HPV-16) L1 expression in plants: comparison of the suitability of different HPV-16 L1 gene variants and different cell-compartment localization. *Journal of General Virology,* 88**,** 1460-1469.

MARGOLIN, E., CHAPMAN, R., WILLIAMSON, A. L., RYBICKI, E. P. & MEYERS, A. E. 2018. Production of complex viral glycoproteins in plants as vaccine immunogens. *Plant Biotechnol J,* 16**,** 1531-45.

MATTHIAS, K. A., CONNOLLY, K. L., BEGUM, A. A., JERSE, A. E., MACINTYRE, A. N., SEMPOWSKI, G. D. & BASH, M. C. 2021. Meningococcal Detoxified Outer Membrane Vesicle Vaccines Enhance Gonococcal Clearance in a Murine Infection Model. *The Journal of Infectious Diseases,* 225**,** 650-660.

MISTRY, N., WIBOM, C. & EVANDER, M. 2008. Cutaneous and mucosal human papillomaviruses differ in net surface charge, potential impact on tropism. *Virology Journal,* 5**,** 118.

MÓDOLO, D. G., ARALDI, R. P., MAZZUCHELLI-DE-SOUZA, J., PEREIRA, A., PIMENTA, D. C., ZANPHORLIN, L. M., BEÇAK, W., MENOSSI, M., DE CASSIA STOCCO, R. & DE CARVALHO, R. F. 2017. Integrated analysis of recombinant BPV-1 L1 protein for the production of a bovine papillomavirus VLP vaccine. *Vaccine,* 35**,** 1590-1593.

MOHAMMADZADEH, S., ROOHVAND, F., MEMARNEJADIAN, A., JAFARI, A., AJDARY, S., SALMANIAN, A.-H. & EHSANI, P. 2016. Co-expression of hepatitis C virus polytope–HBsAg and p19-silencing suppressor protein in tobacco leaves. *Pharmaceutical biology,* 54**,** 465-473.

MOHSEN, M. O., ZHA, L., CABRAL-MIRANDA, G. & BACHMANN, M. F. 2017. Major findings and recent advances in virus–like particle (VLP)-based vaccines. *Seminars in Immunology,* 34**,** 123-132.

MOODY, C. A. & LAIMINS, L. A. 2010. Human papillomavirus oncoproteins: pathways to transformation. *Nat Rev Cancer,* 10**,** 550-60.

MOSMANN, T. R. & COFFMAN, R. L. 1989. TH1 and TH2 cells: different patterns of lymphokine secretion lead to different functional properties. *Annu Rev Immunol,* 7**,** 145-73.

MÜHLECKER, W., GULATI, S. S., JUTAMAS. RAM, SANJAY. RICE, PETER A., MCQUILLEN, D. P., RAM, S., RICE, P. A. & REINHOLD, V. N. 1999. An essential saccharide binding domain for the mAb 2C7 established for Neisseria gonorrhoeae LOS by ES-MS and MS n. *Glycobiology,* 9**,** 157-171.

NAUD, P. S., ROTELI-MARTINS, C. M., DE CARVALHO, N. S., TEIXEIRA, J. C., DE BORBA, P. C., SANCHEZ, N., ZAHAF, T., CATTEAU, G., GEERAERTS, B. & DESCAMPS, D. 2014. Sustained efficacy, immunogenicity, and safety of the HPV-16/18 AS04-adjuvanted vaccine. *Human Vaccines & Immunotherapeutics,* 10**,** 2147-2162.

NEEFJES, M., HOUSMANS, B. A. C., VAN DEN AKKER, G. G. H., VAN RHIJN, L. W., WELTING, T. J. M. & VAN DER KRAAN, P. M. 2021. Reporter gene comparison demonstrates interference of complex body fluids with secreted luciferase activity. *Scientific Reports,* 11.

NETO, A., SEVILHA, J., SEABRA, D., OLIVEIRA, I., SANTOS, R. P., ANDRADE, A., PINHO, P., COSTA, P. M., VIANA, M. & PINTO, P. 2021. Acute Aortic Regurgitation Due to Endocarditis Caused by Disseminated Gonococcal Infection: A Case Report. *Sexually Transmitted Diseases,* 48**,** e48-e50.

NGAMPASUTADOL, J., RICE, P. A., WALSH, M. T. & GULATI, S. 2006. Characterization of a peptide vaccine candidate mimicking an oligosaccharide epitope of Neisseria gonorrhoeae and resultant immune responses and function. *Vaccine,* 24**,** 157-170.

NGAMPASUTADOL, J., TRAN, C., GULATI, S., BLOM, A. M., JERSE, E. A., RAM, S. & RICE, P. A. 2008. Species-specificity of Neisseria gonorrhoeae infection: do human complement regulators contribute? *Vaccine,* 26 Suppl 8**,** I62-6.
OBEMBE, O. O., POPOOLA, J. O., LEELAVATHI, S. & REDDY, S. V. 2011. Advances in plant molecular farming. *Biotechnology Advances,* 29**,** 210-222.
OSAKA, K., TAKAHATA, M., TAKAKURA, T., NARUKAWA, K., ENDO, K., KIYOTA, H. & ONODERA, S. 2008. Analysis of amino acid sequences of penicillin-binding protein 2 in clinical isolates of Neisseria gonorrhoeae with reduced susceptibility to cefixime and ceftriaxone. *Journal of Infection and Chemotherapy,* 14**,** 195-203.
PASMANS, H., BERKOWSKA, M. A., DIKS, A. M., DE MOOIJ, B., GROENLAND, R. J., DE ROND, L., NICOLAIE, M. A., VAN DER BURG, S. H., VAN DONGEN, J. J. M., VAN DER KLIS, F. R. M. & BUISMAN, A. M. 2022. Characterization of the early cellular immune response induced by HPV vaccines. *Front Immunol,* 13**,** 863164.
PASTRANA, D. V., BUCK, C. B., PANG, Y. Y., THOMPSON, C. D., CASTLE, P. E., FITZGERALD, P. C., KRÜGER KJAER, S., LOWY, D. R. & SCHILLER, J. T. 2004. Reactivity of human sera in a sensitive, high-throughput pseudovirus-based papillomavirus neutralization assay for HPV16 and HPV18. *Virology,* 321**,** 205-16.
PENG, S., FRAZER, I. H., FERNANDO, G. J. & ZHOU, J. 1998. Papillomavirus virus-like particles can deliver defined CTL epitopes to the MHC class I pathway. *Virology,* 240**,** 147-57.
PETERS, B. S., CHEINGSONG-POPOV, R., CALLOW, D., FOXALL, R., PATOU, G., HODGKIN, K. & WEBER, J. N. 1997. A pilot phase II study of the safety and immunogenicity of HIV p17/p24:VLP (p24-VLP) in asymptomatic HIV seropositive subjects. *Journal of Infection,* 35**,** 231-235.
PETOUSIS-HARRIS, H., PAYNTER, J., MORGAN, J., SAXTON, P., MCARDLE, B., GOODYEAR-SMITH, F. & BLACK, S. 2017. Effectiveness of a group B outer membrane vesicle meningococcal vaccine against gonorrhoea in New Zealand: a retrospective case-control study. *Lancet,* 390**,** 1603-1610.
PINEO, C. B., HITZEROTH, INGA I., RYBICKI, EDWARD P. & 2013. Immunogenic assessment of plant-produced human papillomavirus type 16 L1/L2 chimaeras.
PINTO, L. A., DILLNER, J., BEDDOWS, S. & UNGER, E. R. 2018. Immunogenicity of HPV prophylactic vaccines: Serology assays and their use in HPV vaccine evaluation and development. *Vaccine,* 36**,** 4792-4799.
PLOTKIN, S. A. 2010. Correlates of protection induced by vaccination. *Clin Vaccine Immunol,* 17**,** 1055-65.
PULENDRAN, B. & AHMED, R. 2011. Immunological mechanisms of vaccination. *Nature Immunology,* 12**,** 509-517.
QIAN, C., LIU, X., XU, Q., WANG, Z., CHEN, J., LI, T., ZHENG, Q., YU, H., GU, Y., LI, S. & XIA, N. 2020. Recent Progress on the Versatility of Virus-Like Particles. *Vaccines,* 8**,** 139.
QUILLIN, S. J. & SEIFERT, H. S. 2018. Neisseria gonorrhoeae host adaptation and pathogenesis. *Nature Reviews Microbiology,* 16**,** 226-240.
QULU, W., MTSHALI, A., OSMAN, F., NDLELA, N., NTULI, L., MZOBE, G., NAICKER, N., GARRETT, N., ROMPALO, A., MINDEL, A., NGCAPU, S. & LIEBENBERG, L. 2023. High-risk human papillomavirus prevalence among South African women diagnosed with other STIs and BV. *PLOS ONE,* 18**,** e0294698.
RAFF, A. B., WOODHAM, A. W., RAFF, L. M., SKEATE, J. G., YAN, L., SILVA, D. M. D., SCHELHAAS, M. & KAST, W. M. 2013. The Evolving Field of Human Papillomavirus Receptor Research: a Review of Binding and Entry. *Journal of Virology,* 87**,** 6062-6072.
RAM, S., GULATI, S., LEWIS, L. A., CHAKRABORTI, S., ZHENG, B., DEOLIVEIRA, R. B., REED, G. W., COX, A. D., LI, J., ST MICHAEL, F., STUPAK, J., SU, X. H., SAHA, S.,

LANDIG, C. S., VARKI, A. & RICE, P. A. 2018. A novel sialylation site on Neisseria gonorrhoeae lipooligosaccharide links heptose II lactose expression with pathogenicity. *Infect Immun***,** e00285-18.
RAM, S. G., SUNITA; LEWIS, LISA A; CHAKRABORTI, SRINJOY; ZHENG, BO; DEOLIVEIRA, ROSANE B; REED, GEORGE W; COX, ANDREW D; LI, JIANJUN; MICHAEL, FRANK ST; STUPAK, JACEK; SU, XIAO-HONG; SAHA, SUDESHNA; LANDIG, CORINNA S; VARKI, AJIY; RICE, PETER. 2018. A Novel Sialylation Site on Neisseria gonorrhoeae Lipooligosaccharide Links Heptose II Lactose Expression with Pathogenicity. *Infection And Immunity,* 86.
RATERMAN, E. L. & JERSE, A. E. 2019. Female Mouse Model of Neisseria gonorrhoeae Infection. *Methods Mol Biol,* 1997**,** 413-429.
REST, R. F. & FRANGIPANE, J. V. 1992. Growth of Neisseria gonorrhoeae in CMP-N-acetylneuraminic acid inhibits nonopsonic (opacity-associated outer membrane protein-mediated) interactions with human neutrophils. *Infect Immun,* 60**,** 989-97.
RICE, P. A., SHAFER, W. M., RAM, S. & JERSE, A. E. 2017. Neisseria gonorrhoeae: Drug Resistance, Mouse Models, and Vaccine Development. *Annual Review of Microbiology,* 71**,** 665-686.
RICHARDS, R. M., LOWY, D. R., SCHILLER, J. T. & DAY, P. M. 2006. Cleavage of the papillomavirus minor capsid protein, L2, at a furin consensus site is necessary for infection. *Proc Natl Acad Sci U S A,* 103**,** 1522-7.
ROBERTS, J. N., BUCK, C. B., THOMPSON, C. D., KINES, R., BERNARDO, M., CHOYKE, P. L., LOWY, D. R. & SCHILLER, J. T. 2007. Genital transmission of HPV in a mouse model is potentiated by nonoxynol-9 and inhibited by carrageenan. *Nature Medicine,* 13**,** 857-861.
RODEN, R. B., GREENSTONE, H. L., KIRNBAUER, R., BOOY, F. P., JESSIE, J., LOWY, D. R. & SCHILLER, J. T. 1996. In vitro generation and type-specific neutralization of a human papillomavirus type 16 virion pseudotype. *J Virol,* 70**,** 5875-83.
RODEN, R. B. S., DAY, P. M., BRONZO, B. K., YUTZY, W. H., YANG, Y., LOWY, D. R. & SCHILLER, J. T. 2001. Positively Charged Termini of the L2 Minor Capsid Protein Are Necessary for Papillomavirus Infection. *Journal of Virology,* 75**,** 10493-10497.
ROSALES-MENDOZA, S. 2020. Will plant-made biopharmaceuticals play a role in the fight against COVID-19? *Expert opinion on biological therapy,* 20**,** 545-548.
ROSS, J. D. 1996. Systemic gonococcal infection. *Sexually Transmitted Infections,* 72**,** 404-407.
ROSS, J. D., MOYES, A. & YOUNG, H. 1995. Serovar specific immunity to Neisseria gonorrhoeae: does it exist? *Sexually Transmitted Infections,* 71**,** 367-369.
RYBICKI, E. P. 2010. Plant-made vaccines for humans and animals. *Plant Biotechnol J,* 8**,** 620-37.
SADARANGANI, M., POLLARD, A. J. & GRAY-OWEN, S. D. 2011. Opa proteins and CEACAMs: pathways of immune engagement for pathogenic Neisseria. *FEMS Microbiol Rev,* 35**,** 498-514.
SAINSBURY, F., THUENEMANN, E. C. & LOMONOSSOFF, G. P. 2009. pEAQ: versatile expression vectors for easy and quick transient expression of heterologous proteins in plants. *Plant Biotechnology Journal,* 7**,** 682-693.
SANCTA, S. C. B., LINDLEY. WORKOWSKI, KIMBERLY A. BACHMANN, LAURA H. PHAM, CAU. SCHLANGER, KAREN. TORRONE, ELIZABETH. WEINSTOCK, HILLARD. KERSH, ELLEN N. THORPE, PHOEBE. 2020. Update to CDC's Treatment Guidelines for Gonococcal Infection. *Morbidity and Mortality Weekly Report,* 69**,** 1911 - 1916.
SAPP, M. & BIENKOWSKA-HABA, M. 2009. Viral entry mechanisms: human papillomavirus and a long journey from extracellular matrix to the nucleus. *Febs j,* 276**,** 7206-16.
SCHMIDT, K. A., SCHNEIDER, H., LINDSTROM, J. A., BOSLEGO, J. W., WARREN, R. A., VAN DE VERG, L., DEAL, C. D., MCCLAIN, J. B. & GRIFFISS, J. M. 2001.

Experimental Gonococcal Urethritis and Reinfection with Homologous Gonococci in Male Volunteers. *Sexually Transmitted Diseases,* 28**,** 555-564.
SCURTU, L. G., JINGA, V. & SIMIONESCU, O. 2022. Fascinating Molecular and Immune Escape Mechanisms in the Treatment of STIs (Syphilis, Gonorrhea, Chlamydia, and Herpes Simplex). *International Journal of Molecular Sciences,* 23**,** 3550.
SEMCHENKO, E. A. & SEIB, K. L. 2022. Outer membrane vesicle vaccines for Neisseria gonorrhoeae. *Nature Reviews Urology,* 19**,** 5-6.
SEMCHENKO, E. A., TAN, A., BORROW, R. & SEIB, K. L. 2019. The serogroup B meningococcal vaccine Bexsero elicits antibodies to Neisseria gonorrhoeae. *Clinical Infectious Diseases,* 69**,** 1101-1111.
SHAUGHNESSY, J., CHABEDA, A., TRAN, Y., ZHENG, B., NOWAK, N., STEFFENS, C., DEOLIVEIRA, R. B., GULATI, S., LEWIS, L. A., MACLEAN, J., MOSS, J. A., WYCOFF, K. L. & RAM, S. 2022. An optimized Factor H-Fc fusion protein against multidrug-resistant Neisseria gonorrhoeae. *Frontiers in Immunology,* 13.
SHAUGHNESSY, J., GULATI, S., AGARWAL, S., UNEMO, M., OHNISHI, M., SU, X.-H., MONKS, B. G., VISINTIN, A., MADICO, G., LEWIS, L. A., GOLENBOCK, D. T., REED, G. W., RICE, P. A. & RAM, S. 2016. A Novel Factor H–Fc Chimeric Immunotherapeutic Molecule against Neisseria gonorrhoeae. *The Journal of Immunology,* 196**,** 1732-1740.
SHI, S., ZHU, H., XIA, X., LIANG, Z., MA, X. & SUN, B. 2019. Vaccine adjuvants: Understanding the structure and mechanism of adjuvanticity. *Vaccine,* 37**,** 3167-3178.
SINGH, D., VIGNAT, J., LORENZONI, V., ESLAHI, M., GINSBURG, O., LAUBY-SECRETAN, B., ARBYN, M., BASU, P., BRAY, F. & VACCARELLA, S. 2023. Global estimates of incidence and mortality of cervical cancer in 2020: a baseline analysis of the WHO Global Cervical Cancer Elimination Initiative. *The Lancet Global Health,* 11**,** e197-e206.
SMIRNOV, A., DAILY, K. P., GRAY, M. C., RAGLAND, S. A., WERNER, L. M., BRITTANY JOHNSON, M., EBY, J. C., HEWLETT, E. L., TAYLOR, R. P. & CRISS, A. K. 2023. Phagocytosis via complement receptor 3 enables microbes to evade killing by neutrophils. *Journal of Leukocyte Biology,* 114**,** 1-20.
ST CYR, S. B., LINDLEY. WORKOWSKI, KIMBERLY A. BACHMANN, LAURA H. PHAM, CAUL. SCHLANGER, KAREN. TORRONE, ELIZABETH. WEINSTOCK, HILLARD. KERSH, ELLEN N. THORPE, PHOEBE. 2020. Update to CDC's Treatment Guidelines for Gonococcal Infection, 2020. *Morbidity and Mortality Weekly Report,* 69.
SU, H., VAN EERDE, A., RIMSTAD, E., BOCK, R., BRANZA-NICHITA, N., YAKOVLEV, I. A. & CLARKE, J. L. 2023. Plant-made vaccines against viral diseases in humans and farm animals. *Frontiers in Plant Science,* 14.
SU, X., LE, W., ZHU, X., LI, S., WANG, B., MADICO, G., YANG, Z., CHAISSON, C. E., MCLAUGHLIN, R. E., GANDRA, S., YOON, J., ZHENG, B., LEWIS, L. A., GULATI, S., REED, G. W., RAM, S. & RICE, P. A. 2022. Neisseria gonorrhoeae Infection in Women Increases With Rising Gonococcal Burdens in Partners: Chlamydia Coinfection in Women Increases Gonococcal Burden. *J Infect Dis,* 226**,** 2192-2203.
SUAY-GARCÍA, B. & PÉREZ-GRACIA, M. 2018. Future Prospects for Neisseria gonorrhoeae Treatment. *Antibiotics,* 7**,** 49.
SUN, B., ZHAO, D., ZHANG, X., GU, T., YU, X., SUN, S., ZHAO, X., WEI, L., LIU, D., YAN, H., MENG, X., KONG, W., XU, F., YANG, P. & JIANG, C. 2016. Development a scalable production process for truncated human papillomavirus type-6 L1 protein using WAVE Bioreactor and hollow fiber membrane. *Applied Microbiology and Biotechnology,* 100**,** 1231-1240.
SWAIN, S. L., MCKINSTRY, K. K. & STRUTT, T. M. 2012. Expanding roles for CD4+ T cells in immunity to viruses. *Nature Reviews Immunology,* 12**,** 136-148.
SYOMIN, B. V. & ILYIN, Y. V. 2019. Virus-Like Particles as an Instrument of Vaccine Production. *Molecular Biology,* 53**,** 323-334.

TAKEDA, A., SUGIYAMA, K., NAGANO, H., MORI, M., KAIDO, M., MISE, K., TSUDA, S. & OKUNO, T. 2002. Identification of a novel RNA silencing suppressor, NSs protein of Tomato spotted wilt virus. *FEBS letters,* 532**,** 75-79.

TSEVAT, D. G., WIESENFELD, H. C., PARKS, C. & PEIPERT, J. F. 2017. Sexually transmitted diseases and infertility. *American Journal of Obstetrics and Gynecology,* 216**,** 1-9.

UDENIGWE, C. C., OKOLIE, C. L., QIAN, H., OHANENYE, I. C., AGYEI, D. & ALUKO, R. E. 2017. Ribulose-1,5-bisphosphate carboxylase as a sustainable and promising plant source of bioactive peptides for food applications. *Trends in Food Science & Technology,* 69**,** 74-82.

UNEMO, M., LAHRA, M. M., COLE, M., GALARZA, P., NDOWA, F., MARTIN, I., DILLON, J.-A. R., RAMON-PARDO, P., BOLAN, G. & WI, T. 2019a. World Health Organization Global Gonococcal Antimicrobial Surveillance Program (WHO GASP): review of new data and evidence to inform international collaborative actions and research efforts. *Sexual Health,* 16**,** 412.

UNEMO, M., LAHRA, M. M., ESCHER, M., EREMIN, S., COLE, M. J., GALARZA, P., NDOWA, F., MARTIN, I., DILLON, J.-A. R., GALAS, M., RAMON-PARDO, P., WEINSTOCK, H. & WI, T. 2021a. WHO global antimicrobial resistance surveillance for Neisseria gonorrhoeae 2017–18: a retrospective observational study. *The Lancet Microbe,* 2**,** e627-e636.

UNEMO, M. & NICHOLAS, R. A. 2012. Emergence of multidrug-resistant, extensively drug-resistant and untreatable gonorrhea. *Future Microbiology,* 7**,** 1401-1422.

UNEMO, M., SEIFERT, H. S., HOOK, E. W., HAWKES, S., NDOWA, F. & DILLON, J.-A. R. 2019b. Gonorrhoea. *Nature Reviews Disease Primers,* 5.

UNEMO, M. & SIKORA, A. E. 2017. Proof of principle for effectiveness of a gonorrhoea vaccine. *Nature Reviews Urology,* 14**,** 643-644.

UNEMO, M. L., MONICA M;, ESCHER, M., EREMIN, S., COLE, M. J., GALARZA, P. N., FRANCIS; MARTIN, IRENE; DILLION, JO-ANNE R;, GALAS, M. R.-P., PILAR;, WEINSTOCK, H. W., TEODORA. & 2021b. WHO global antimicrobial resistance surveillance for Neisseria gonorrhoeae. 2**,** 627-636.

UNEMO, M. S., WILLIAM M. 2014. Antimicrobial resistance in Neisseria gonorrhoeae in the 21st Century: Past, evolution, and future. 27**,** 587-613.

VALERO-PACHECO, N., PÉREZ-TOLEDO, M., VILLASÍS-KEEVER, M. Á., NÚÑEZ-VALENCIA, A., BOSCÓ-GÁRATE, I., LOZANO-DUBERNARD, B., LARA-PUENTE, H., ESPITIA, C., ALPUCHE-ARANDA, C., BONIFAZ, L. C., ARRIAGA-PIZANO, L., PASTELIN-PALACIOS, R., ISIBASI, A. & LÓPEZ-MACÍAS, C. 2016. Antibody Persistence in Adults Two Years after Vaccination with an H1N1 2009 Pandemic Influenza Virus-Like Particle Vaccine. *PLOS ONE,* 11**,** e0150146.

VARSANI, A., WILLIAMSON, A.-L., VILLIERS, D. D., BECKER, I., CHRISTENSEN, N. D. & RYBICKI, E. P. 2003. Chimeric Human Papillomavirus Type 16 (HPV-16) L1 Particles Presenting the Common Neutralizing Epitope for the L2 Minor Capsid Protein of HPV-6 and HPV-16. *Journal of Virology,* 77**,** 8386-8393.

VIDAURRAZAGA, M. M. & PERLMAN, D. C. 2020. A case of purulent gonococcal arthritis. *IDCases,* 19**,** e00662.

WANG, H., JIANG, Y., WANG, Q., LAI, Y. & HOLLOWAY, A. 2023. The status and challenges of HPV vaccine programme in China: an exploration of the related policy obstacles. *BMJ Global Health,* 8**,** e012554.

WETZLER, L. M., BLAKE, M. S., BARRY, K. & GOTSCHLICH, E. C. 1992. Gonococcal porin vaccine evaluation: comparison of Por proteosomes, liposomes, and blebs isolated from rmp deletion mutants. *J Infect Dis,* 166**,** 551-5.

WHO, W. H. O. 2014. Report on global sexually transmitted infection surveillance 2013. *Sexual and reproductive health*.

WHO, W. H. O. 2018. *Report on global sexually transmitted infection surveillance 2018*, World Health Organization.
WHO, W. H. O. 2022. Human papillomavirus vaccines: WHO position paper, December 2022. *Weekly Epidemiological Record No 50,* 97**,** 645-672.
WI, T., LAHRA, M. M., NDOWA, F., BALA, M., DILLON, J.-A. R., RAMON-PARDO, P., EREMIN, S. R., BOLAN, G. & UNEMO, M. 2017. Antimicrobial resistance in Neisseria gonorrhoeae: Global surveillance and a call for international collaborative action. *PLOS Medicine,* 14**,** e1002344.
WORLD HEALTH ORGANIZATION, W. 2015. Progress report of the implementation of the global strategy for prevention and control of sexually transmitted infections: 2006-2015: document for the World Health Assembly. Geneva: World Health Organization.
XU, Y. F., ZHANG, Y. Q., XU, X. M. & SONG, G. X. 2006. Papillomavirus virus-like particles as vehicles for the delivery of epitopes or genes. *Archives of Virology,* 151**,** 2133-2148.
YAMASAKI, R., KOSHINO, H., KURONO, S., NISHINAKA, Y., MCQUILLEN, D. P., KUME, A., GULATI, S. S., JUTAMAS. RAM, SANJAY. & RICE, P. A. 1999. Structural and Immunochemical Characterization of aNeisseria gonorrhoeae Epitope Defined by a Monoclonal Antibody 2C7; the Antibody Recognizes a Conserved Epitope on Specific Lipo-oligosaccharides in Spite of the Presence of Human Carbohydrate Epitopes*. *Journal of Biological Chemistry,* 274**,** 36550-36558.
YEAGER, M. D., ASTE-AMEZAGA, M., BROWN, D. R., MARTIN, M. M., SHAH, M. J., COOK, J. C., CHRISTENSEN, N. D., ACKERSON, C., LOWE, R. S., SMITH, J. F., KELLER, P. & JANSEN, K. U. 2000. Neutralization of Human Papillomavirus (HPV) Pseudovirions: A Novel and Efficient Approach to Detect and Characterize HPV Neutralizing Antibodies. *Virology,* 278**,** 570-577.
ZAHIN, M., JOH, J., KHANAL, S., HUSK, A., MASON, H., WARZECHA, H., GHIM, S.-J., MILLER, D. M., MATOBA, N. & JENSON, A. B. 2016. Scalable Production of HPV16 L1 Protein and VLPs from Tobacco Leaves. *PLOS ONE,* 11**,** e0160995.
ZHANG, L., XU, W., MA, X., SUN, X., FAN, J. & WANG, Y. 2023. Virus-like Particles as Antiviral Vaccine: Mechanism, Design, and Application. *Biotechnol Bioprocess Eng,* 28**,** 1-16.
ZHAO, K. N., SUN, X. Y., FRAZER, I. H. & ZHOU, J. 1998. DNA packaging by L1 and L2 capsid proteins of bovine papillomavirus type 1. *Virology,* 243**,** 482-91.
ZHAO, Q., ALLEN, M. J., WANG, Y., WANG, B., WANG, N., SHI, L. & SITRIN, R. D. 2012. Disassembly and reassembly improves morphology and thermal stability of human papillomavirus type 16 virus-like particles. *Nanomedicine: Nanotechnology, Biology and Medicine,* 8**,** 1182-1189.
ZHAO, T., CAI, Y., JIANG, Y., HE, X., WEI, Y., YU, Y. & TIAN, X. 2023. Vaccine adjuvants: mechanisms and platforms. *Signal Transduct Target Ther,* 8**,** 283.
ZHU, W. C., CHING JU. THOMAS, CHRISTOPHER E. ANDERSON, JAMES E. JERSE, ANN E. SPARLING, P. FREDERICK & 2011. Vaccines for gonorrhea: Can we rise to the challenge? *Frontiers in Microbiology,* 2.